Morphological studies on the genital organ in the raccoon (*Procyon lotor*)

2023

Doctoral Program of Veterinary Science
Graduate School of Animal and Veterinary Sciences and Agriculture
Obihiro University of Agriculture and Veterinary Medicine

ISHIGURO Yuki

アライグマ生殖器の形態学的研究

令和 5 年

（2023）

帯広畜産大学大学院畜産学研究科
獣医学専攻博士課程

石黒佑紀

CONTENTS

General Introduction

Overview

The raccoon (*Procyon loter*) is a member of Procyonidae belonging to Carnivora, which is a middle-sized mammal and skillfully use the forelimbs (Kamioka et al., 2017). The raccoon lives in various environments, especially prefer waterfront and is omnivore with a various diet such as insects, reptiles, crustaceans, birds, small mammals, fruits and crops (Ikeda et al., 2004).

The raccoon native to North America was introduced into Japan in 1970s and has been naturalized in almost every prefecture of Japan (Ikeda et al., 2004). In Hokkaido, Japan, its population has not decreased although the extermination of raccoons has been carried out since 1997. With their population increase, many problems such as predation of Japanese native species, eating damage to agricultural crops and increased risk of zoonosis, are caused by them (Ikeda et al., 2004; Koizumi et al., 2009; Oe et al., 2020). In Hokkaido, the concentrated capture of raccoons during the breeding season and subsequent suckling period (pregnant animals and mothers with cubs) is recommended for efficient population control. Therefore it needs to reveal the reproductive characteristics of raccoons in Japan.

Raccoons are considered seasonal breeders, although their breeding season varies from region to region. Gehert (2003) said that most of the raccoon mate during February to March in the many parts of North America. In Hokkaido also which is a prefecture located at the highest latitude in Japan, the mating season peaks in February (Asano et al., 2003). However, in the lower latitude of North America (Gehert, 2003) and Japan (Kato et al., 2009), raccoons tend to prolong the mating period as compared with the higher latitude. It has been reported that, moreover, in same region, some raccoons maintain the spermatogenesis in the non-breading season (Okuyama et al., 2014). Therefore, it seems that there are regional and individual differences in the seasonal breeding of raccoons, but it is not fully elucidated why such differences occur.

Seasonal breeding is a common reproductive style for wild animals at all latitude, and their breeding season is affected by environment such as photoperiod and foraging condition (Bronson, 2009). Environmental conditions are mainly reflected in blood sex hormone levels, which change with seasons and regulate reproductive functions. During the breeding season, the levels of blood sex hormone such as androgen or estrogen increase, and the cells which compose genital organs develop through the hormone receptors. On the other hand, during the non-breeding season, the blood sex hormone levels decrease and genital organs are regressed. In roe deer, testosterone showed high concentration during the breeding season, and the testosterone level plummeted after the breeding season (Goeritz et al., 2003). The blood testosterone level of Iberian moles decreased when testes were regressed (Dadhich et al., 2013). In the genital organs of raccoons, histological seasonal changes are partly known about testes (Kaneko et al., 2005; Okuyama et al., 2012; Okuyama et al., 2014) and ovaries (Sanderson and

Nalbandov, 1973) in adult, but largely unknown. In general, the genital organs undergo significant morphological changes with functional quiescent during the early postnatal development, and at onset of puberty, begin to develop toward sexual maturity, which means that individuals have a reproductive ability. In wild animals, the starting period and duration of puberty affects the number of breeding in life and the population growth and understanding the timing of sexual maturity is important for appropriate correspondence in breeding.

The following is known about the postnatal development of raccoons. Mated female raccoons stays pregnant for about 63 days and give birth to an average of 3-4 cubs (Gehert, 2003). Cubs are nursed until about 16 weeks of age, and juvenile raccoons become independent during autumn (Gehert, 2003). Raccoons reach sexual maturity at 10-12 months old in the North America (Sanderson and Nalbandov, 1973). While male raccoons reach sexual maturity at different times, and a few raccoons mature precociously (Okuyama et al., 2013). However, information on morphological changes in the raccoon genital organs with postnatal development, with seasonal change and during pregnancy is limited. In this study, therefore, morphological and functional changes were examined in the male genital organs, such as testes and prostate glands, during developmental and seasonal changes, and in female, morphological and functional dynamics of the uterus, especially cervix during pregnancy were investigated.

Objective of Studies

The main objectives of this study are to reveal the histological and functional dynamics of genital organs in raccoons during development and season.

To accomplish the objective, following points were investigated in raccoons:

Chapter 1. Developmental and seasonal changes in the testis of raccoons.

Chapter 2. Developmental and seasonal changes in the prostate gland of raccoons.

Chapter 3. Developmental changes in the prostatic utricle of raccoons.

Chapter 4. Morphological changes in the cervix of raccoons during pregnancy.

General Materials and Methods

Animals and treatments

The carcasses of 165 feral male raccoons and 46 feral female raccoons exterminated by the wildlife protection and population control services in the Tokachi area, Hokkaido, Japan, between May 2016 and April 2022 were obtained. The number and season of captured raccoons were shown in Table G.1. The animals were brought into the laboratory shortly after death and were dissected to examine male genital organs (testes with the epididymis and prostate glands) and female genital organs (uteri). For male, testes with the epididymis, prostate glands were immediately removed, and then the weight of the samples was measured. For female, uteri were immediately removed and were cut open. In non-pregnant, placental scars were checked. In the pregnant females, the crown-rump length (CRL) of the fetus was measured. The tissue samples were fixed in 10% formalin or Bouin's fluid. The samples were dehydrated in a graded series of ethanol, cleared in xylene, and embedded in paraffin. Samples were serially sectioned with a thickness of 4 μm for staining with hematoxylin-eosin (HE), periodic acid-Schiff (PAS), or alcian blue (AB) (pH 2.5) and immunohistochemistry (IHC).

Immunohistochemistry

The sections were deparaffinized and immunohistochemically stained using the avidin-biotin-peroxidase complex (ABC) method. The sections were treated using a high pH target retrieval solution (1:10, S3307; DakoCytomation, Inc., Carpinteria, CA, USA) and by microwaving for 20 min to retrieve antigenicity, and then immersed in methanol containing 0.3% H_2O_2 for 10 min at room temperature (RT) to block endogenous peroxidase activity, and incubated with normal goat serum (1:50, S-1000; Vector Laboratories, Burlingame, CA, USA) for 30 min at RT to prevent nonspecific staining. Then, the sections were incubated overnight with a monoclonal anti-vimentin antibody raised in the mouse (1:1, V9; Dako, Glostrup, Denmark), a polyclonal anti-cytochrome P450 side-chain cleavage enzyme (P450scc) antibody raised in the rabbit (1:200, AB1244; Chemicon International, Temecula, CA, USA), a monoclonal anti-p63 antibody raised in the mouse (1:50, ab735; Abcam, Temecula, CA, USA), a polyclonal anti-androgen receptor (AR) antibody raised in the rabbit (1:50, N-20; Santa Cruz Biotechnology, CA, USA) and a monoclonal anti-proliferating cell nuclear antigen (PCNA) antibody raised in the mouse (1:10, PC10; ICN Pharmaceuticals, Inc. CA, USA) at 4°C in a moisture chamber. After incubation with primary antibodies, biotinylated anti-rabbit IgG or anti-mouse IgG raised in the goat (1:200, BA-1000, BA-9200, respectively; Vector Laboratories, Inc.) was applied for 30 min, and then the sections were incubated with ABC reagent for 30 min (1:2, PK-6100, Vectastain Elite ABC Kit; Vector Laboratories). The binding sites were visualized with Tris-HCl buffer (pH 7.4) containing 0.02% 3,3'-diaminobenzidine hydrochloride and 0.006% H_2O_2. After incubation, the sections were washed

with 0.01 M PBS (pH 7.4), dehydrated in a graded series of ethanol, cleared in xylene, coverslipped, and observed under a conventional light microscope. The negative control sections were treated with normal goat serum instead of primary antibodies.

Age determination

In both of male and female raccoons, their heads were collected at dissection and cranial specimens were prepared, and then I examined the closure of root foramina (Grau et al., 1970), the tooth eruption (Montgomery, 1964) and the obliteration of cranial sutures (Junge and Hoffmeister, 1979) to determine the ages (Table G.2). As results, the ages of raccoons were categorized as 1, 2, 3, 4, 5, 6, 8, 10, 12 and over 12 months of age.

Table G.1. Number of captured feral raccoons in this study

month	sex	
	male	female
January	1	0
February	4	1
March	8	8
April	12	6
May	27	8
June	43	7
July	21	6
August	19	1
September	11	4
October	12	3
Nobember	6	2
December	1	0
Total	165	46

Table G.2. Estimated age of captured feral raccoons in this study

month	sex	
	male	female
1 month	1	0
2 month	5	0
3 month	12	0
4 month	5	0
5 month	6	0
6 month	15	5
8 month	5	0
10 month	14	1
12 month	14	0
over 12 month	88	40
Total	165	46

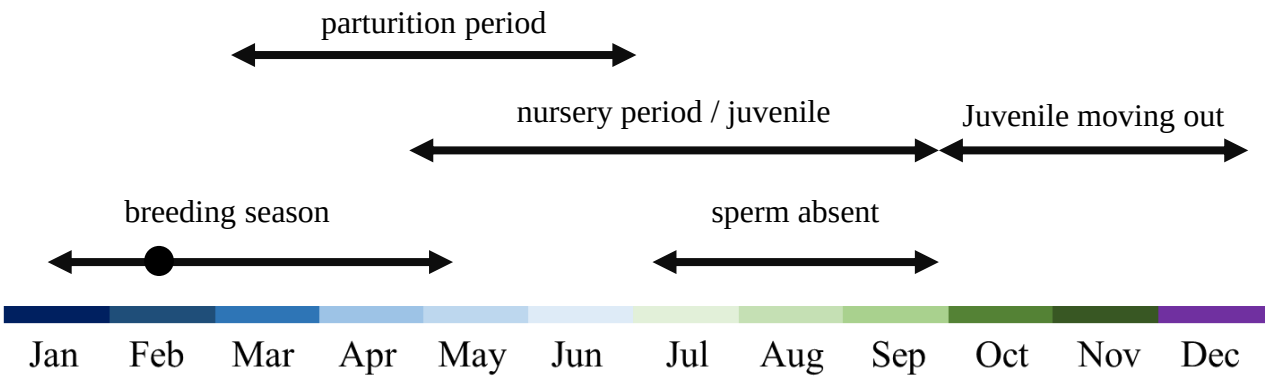

Fig. G.1. Seasonal cycle of raccoon breeding.
Breeding season and parturition period were based on the report in Illinois (Sanderson and Nalbandov, 1973). Nursery period and moving out timing were based on the review report (Gehrt, 2003). Sperm absent period was based on the report in Hokkaido (Okuyama et al., 2014). Black circle indicates peak of mating.

Chapter 1
Developmental and Seasonal Changes in the Testis of Raccoons

1.1 Introduction

Testes have two main functions such as spermatogenesis and hormone production, especially testosterone, which is one of the androgens, and in seasonal breeders, the testis is generally regulated with the seasonal change. During the breeding season, testicular functions are most activated, and spermatogenesis and testosterone production are at their peak. Whereas, during the non-breeding season, testes regress and testosterone levels drop. The degree to which the testes regress varies from species to species. For example, during the non-breeding season, horses produce less sperm (Johnson and Tatum, 1989), and hedgehogs (Massoud et al., 2018) and raccoon dogs (Qiang et al., 2003) keep spermatogenic cells up to spermatocytes and spermatogonia, respectively. Raccoons also have a testicular regression period of 3-4 months in North America (Sanderson and Nalbandov, 1973) and in Japan (Kaneko et al., 2005; Okuyama et al., 2012). In the same region, however, some raccoons maintained spermatogenesis in the non-breeding season, and it is suggested that aromatase expression may be involved in the maintenance of spermatogenesis in a testicular regression period (Okuyama et al., 2014).

Sexual maturity means that individuals have the reproductive ability, and sexually matured males can impregnate females by mating. Puberty is the growth period until sexual maturity is completed, and puberty animals grow until they are the same body size and reproductive condition as adult. During puberty, therefore, spermatogenesis in testes begins and completes. The timing of sexual maturation in Hokkaido raccoons has already been reported (Okuyama et al., 2013), but the histological progression of spermatogenesis during postnatal development has not been elucidated. The mechanisms for testicular completion during sexual maturation may be similar to those for relapse from regression testes during seasonal changes in adults. To understand spermatogenic features in the raccoon testes, it is necessary to compare the process of sexual maturation and the relapse from seasonal regression. However, the detailed examinations to understand histological testicular features during sexual maturation and seasonal changes have not yet been reported in raccoons.

In the Chapter 1, the aim is to reveal the histological characteristics in the raccoon testes during sexual maturation and during seasonal changes.

1.2 Materials and Methods

Testes and epididymides of 165 feral male raccoons from 1 month to over 12 months of age were used in this study. Sexual maturity was determined based on the progress of spermatogenesis (presence of elongated spermatids) in the testis and the presence of spermatozoa in the cauda epididymis. In June-

August of over 12 months, many regressed testes appeared (Table 1.1). Therefore, this period is defined as spermatogenetic-declined season. For analysis of seasonal changes, only adult raccoon testes were investigated, and the testes of all stage were examined for understanding testicular development.

Animals and sample preparation are described in the General Materials and Methods. Histological sections of testes were stained with HE. The immunostaining for vimentin, P450scc and PCNA was carried out.

In the Chapter 1, testes in various ages were used for histological observation (n=165) (Table G2). The diameter of seminiferous tubules was measured in formalin-fixed samples which testes weight was known (n=73). The breakdown of the 73 raccoons was 33 non-adults and 40 adults. The measurements of the diameter were performed on at least 20 seminiferous tubules in 3 random fields. Measurements were taken on seminiferous tubules that are nearly circular, minor and major axes were measured in one seminiferous tubule, and the diameter average of two axes was treated as the diameter for one seminiferous tubule. Then, the average of all values of the seminiferous tubules was used as the diameter for one testis. In this study, the left testis was adopted for the testis weight.

1.3 Results

Histological and immunohistochemical observations of testes during seasonal changes

The condition which the elongated spermatids were formed in the testes, and spermatozoa existed in the cauda epididymis, was defined as developed testes (Fig. 1.1A, C). Developed testes were observed through all season except January in which samples were not corrected (Table 1). The condition which the elongated spermatids were not formed in the testes, and/or spermatozoa were absent in the cauda epididymis, was defined as regressed testes (Fig. 1.1B, D). Twenty four regressed testes were observed only in end of May to September (Table 1). In this study, 3 months from June to August was defined as the spermatogenetic-declined season because most of the regressed testes were observed in this period and the percentage of presence of regressed testes was 49% (20/41) (Table 1).

In all regressed testes, most advanced germ cells were mostly round spermatids (19/24) and some primary spermatocytes (5/24). In the seminiferous tubules of the regressed testes, the detachment of germ cells, multinucleated giant cells, and sperm accumulation at the base of the seminiferous tubules were observed. The detachment of germ cells was observed in the seminiferous tubules of all regressed testes (Fig. 1.2A). Multinucleated giant cells were observed in the seminiferous tubule of 64% regressed testes (16/24) (Fig. 1.2B). Sperm accumulation at the basal area of the seminiferous tubules were observed in 68% regressed testes (17/24) (Fig. 1.2C).

Some spermatogonia and spermatocytes were PCNA-positive not only in the developed testes in the breeding season (spring) (Fig. 1.3A), but also in the developed (Fig. 1.3B) and regressed testes (Fig.

1.3C) in the spermatogenetic-declined season. Leydig cells showed more PCNA-positive in the breeding season (spring) than in the spermatogenetic-declined season (summer) (Fig. 1.3). In the spermatogenetic-declined season, the developed testes had a few PCNA-positive Leydig cells (Fig. 1.3B), while the regressed testes had few positive Leydig cells (Fig. 1.3C).

In the developed testes, vimentin in Sertoli cells was elongated towards the lumen of seminiferous tubule and detected around the nucleus (Fig. 1.4A). In the regressed testes, vimentin in Sertoli cells showed the same distribution as the developed testes regardless of the germ cell shedding (Fig. 1.4B).

The developed testes in the breeding season had larger interstitial region with P450scc immunoreactivity as compared with the regressed and developed testes in the spermatogenetic-declined season (Fig. 1.5A-C). In size, Leydig cells were larger in the breeding season than in the spermatogenetic-declined season (Fig. 1.5D-E).

The seasonal changes of diameter of the seminiferous tubules in 40 adult raccoons were shown in the Figure 1.6. Seminiferous tubules in the regressed testes were smaller than those in the developed testes. In the spermatogenetic-declined season, the diameter of the seminiferous tubules in the developed testes also decreased compared to those in other season (Fig. 1.6).

The testis weight was lighter in the regressed testes than in the developed testes, and the testis weight in the developed testes also decreased in spermatogenetic-declined season (Fig. 1.7). Testis weight tends to be higher in the seasons from January to April than in other seasons (Fig. 1.7).

Histological and immunohistochemical observations of testes during postnatal development

The gonocytes was observed within the seminiferous tubules at all raccoons until 4 months old inclusive (Figs. 1.8A and 1.9). From 5 months old, primary spermatocytes began to appear, although gonocytes still occupy half of spermatogenic cells, and the seminiferous tubules became to form the lumen around 6 months age (Figs. 1.8B, C and 1.9). Between 6 months and 10 months old, the spermatogenesis progressed, and round and elongated spermatids began to appear in the most testes (Figs. 1.8D, and 1.9), moreover, a few precocious raccoons (3/34) reached sexual maturity during this period (Fig. 1.9). Precocious raccoons were observed before or during the first half of spermatogenetic-declined season (June-August) (Fig. 1.10). In 12 months old, elongated spermatid were formed in more than half of the raccoons, and in most of them, sperms were not yet observed in the cauda epididymis (Figs. 1.8E, F, and 1.9). Over 12 months of age, all raccoons reached sexual maturity (presence of elongated spermatids and of spermatozoa in the cauda epididymis) and became to show the seasonal changes (Figs. 1.1, 1.6, and 1.7).

In early development, up to 5 months of age, vimentin expression of Sertoli cells was present only beneath the nucleus (Fig. 1.11A). Vimentin in Sertoli cells was seen beneath the nucleus and in the

perinuclear area when primary spermatocytes were present, and the seminiferous tubules were not canalized (Fig. 1.11B). With the formation of the lumen, vimentin expression in Sertoli cells extended toward the lumen (Fig. 1.11C). Vimentin expression in Sertoli cells was similarly elongated when the most advanced germ cells were round spermatids (Fig. 1.11D). In the seminiferous tubules with elongated spermatids in the developing testes, vimentin expression in Sertoli cells was elongated as those in adults (Fig. 1.11E, F).

In the intestinal tissue of the developing testis, the cytoplasm of Leydig cells was consistently positive for P450scc, and P450scc-posotive Leydig cells increased with development (Fig. 1.12).

The relationship between seminiferous tubule diameter and age, and between testis weight and age, is shown in the Figures 1.13 and 1.14, respectively. The seminiferous tubule diameter and testis weight tended to increase although each data varied from 6 months of age. The relationship among seminiferous tubule diameter, testis weight and the most advanced germ cells is shown in the Figure 1.15. The seminiferous tubule diameter increased with increasing of the testis weight, and spermatogenesis was more advanced in testes with heavier testis weights and larger seminiferous tubule diameters.

1.4 Discussion

Histological and immunohistochemical observation of testes in seasonal change

Testes of seasonal breeders often regress during the non-breeding season, and regressed testes no longer continue spermatogenesis, resulting in lower fertility. Extent of its regression varies by species. There are three cases of degrees of regression in seasonal breeders: Case 1, the amount of sperm decreases; Case 2, primary spermatocytes, spermatogonia and Sertoli cells remain; Case 3, spermatogonia and Sertoli cells remain. The species with Case 1 include sheep (Hochereau-de Reviers et al., 1985) and horses (Johnson and Tatum, 1989). The species with Case 2 include northern fur seals (Tsubota et al., 2001), brown hares (Štrbenc et al., 2003), Egyptian long-eared hedgehogs (Massoud et al., 2018), Syrian hamsters (Seco-Rovira et al., 2015) and Daurian ground squirrels (Li et al., 2015). The species with Case 3 include roe deer (Klonisch et al., 2006), black bears (Komatsu et al., 1997), raccoon dogs (Qiang et al., 2003) and cacomistles (Poglayen-Neuwall and Shively, 1991). In this study, most of the regressed testes of raccoons had round spermatids remaining, but some raccoon testes regressed to primary spermatocytes. Previous reports in the raccoons inhabiting Hokkaido do not contradict this (Kaneko et al., 2005; Okuyama et al., 2012). It is thought that observed differences in the extent of germ cell regression may reflect the length and intensity of regression.

Characteristics of regressed testes in raccoons were sperm accumulation at the basal area of the seminiferous tubules, detachment of germ cells and appearance of multinucleated giant cells. It has been reported that Sertoli cells phagocytize sperm that are not released due to defective sperm maturation

(Chatani and Kandori, 2017). It is thought that, therefore, the accumulating sperm is able to be phagocytized by Sertoli cells in the raccoon testes also. In the regressed testes of the Iberian mole, germ cell detachment precedes the contractions of seminiferous tubules (Dadhich et al., 2013). In raccoons as well, the detachment of germ cells occurred in all regressed testes, so it may be a phenomenon that always occurs during regression. The appearance of multinucleated giant cells was observed in the seminiferous tubules of various species: humans (Nistal et al., 1986), rabbits (Morton et al., 1986), dogs (Rehm, 2000; Goedken et al., 2008) and minipigs (Thuilliez et al., 2014). Such multinucleated giant cells are seen when the damage to the testis is mild to moderate (Morton et al., 1986). In addition, multinucleated giant cells are commonly found in pubertal animals before and after the blood–testis barrier (BTB) formation (Haruyama et al., 2012; Kangawa et al., 2016), and the formation of multinucleated giant cells is thought to be due to incomplete BTB formation. BTB isolates inner area (adluminal compartment) from outer area (basal compartment) in the seminiferous tubules, and protects spermatocytes and spermatids from the recognition by own antigens (Kaur et al., 2014). When the function of BTB is destroyed, germ cells from the primary spermatocytes are eliminated by the immune system (Morales et al., 2007). It has been demonstrated that in Djungarian hamsters, BTB becomes non-functional in photoperiods as the non-breeding season (Kliesch et al., 1991), and BTB disruption during the non-breeding season has also been reported in minks (Pelletier, 1986). In this study, direct proof was not possible, but similarly, it was suggested that the BTB was disrupted in the regressed testes of raccoons during the spermatogenetic-declined season.

In raccoons, since PCNA-positive germ cells were continuously observed in the seminiferous tubules throughout the year, therefore, spermatogenesis itself may not be stagnant even in the regressed testes. In the absence of functional BTB formation during the non-breeding season, primary spermatocytes and subsequent germ cells are subject to immunological elimination mechanisms (Morales et al., 2007). Several studies have so far examined the proliferative activity of germ cells during the non-breeding season (Štrbenc et al., 2003; Seco-Rovira et al., 2015; Massoud et al., 2018). In Egyptian long-eared hedgehogs, germ cell proliferative activity is not reduced even in regressing testes, and it is thought that meiotic progression does not stop even during regression in the non-breeding season (Massoud et al., 2018). Similarly, it was suggested that meiosis was not arrested in raccoons as well during the spermatogenetic-declined season, and then spermatocytes and subsequent germ cells may be affected by immunological elimination.

Immunostaining for vimentin was performed to observe the cytoskeletal dynamics of Sertoli cells in this study. Vimentin expression in raccoon Sertoli cells elongated toward the lumen of the seminiferous tubule and was often found in the upper part of the nucleus, and moreover, it was located under the nucleus of Sertoli cells also. This location of vimentin expression has been observed in mouse

deer (Sasaki et al., 2010). Vimentin below the nuclear of Sertoli cells in developed testes appears to be associated with the location of Sertoli cell nucleus. In the regressed testis, vimentin distribution of Sertoli cells in the seminiferous tubules, which remained to the primary spermatocytes, did not show major difference from that in the developed testis. Vimentin in Sertoli cells extending toward the lumen was maintained in the regressed raccoon testes. Similarly, expression of vimentin in the regressed testes was also examined in Japanese black bears, but it has been concluded that it does not change between developed and regressed (Komatsu et al., 1998). Vimentin in Sertoli cells is restored in experimentally regressed rat testes, dependent on germ cell regeneration (Kopecky et al., 2005). When spermatocytes reappear in the seminiferous tubules, vimentin in Sertoli cells reorganizes, and apical vimentin filaments were restored (Kopecky et al., 2005). The presence of primary spermatocytes in the regressing testes of raccoons may keep vimentin in Sertoli cells in an elongated state, similar to rats (Kopecky et al., 2005).

The interstitial area in the testes of raccoons was wider during the breeding season (spring), and narrower during the spermatogenetic-declined season (summer) regardless of situation of the spermatogenesis (in both of developed and regressed testes). In raccoons, Leydig cells were the largest in the breeding season and smaller in the spermatogenetic-declined season, and showed a lot of proliferative activity in the breeding season, but little proliferative activity was observed in the spermatogenetic-declined season. Seasonal changes in Leydig cells have also been reported in other seasonal breeders. In European hedgehogs, Leydig cells proliferate and enlarge during the breeding season compared to the non-breeding season (Dutourné and Sanboureau, 1983). In roe deer, number of Leydig cells and volume of interstitium increased in the breeding season, while decreased in the non-breeding season（Klonisch et al., 2006）. Similarly, in raccoons, Leydig cells proliferate and enlarged in the breeding season, and thus the area of the interstitium was widen.

Seminiferous tubule diameters of raccoons were greatly reduced in the regressed raccoon testes. It is thought that this is due to the shedding of many germ cells in the seminiferous tubules. At the same time, testicular weight is significantly reduced in the regressed testes. Similarly, previous studies have also confirmed reduced testis weight in raccoons associated with decrease in seminiferous tubule diameter and reduced spermatogenesis (Kaneko et al., 2005; Okuyama et al., 2012). The decrease in the testis weight during the non-breeding season have been reported in most seasonal breeders: cacomistles (Poglayen-Neuwall and Shively, 1991), roe deer (Blottner et al., 1996), Daurian ground squirrels (Li et al., 2015) and *Myotis levis* (Farias et al., 2020). Roe deer in the non-breeding showed regressive change in both the tubules and stroma of testes (Klonisch et al., 2006). In raccoons as well, it was suggested that the loss of germ cells within the seminiferous tubules and decrease in the number and size of Leydig cells in the spermatogenetic-declined season affected to the decrease in testicular weight.

Postnatal development in raccoon testes

Postnatal development of the testis is particularly well studied in laboratory animals as rats (Picut et al., 2015), dogs (Kawakami et al., 1991) and microminipigs (Kangawa et al., 2016). During postnatal development from birth to sexural maturity, gonocytes in the seminiferous tubules transform into spermatogonia, Sertoli cells mature to form BTBs, meiosis progresses, and round and elongated spermatids in the seminiferous tubules are formed (Picut et al., 2018). Presence of spermatids with final step and appearance of sperm in the epididymis signifies that sexual maturity has been reached (Picut et al., 2018). The above developmental processes are common in mammals, but the timing of those occurrence differs among species (Picut et al., 2018).

In raccoons, gonocytes were the predominant cell type until 4 months of age, decreased by half in 5 months of age and disappear in most raccoons by 6 months of age. The transition of gonocytes to spermatogonia may be less sensitive to environmental factors, as there was little difference of its timing among raccoons. Primary spermtocytes began to appear in some raccoons from 5 months of age. In dogs, only Sertoli cells and gonocytes are present in the seminiferous tubules at birth, primary spermatocytes begin to appear in dogs at 20 weeks of age, and gonocytes hardly became find over 20 weeks of age (Kawakami et al., 1991). Therefore, the timing of the disappearance of gonocytes and the appearance of primary spermatocytes in raccoons is similar to it in dogs.

In raccoons, the seminiferous tubules were not canalized at 5 months of age, and the seminiferous tubules of most raccoons began to be canalized at 6 months of age. This indicates that in raccoons, the seminiferous tubules were canalized after the emergence of primary spermatocytes. In rats, seminiferous tubules are canalized after the appearance of primary spermatocytes, and BTBs are formed along with luminal formation (Bergmann and Dierichs, 1983; Pelletier, 1986; Morales et al., 2007). In humans also, the appearance of primary spermatocytes precedes the formation of BTB (Picut et al., 2018). It may be assumed that the appearance of primary spermatocytes in raccoons precedes BTB formations like in humans and rats.

From 6 months of age, the seminiferous tubules in most raccoons were canalized, and the primary spermatocytes developed. In raccoons, spermatogenesis progressed with varying degrees between 6 and 10 months, including the appearance of round and elongated spermatids also. In dogs, round spermatids appear at 22 weeks of age, and elongated spermatids appear at 26 weeks of age (Kawakami et al., 1991). There were a few raccoons that already showed complete spermatogenesis (spermiogenesis) in the testis at 6 months of age and had sperm in the cauda epididymis in this study. Okuyama et al. (2013) reported that some individuals reach sexual maturity earlier than most other individuals, and are considered precocious individuals. Precocious raccoons may show roughly the same timing of the sexual maturity of dogs (35-40 weeks of age). However, during 6-10 months of age, the most advanced germ cells of

most raccoons remained primary spermatocytes or round spermatids.

At 12 months of age, in more than half of the raccoons, the most advanced germ cells were elongated spermatids, and all raccoons reached sexual maturity at over 12 months of age. It has been reported that raccoons reach sexual maturity at 10-12 months old in the North America (Sanderson and Nalbandov, 1973). In this study, all individuals reached sexual maturity at over 12 months of age in the breeding season (spring), although mature raccoon were partially recognized at 6, 10 and 12 months old. This difference in sexual maturity may be a regional factor. In this studies, I define under 6 months old as infantile, 6-12 months old as juvenile and over 12 months as adult. Dogs reach sexual maturity at 35-40 weeks of age (James and Heywood, 1979). Many raccoons seem to reach sexual maturity later than dogs although a few precocious individuals were present. The timing of the onset of spermatogenesis in raccoons approximately equal that in dogs, thus, raccoons may take longer than dogs to complete spermatogenesis basically.

Overlapping non-breeding periods during development may impede sexual maturation by the same mechanism that causes adult animal testes to regress. A few precocious raccoons reached sexual maturity already in the first breeding season, but most raccoons did not reach sexual maturity until after the non-breeding season. Similarly, testicular development in fawn roe deer is not activated until the maximum testicular regression period in adults, and then becomes inspired after the period (Blottner et al., 1996). In Djungarian hamsters, rearing with a day length during the non-breeding season delays sexual maturity (Hoffmann, 1978). In minks, the BTBs are formed at 8 months of age, and BTB disruption occurs during the non-breeding season in adult (Pelletier, 1986). In adult animals, BTB disruption occurs and affects spermatogenesis during the non-breeding season (Pelletier, 1986; Kliesch et al., 1991). Therefore, it is thought that the suspension of BTB formation or disruption of BTB can happen also in the developing testes during the non-breading season. Considering that the spermatogenesis unable to proceed beyond the pachytene primary spermatocyte when the BTB is incomplete, the reason why raccoons have longer immature period as compared with dogs without non-breeding season, may be the presence of spermatogenetic-declined season during the developing period.

In raccoon Sertoli cells, vimentin expression has been localized only under a nucleus up to 5 months. In immature rats (Zhu et al., 1997; Weider et al., 2011) and bulls (Devkota et al., 2006) also, vimentin expression was observed under the nucleus of Sertoli cells. Thus, this state of vimentin expression in immature testes may be common across animals. In raccoons, primary spermatocytes appeared before the canalization of the seminiferous tubules, and vimentin expression was localized on basal and perinuclear area at the early appearance of primary spermatocytes without lumen. After canalization, on the other hand, vimentin expression in Sertoli cells was elongated from the basal to supranuclear area and extended among primary spermatocytes. In the later postnatal development, vimentin expression in

Sertoli cells remains elongated toward the lumen as spermatogenesis progresses, and this distribution of the vimentin was the same in adult testes regardless of developed and regressed. Similar distributional changes of vimentin during the postnatal development were also reported in rats (Zhu et al., 1997). In the postnatal development of raccoon testes, therefore, not only the presence of primary spermatocytes but also canalization of the seminiferous tubules may be essential for apical extension of vimentin.

P450scc was expressed in Leydig cells in all raccoons examined during the postnatal development. P450scc is a steroidogenic enzyme which is involved in the early stage of steroidogenesis; conversion of cholesterol to pregnenolone. In humans and rats, the fetal testes have already started producing testosterone, however, testosterone concentration remains low until puberty (Picut et al., 2018). Sika deer also express P450scc in Leydig cells throughout the postnatal development (Hayakawa et al., 2010). In microminipigs, P450scc remained positive in Leydig cells throughout the postnatal development, and testosterone production continued to increase throughout this period. (Kangawa et al., 2019). In raccoons, the interstitial area with P450scc immunoreactivity increased with testicular development, therefore, the concentration of testosterone suggests to increase with the development. To clarify this, it is necessary to actually measure the amount of circulating testosterone.

In raccoons, during the postnatal development, the seminiferous tubule diameter and testis weight tended to increase, and both values showed a plateau in the developed testes after sexual maturation (over 12 months) although seasonal change occurred. In rats (Kormano and Hovatta, 1972) and peccaries (Costa et al., 2019), the seminiferous tubule diameter and testicular weight increases as they grow. Similar to these animals, raccoons also seem to undergo simultaneous increases in the seminiferous tubule diameter and the testis weight as they grow. In the seminiferous tubule diameter and the testis weight, the individual variation began to appear from 6 months old. In raccoons, the canalization of the seminiferous tubules occurred and various stages of spermatogenesis were observed from 6 months. In this study, the seminiferous tubule diameter, the testis weight and spermatogenic situation (most advanced germ cell) were revealed. It is thought that, therefore, the scattering may be attributed to individual difference in the progression of spermatogenesis.

In conclusion, raccoon testes had both seasonal and developmental changes. In the regressed testes, the ability of germ cell proliferation was maintained, meaning that germ cells shedding is associated with testicular regression in the spermatogenetic-declined season (June-August), and the loss of germ cells and decrease in the number and size of Leydig cells affected to the decrease in testicular weight. In the postnatal testicular development, the canalization of the testes began at 6 months of age and changed the distributional pattern of vimentin in Sertoli cells, and this pattern was maintained in adult also despite developed and regressed.

Table 1.1. The sperm existence and conditions during the year

Sperm existence / spermatogenic condition	Jan.	Feb.	Mar.	Apr.	May	Jun.	Jul.	Aug.	Sep.	Oct.	Nob.	Dec.
developed testes present/elongated	n	3	6	8	15	13	4	4	5	3	2	1
regressed testes	n	0	0	0	3	7	7	6	1	0	0	0
present/no elongated*	n	0	0	0	1	0	1	0	0	0	0	0
no sperm/elongated*	n	0	0	0	0	0	0	0	0	0	0	0
no sperm/no elongated*	n	0	0	0	2	7	6	6	1	0	0	0

elongated, elongated spermatids were present.

no elongated, elongated spermatids were not present.

*: breakdown of regressed testes

n, not corrected.

June-August was defined as spermatogenetic-declined season.

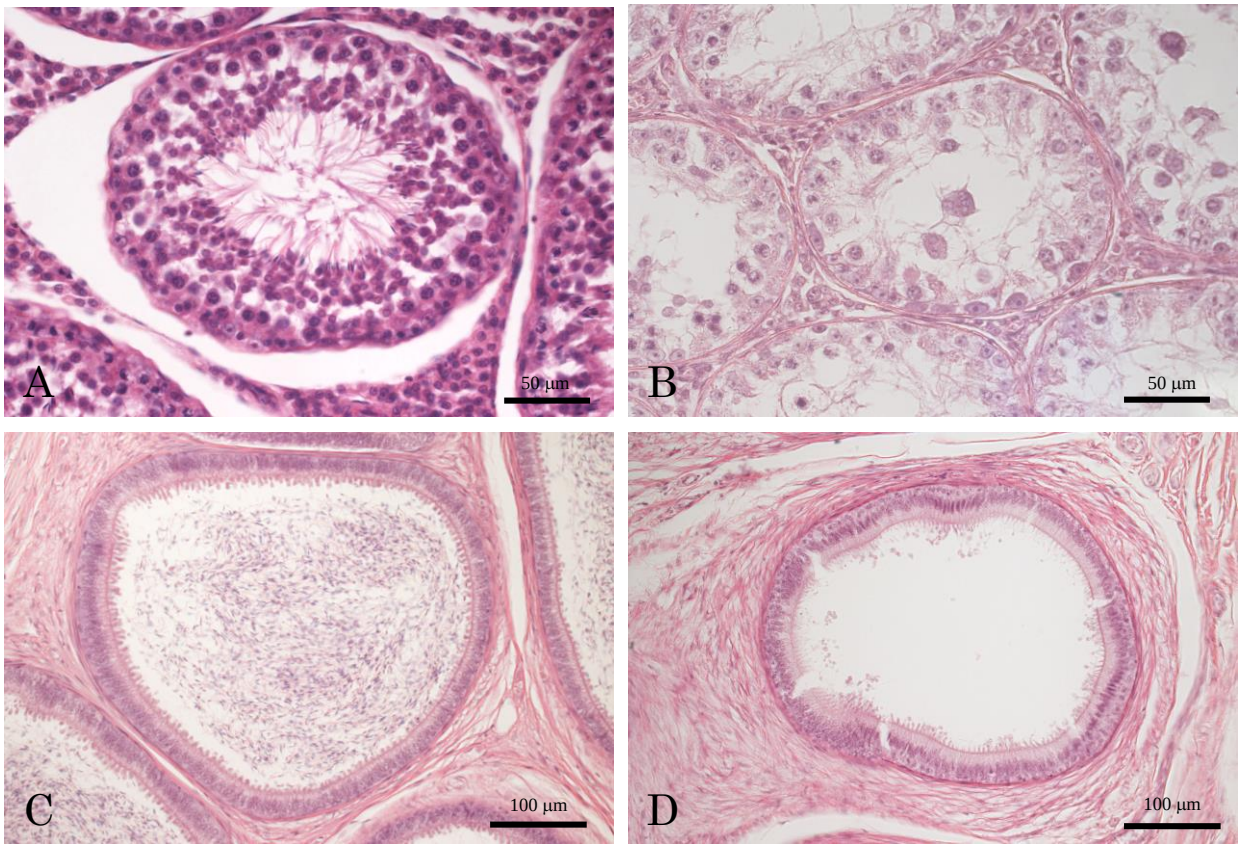

Fig. 1.1. Histological aspects of the developed and regressed testes and sperm existence in the cauda epididymis. (A) Developed testes. (B) Regressed testes. (C) Cauda epididymis with the developed testes stage. Many spermatozoa were observed. (D) Cauda epididymis with the regressed testes stage. HE staining.

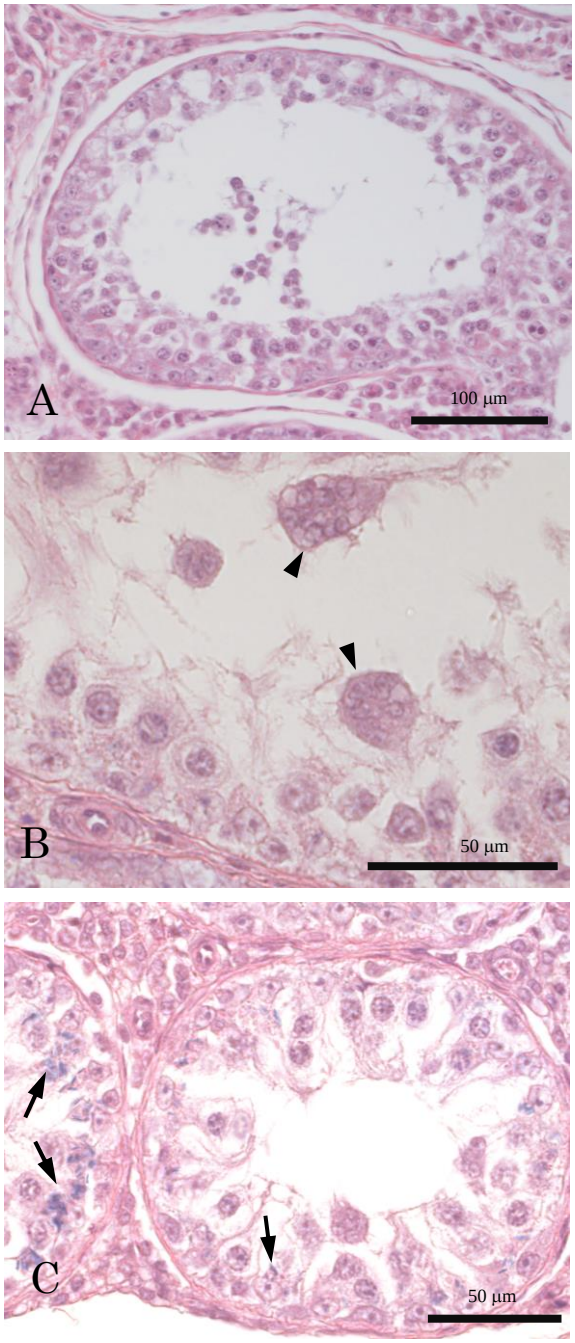

Fig. 1.2. Histological aspects of the seminiferous tubules in the regressed testes. (A) Detachment of germ cells. (B) Appearance of multinucleated giant cells (arrowheads). (C) Spermatozoa located at the basal area (arrows). HE staining.

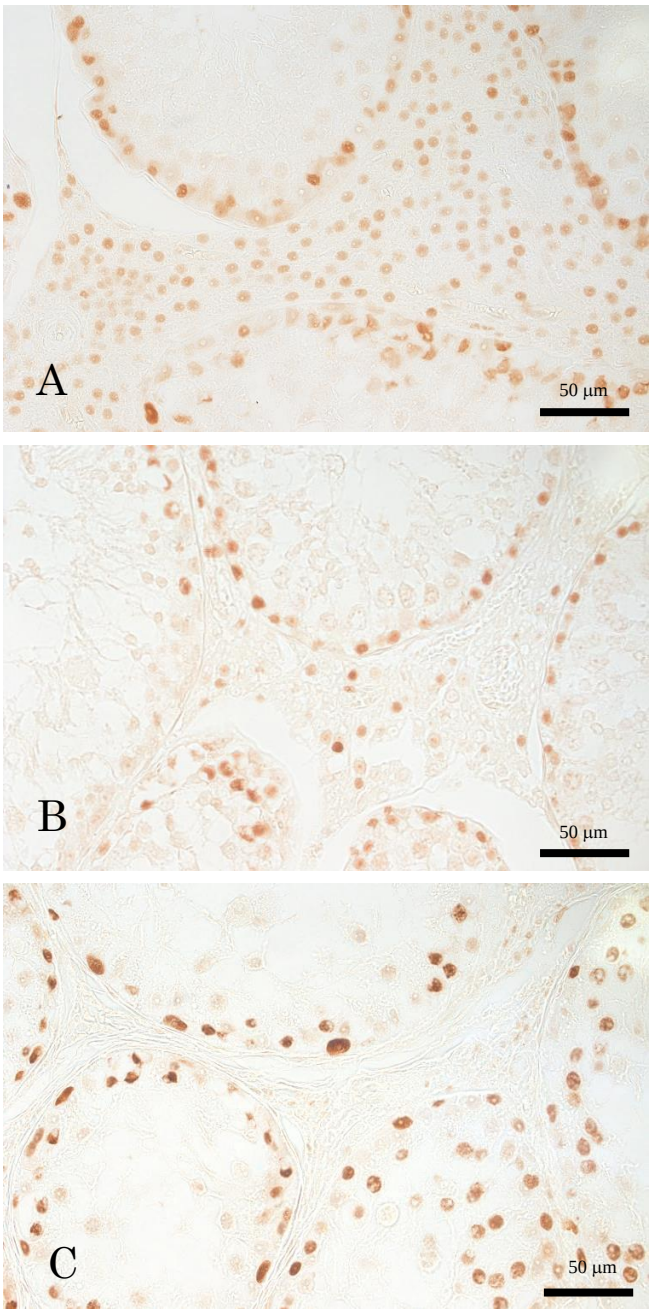

Fig. 1.3. Immunoreactivity for PCNA. (A) Seminiferous tubules with elongated spermatids (developed testis) in the breeding season. Most of Leydig cells showed PCNA-positive reaction. (B) Seminiferous tubules with elongated spermatids (developed testis) in the spermatogenetic-declined season. (C) Seminiferous tubules with no elongated spermatids (regressed testis) in the spermatogenetic-declined season.

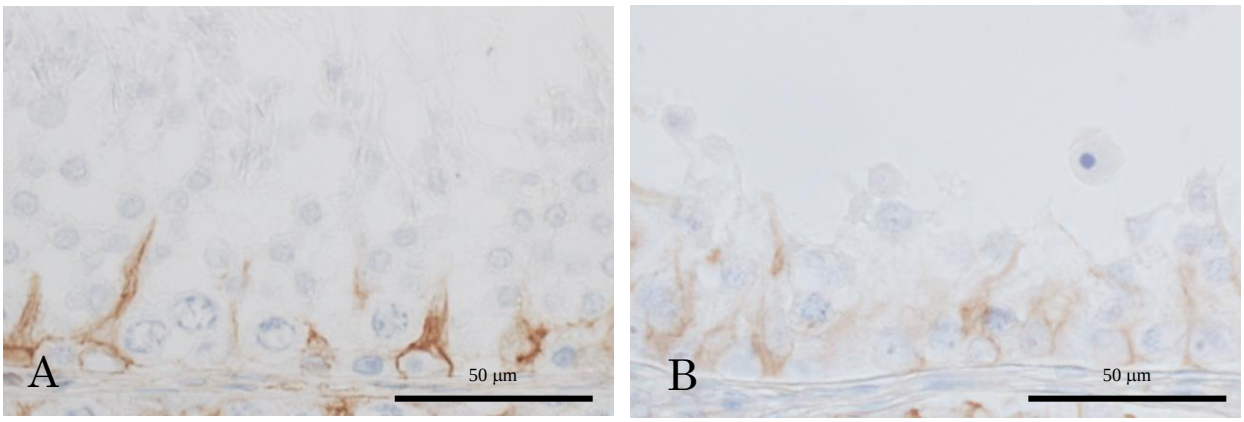

Fig. 1.4. Immunoreactivity for vimentin. (A) Developed testes in the breeding season. (B) Regressed testes in the spermatogenetic-declined season.

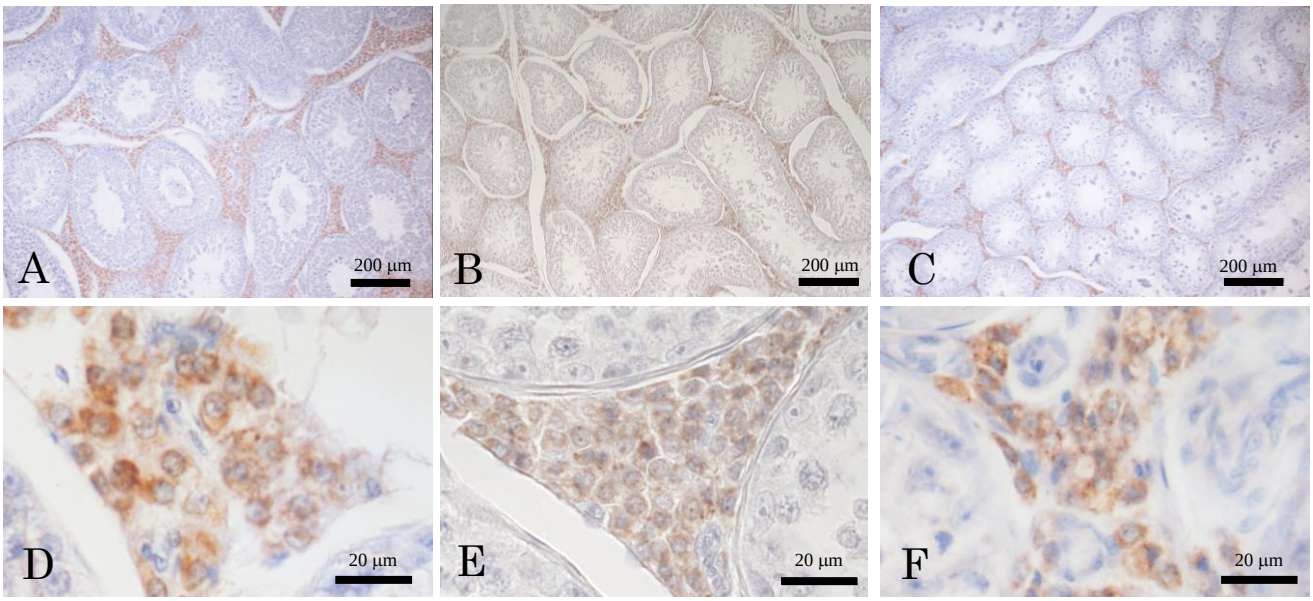

Fig. 1.5. Immunoreactivity for P450scc in the adult testes. (A) Seminiferous tubules with elongated spermatids (developed testis) in the breeding season. (B) Seminiferous tubules with elongated spermatids (developed testis) in the spermatogenetic-declined season. (C) Seminiferous tubules with no elongated spermatids (regressed testis) in the spermatogenetic-declined season. (D), (E) and (F) are enlarged views of Leydig cells in (A), (B) and (C), respectively.

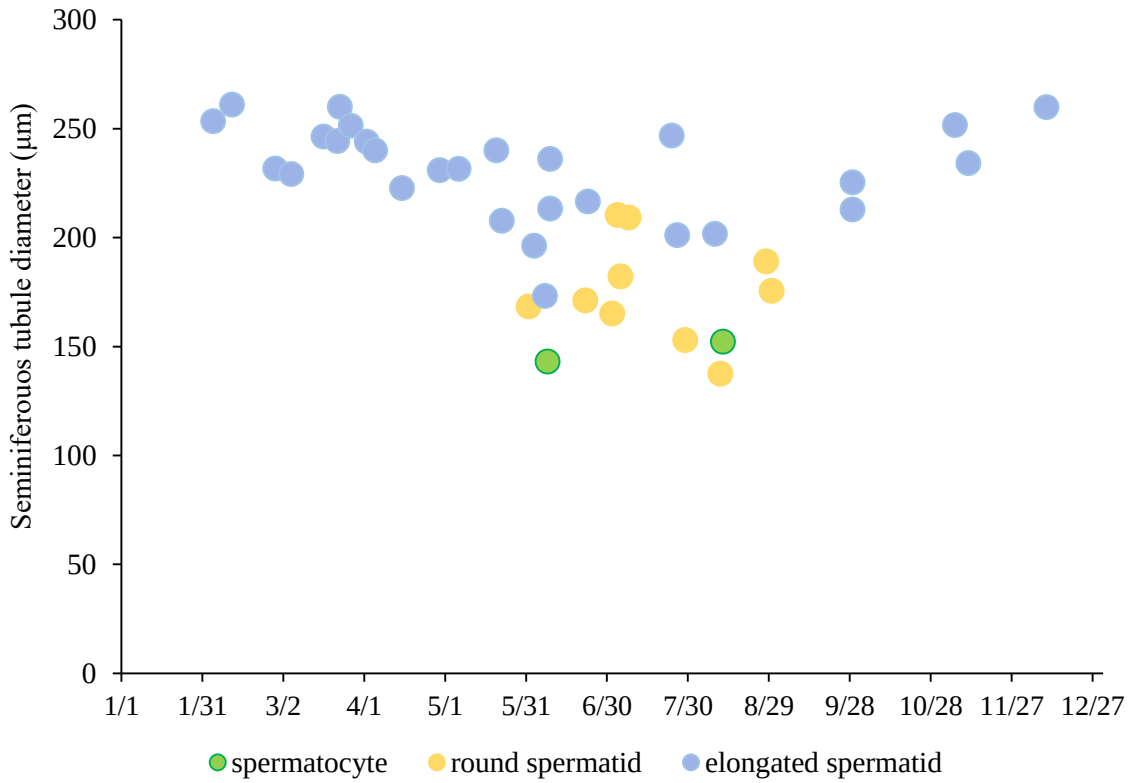

Fig. 1.6. Most advanced germ cells in adult testis during year. The horizontal axis indicates the month, and the vertical axis indicates the seminiferous tubule diameter. One plot represents the status of the seminiferous tubules of one raccoon. Between June and August was spermatogenetic-declined season.

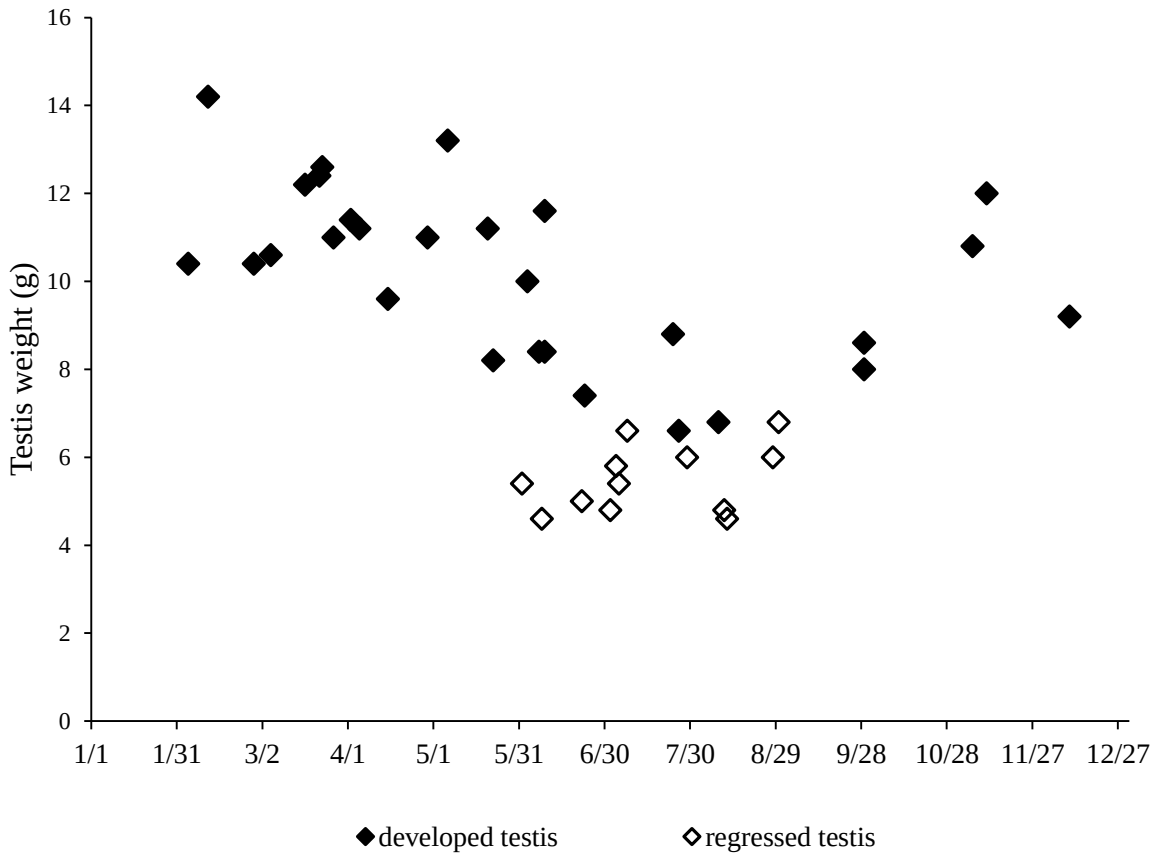

Fig. 1.7. Testicular weight during year. The horizontal axis indicates the month, and the vertical axis indicates the testis weight. One plot represents the status of the seminiferous tubules of one raccoon.

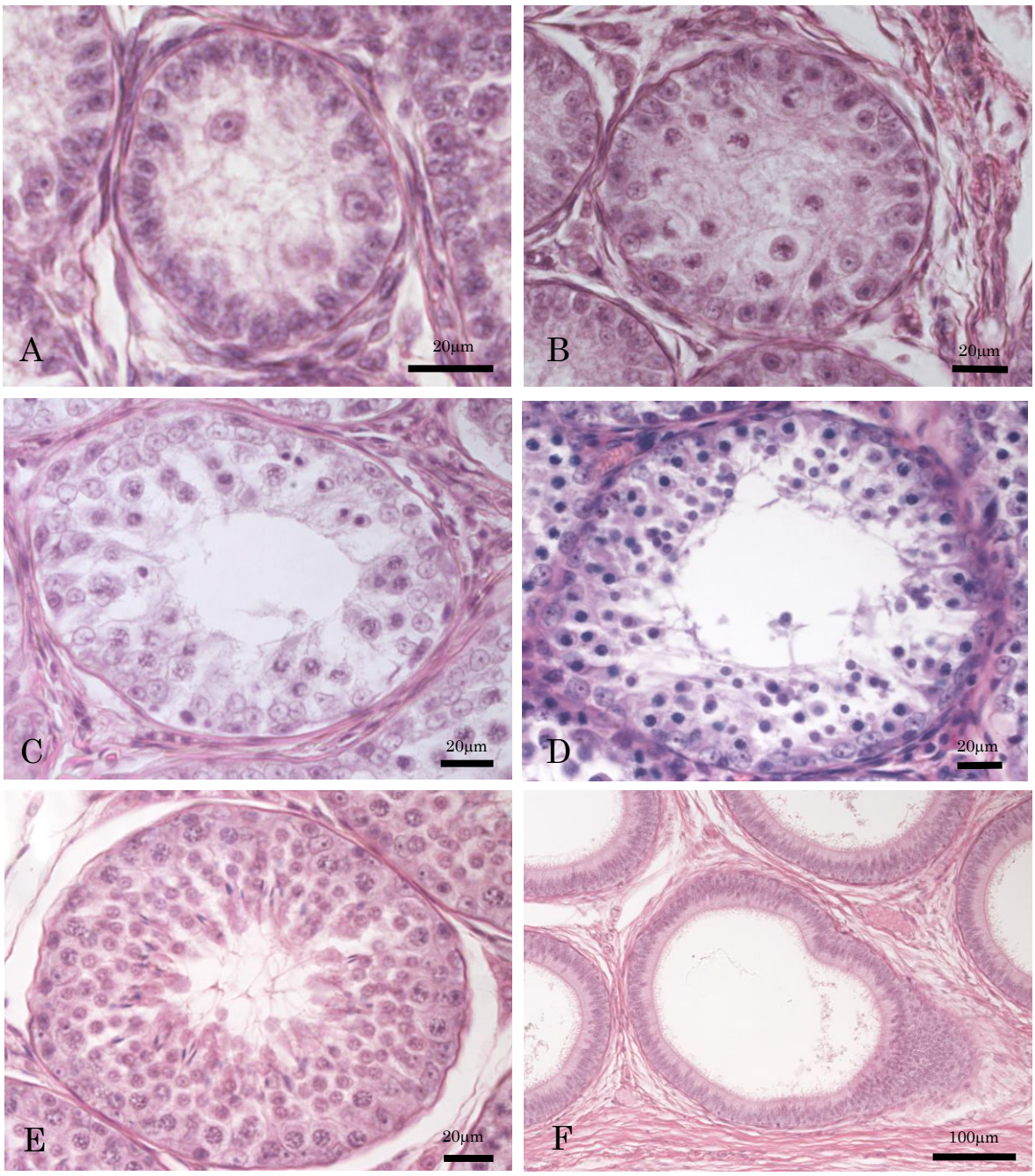

Fig. 1.8. Seminiferous tubules during postnatal development. (A) 2 months old testis. (B) 5 months old. (C) 6 months old. (D) 10 months old without elongated spermatids. (E) 12 months old testis with elongated spermatids. (F) Cauda epididymis in the individual same as E. HE staining.

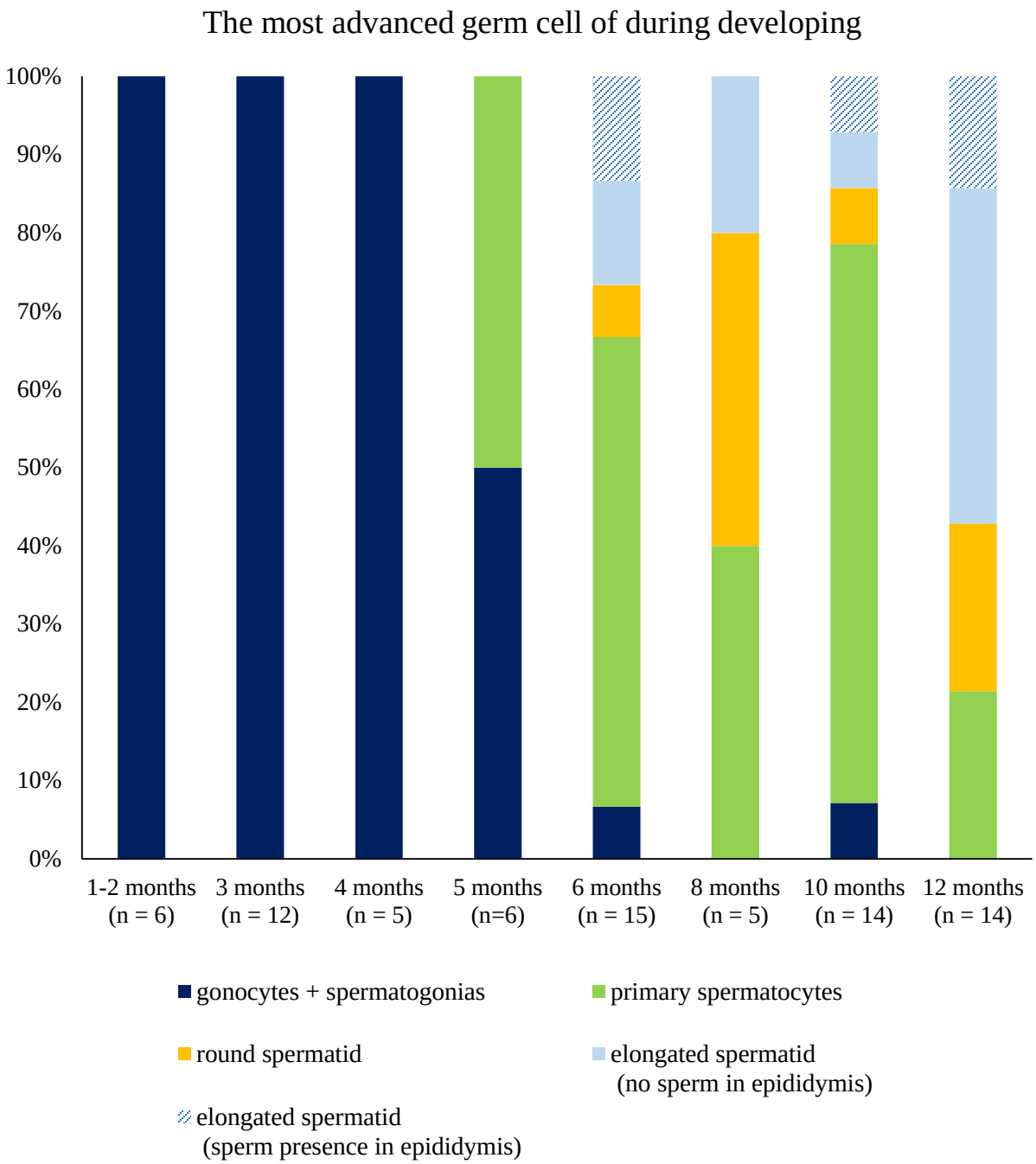

Fig. 1.9. Percentage of most advanced germ cell in raccoons at each age group.

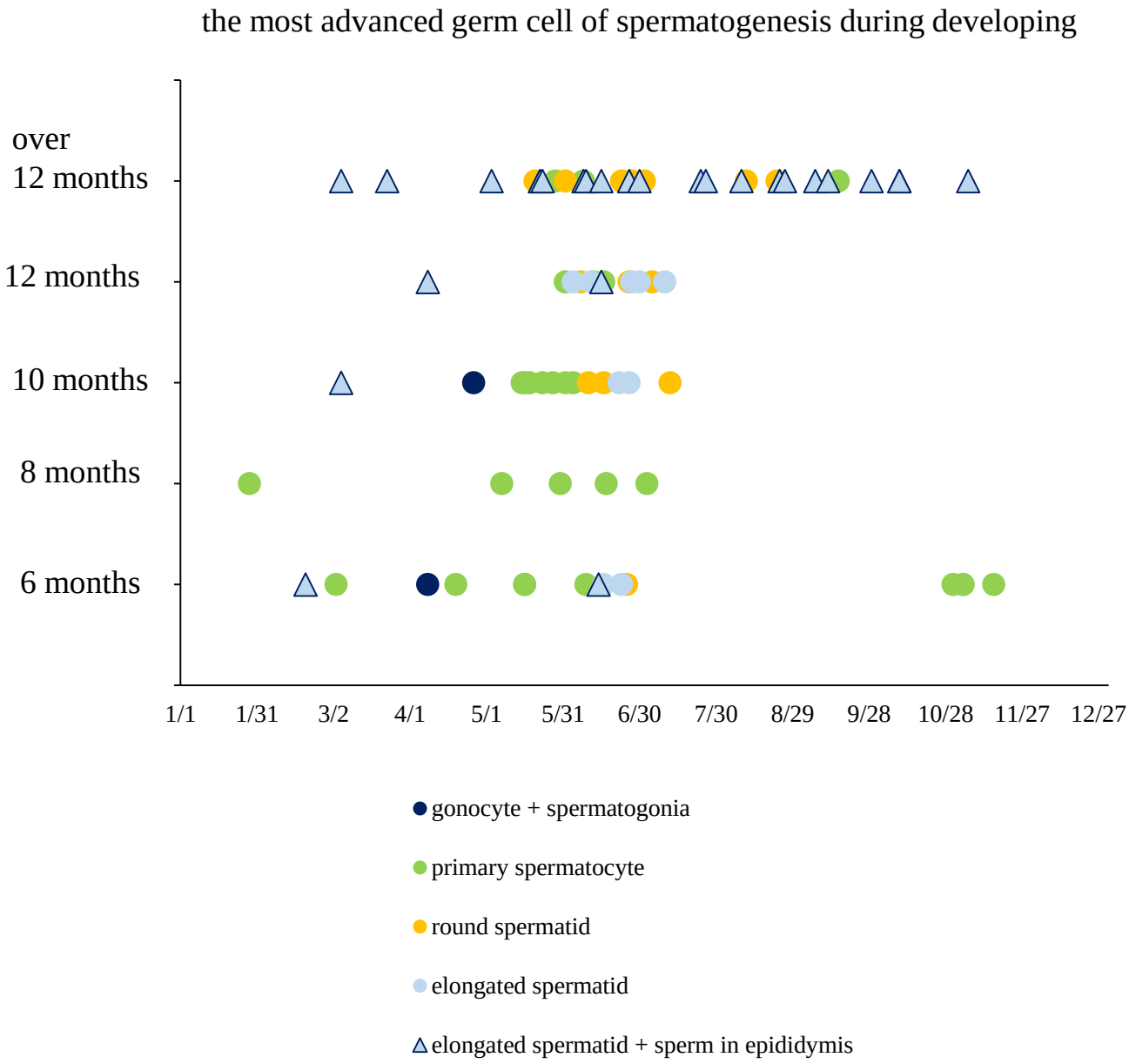

Fig. 1.10. The most advanced germ cell of spermatogenesis during postnatal developing through year. The horizontal axis indicates the month, and the vertical axis indicates age. One plot represents the status of the seminiferous tubules of one raccoon. Each color indicates the most advanced germ cell type in seminiferous tubule, and circular plots indicating no sperm in the cauda epididymis and triangular plots indicating the presence of sperm in the cauda epididymis.

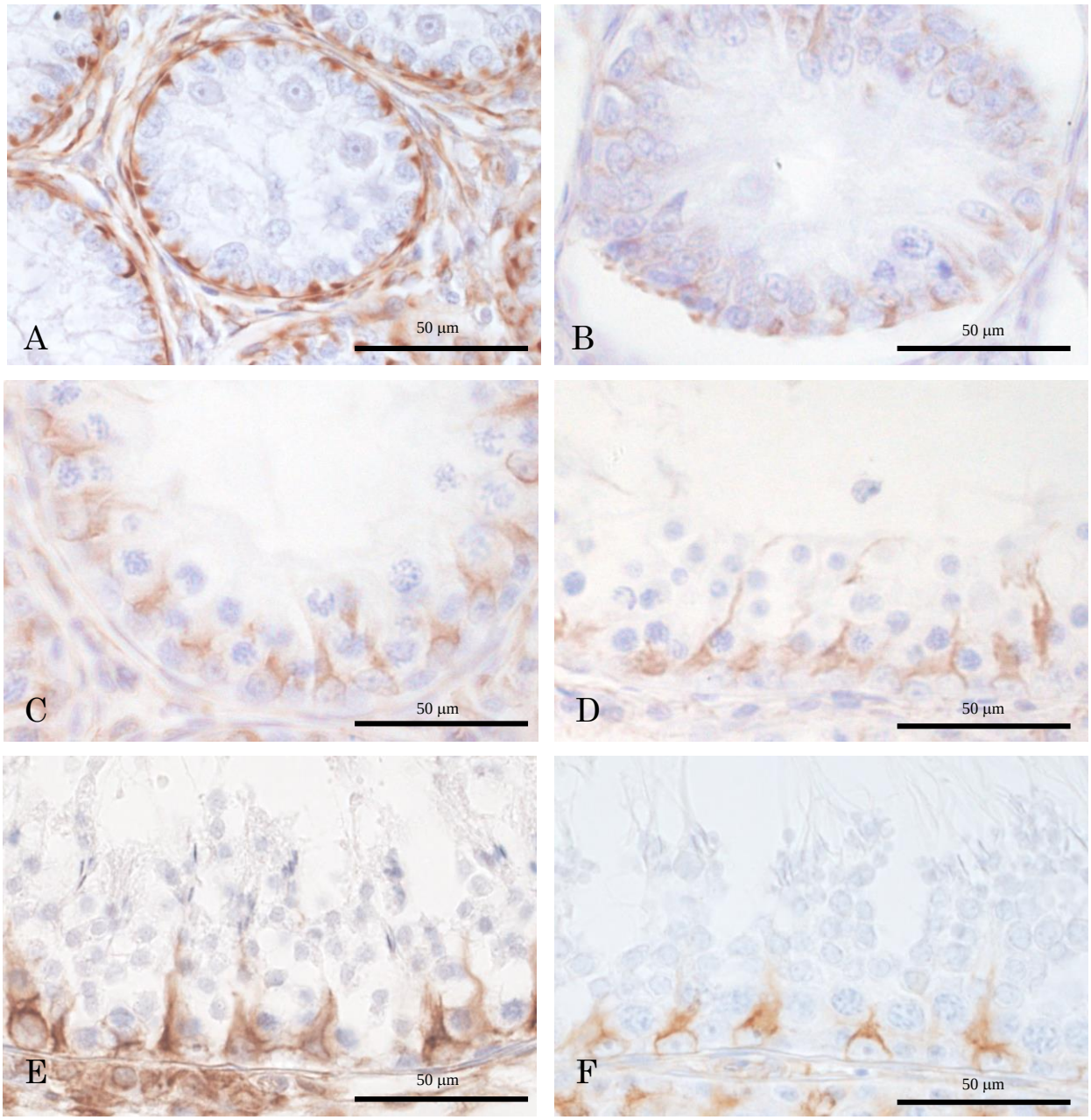

Fig. 1.11. Immunoreactivity for vimentin in the seminiferous tubules during postnatal development. (A) Testis of 3 months old. (B) 6 months old. (C)10 months old. (D)12 months old. (E) 12 month. (F) Adult.

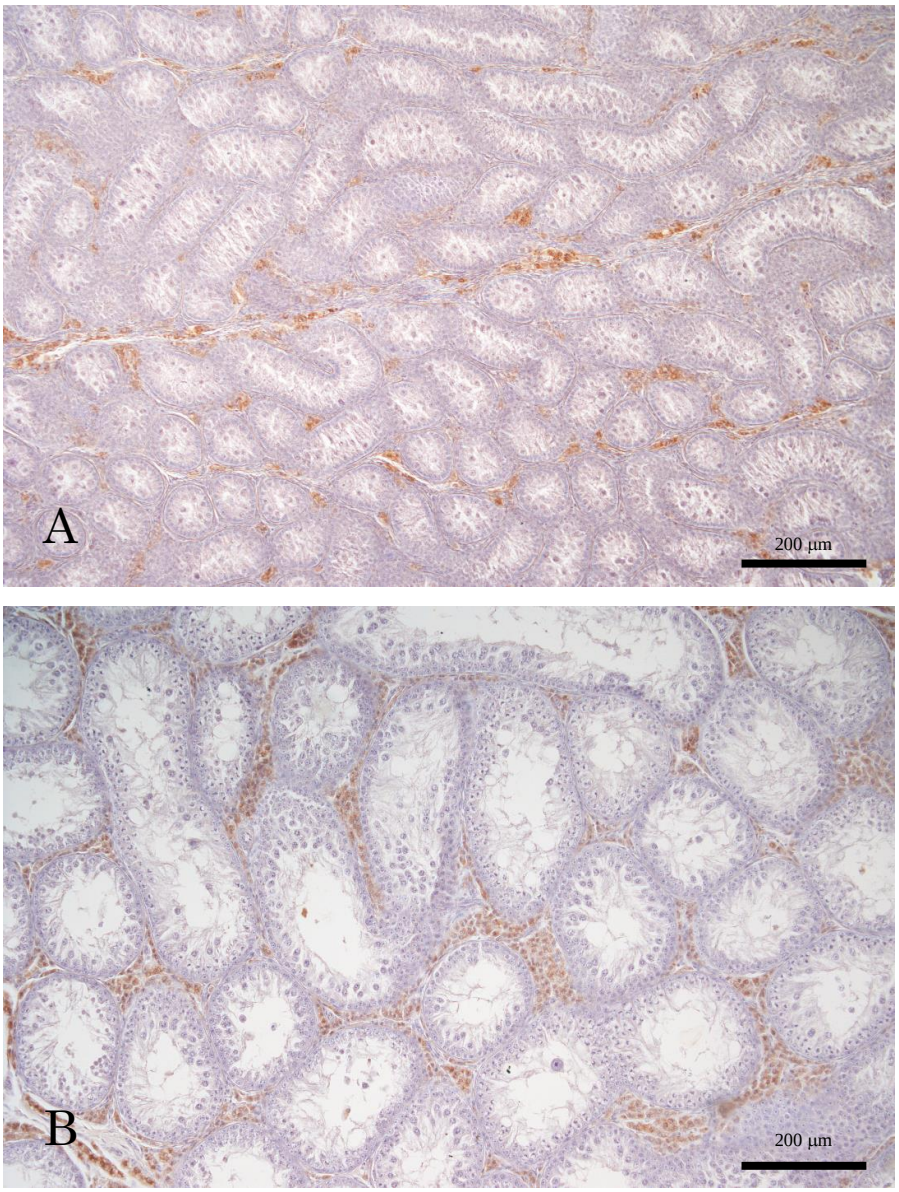

Fig. 1.12. Immunoreactivity for P450scc in the developing testes. (A) Testis of 4 months old. (B) 10 months old.

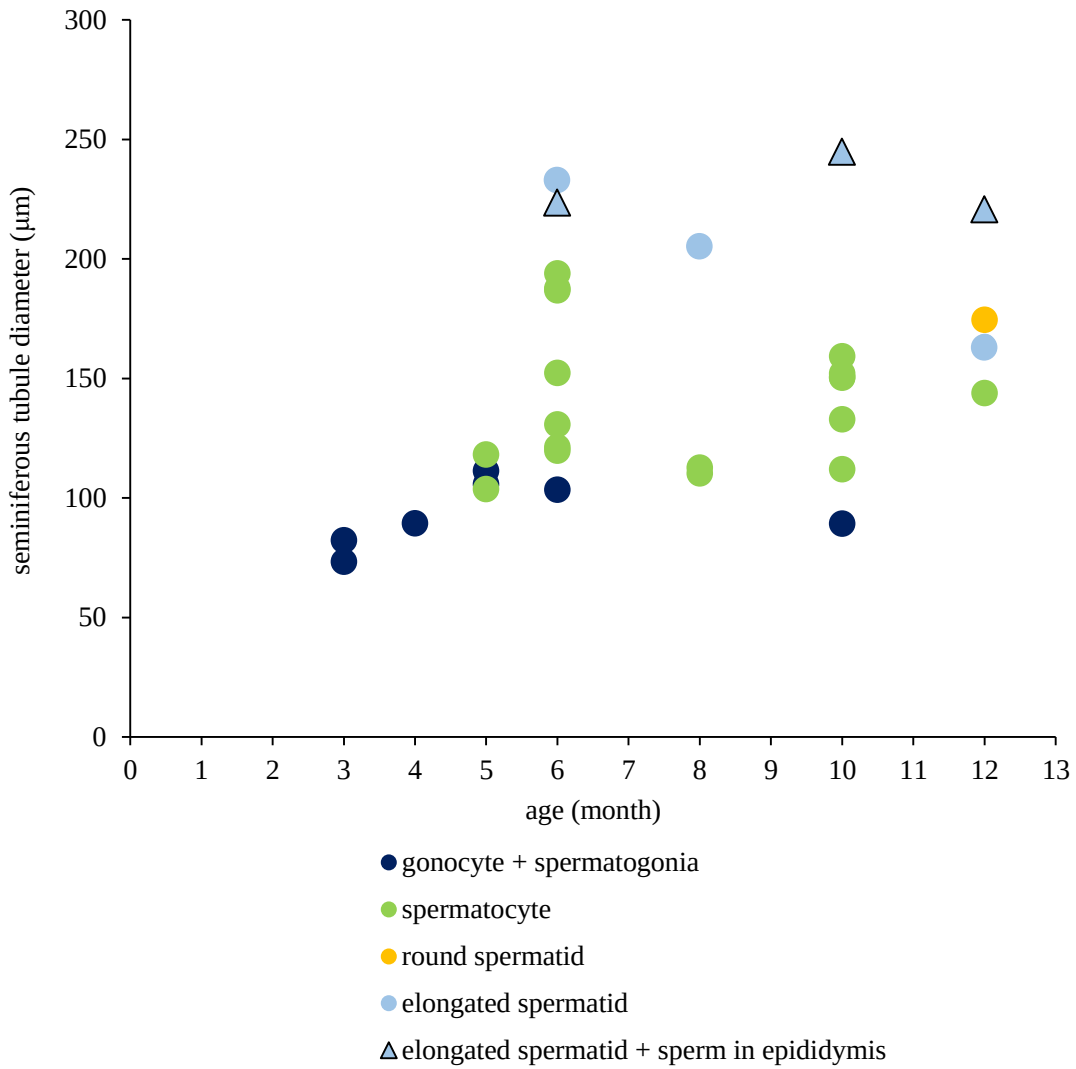

Fig. 1.13. Relationship between seminiferous tubule diameter and age.

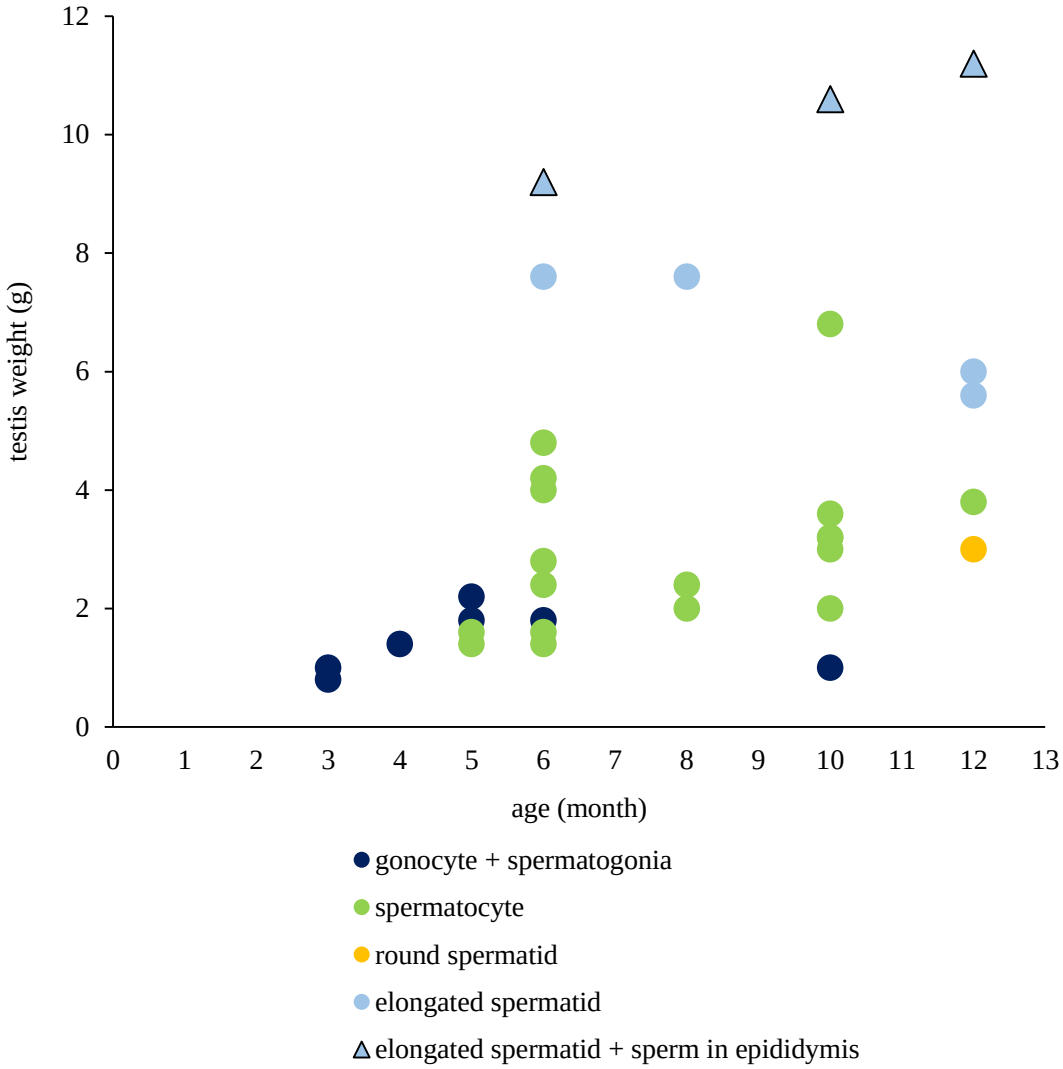

Fig. 1.14. Relationship between testis weight and age.

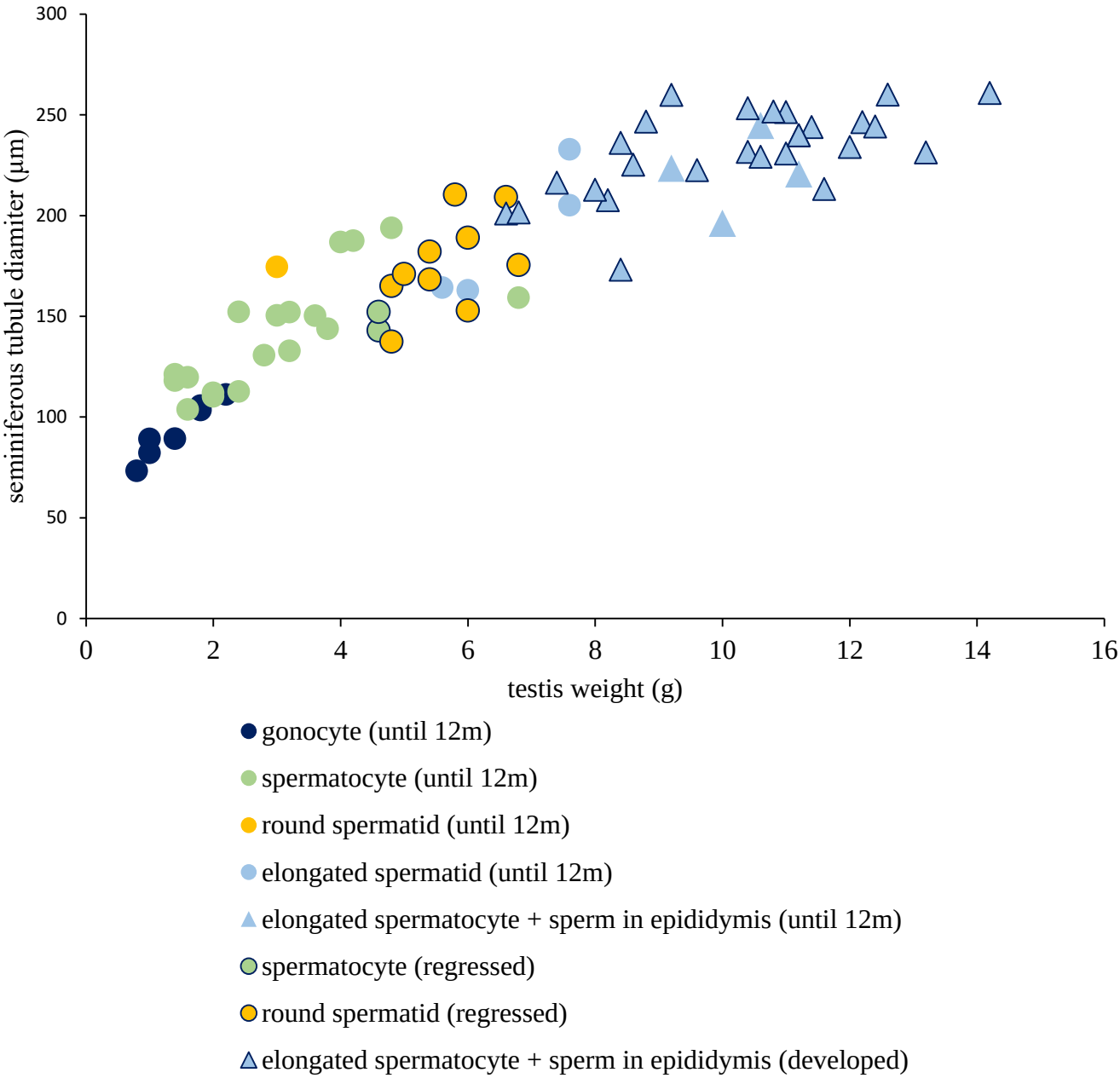

Fig. 1.15. Relationship among testis weight, seminiferous tubule diameter, and the most advanced germ cells. One plot represents the status of the seminiferous tubules of one raccoon. Each color indicates the most advanced germ cell type in seminiferous tubule, and circular plots indicating no sperm in the cauda epididymis and triangular plots indicating the presence of sperm in the cauda epididymis. Marginal plots showed raccoons over 12 months of age.

Chapter 2
Developmental and Seasonal Changes in the Prostate Gland of Raccoons

2.1 Introduction

The raccoon has the ampulla of deferent duct and prostate gland as accessory genital glands as dogs (Sanderson and Nalbandov, 1973). The prostate gland is essential for the success of fertilization, and its main role is the production of prostatic fluid which functions sperm survival and sperm transport during ejaculation (Huggins, 1945; Barsanti and Finco, 1986). The glandular epithelium of prostate glands is composed of luminal (secretory), basal and neuroendocrine (NE) cells (McNeal, 1988; Di Sant'Agnese, 1992; Bonkhoff and Remberger, 1996; Ismail et al., 2002; Ryman-Tubb et al, 2022). The luminal cells are the most abundant epithelial cells, show cuboidal to columnar with basal nuclei, and in dogs, secret prostatic fluid containing the substances such as cholesterol, citrate, lactate and canine prostate-specific arginine esterase (SPSE) which is the homolog of prostate-specific antigen (PSA) of humans (Evans et al., 1993; Gobello et al., 2002). Basal cells which are located on the basement membrane, are second most dominant and involved in the survival of luminal cells, express p63 protein and show the discontinuous layer in dogs unlike in humans (Kurita et al., 2004; Nikitin et al., 2007; Ryman-Tubb et al, 2022). Neuroendocrine cells are rare, secret chromogranin A and synaptophysin, and control the exocrine of secretory cells and the prostate differentiation and growth (Bonkhoff and Remberger, 1996; Di Sant'Agnese, 1992; Ismail et al., 2002; Ryman-Tubb et al, 2022).

It has been reported that the prostate glands of some rodents (Chaves et al., 2015; Kheddache et al., 2017), marsupials (Todhunter and Gemmell, 1987), bats (Puga et al., 2014; Beguelini et al., 2015) and the donkey (Abou-Elhand et al., 2013) show seasonal variation morphologically and histologically. The size and weight of the prostate gland are affected by the development and secretory activity of the glandular epithelial cells depended on testosterone level linked to testicular activity (Huggins, 1945). It has been known that the prostate glands show the morphological and functional changes by castration or experimental treatment in carnivore (Huggins and Clark, 1940; Vanderstichel et al., 2015; Bo et al., 2019; Ryman-Tubb et al, 2022), however, it has been unknown whether carnivore prostates show seasonal change.

Regeneration of regressed prostates are often compared to developmental changes. The prostate glands are formed from prostatic buds consisting of epithelial solid cords extending from the urogenital sinuses during fetal development (Thomson, 2001). The epithelial cells of the cords canalize advancing proximal-to-distal, and differentiate into luminal and basal cells with canalization (Marker et al., 2003). The PAS-positive secretion by luminal cells is observed just before puberty in mice and from the fetal

stage in humans (Marker et al., 2003). The prostate glands remain dormant until puberty when it grows rapidly (Picut et al., 2018). During puberty, in rats, prostate glands grow rapidly, and proliferation of the prostatic epithelium leads to transient epithelial folding (Vilamaior et al., 2006).

Only one histological report on raccoon prostate glands has shown the timing of development (Uno, 2016), but no details have been reported. In raccoons, the characteristics of testicular regression suggests that the prostate gland also would regress as in other seasonally breeding animals, but the details remain unclear. Therefore, in this study, I aimed to define morphological features of the prostate gland in raccoons, and to reveal postnatal developmental and seasonal change. In order to define the characteristics of adults, I first examined seasonality in mature raccoons and then examined their postnatal development.

2.2 Materials and Methods

The prostate glands of 165 feral male raccoons were used in this study. Animals and sample preparations are described in the General Materials and Methods. Histological sections of the prostate gland were stained with HE, PAS, or AB. In addition, PAS staining was also performed after incubation with phosphate-buffered saline (PBS) containing 0.01% diastase for 50 min at 37°C. Moreover, the immunostaining for p63, AR, PCNA was carried out. The prostate glands of under 6 months of age (n=29, infantile), between 6 and 12 months of age (n=48, juvenile) and over 12 months old (n=88, adult) were used for the observations of the prostate glands. Developmental stages ware largely divided into three stages based on results of the testicular spermatogenic conditions and the onset of canalization in the seminiferous tubules in the Chapter 1. In this Chapter, the result of the raccoons at 12 months of age was separated from that of other non-adult raccoons in analysis of the rate of each prostate developmental stage for understanding the situation of the age group closest to adult. Adults were searched for seasonal changes, and developmental searches were conducted at all stages. Moreover, I defined the periods (June to August) as spermatogenetic-declined season based on the results in the Chapter 1.

2.3 Results

Gross anatomy

The prostate gland of raccoons was located caudal to the bladder neck in the pelvic cavity and surrounded the circumference of the urethra (Figs. 2.1 and 2.2A). It was a red-tinged color, solid gland, and protruded slightly to the left and right in the cranial region (Fig. 2.1C). When the urinary bladder and prostatic urethra were cut open and observed ventrally, the urethral crest, which runs from around two ureteric orifices to the seminal colliculus in the prostatic urethra, was observed (Fig. 2.1D). The

seminal colliculus was the highest part of the urethral crest at the center of the dorsal wall of the prostatic urethra (Fig. 2.1D).

Histological and immunohistochemical observation of glands during seasonal change

The prostatic urethra was surrounded by the prostate gland (Fig. 2.2A). On the other hand, the dorsal part of the cranial region was separated due to the presence of connective tissue (Fig. 2.2B). Moreover, the disseminate part of the prostate gland was found under the urethral muscle. At approximately maximum diameter, the urethra exhibited a U-shape due to the presence of the seminal colliculus (Fig. 2.2A). At this location, the prostatic utricle, known as the residual structure corresponding to the female vagina and uterus, sometimes was observed within the connective tissue of the seminal colliculus (Fig. 2.2A). The presence and size of the prostatic utricle depended on the individual. Two ejaculatory ducts were observed in the interstitial tissue dorsal to the urethra, and these ducts finally opened to the seminal colliculus (Figs. 2.1D and 2.2A).

The prostate glands consisted of the glandular parenchyma and interstitium (Fig. 2.2C, D). The prostate parenchyma spread homogenously throughout the gland, and thus, the glandular parenchyma showed no localized distribution within the prostate glands. The interstitial tissue extended from the capsule-separated parenchyma to the lobules (Fig. 2.2C).

In the prostate glands of mature raccoons, two histological conditions were identified: developed and regressed. Each histological aspect is described below.

Developed prostate gland:

The prostate glands showed a branched tubuloalveolar gland, and the glandular lumen was lined by the pseudostratified epithelium with folding, which consisted mainly of numerous luminal cells and relatively few basal cells (Figs. 2.2C, D, and 2.4A-1). In this study, the presence of NE cells has not been investigated.

The luminal cells exhibited a tall columnar shape, and their nuclei were round or ovoid and located in the basal area (Fig. 2.2C, D). The luminal cells had numerous fine secretory granules that were PAS-positive and distributed throughout the cytoplasm (Fig. 2.2E). After digestion with diastase, PAS positivity did not disappear. On the other hand, an AB-positive reaction was not detected (Fig. 2.2F). Moreover, it was revealed by the immunohistochemical localization of p63 that the flat basal cells were scattered in the basal part of the epithelium (Fig. 2.4A-1). The developed prostate glands were found evenly throughout the year, and the prostate glands in spring were mostly composed of developed ones (Table 2.1). In the developed prostate glands, AR-positive cells were shown in most luminal and basal cells of the epithelium, but not all (Fig. 2.4B-1). Immunoreactivity of PCNA was hardly recognized in

the developed prostate glands but was infrequently observed in both luminal and basal cells (Fig. 2.4C-1).

Regressed prostate gland:

Mainly in the spermatogenetic-declined season, all or some lobules of the prostate glands were regressed and they did not show the same epithelial features as the developed prostate glands (Table 2.1, Fig. 2.3A, B). In this paper, the gland in this state was defined as “the regressed gland”. This regressed glandular part tended to initially appear on the craniodorsal and craniolateral regions of the prostate gland, and these changes seemed to be symmetrical (Fig. 2.3A, B).

In raccoon prostate glands, three regressed glandular types were identified in the regressed gland. Type I showed the following characteristics: many luminal cells fell off into the lumen to result in cell debris (Fig. 2.3C, D), flat or cuboidal remaining luminal cells were noticed on the basal cells or basement membrane (Fig. 2.4A-2), basal cells with p63 got closer to each other (Fig. 2.4A-2), the immunoreactivity for AR was mainly detected in the basal cells (Fig. 2.4B-2), and many basal cells showed PCNA-positive reaction, while the luminal cells did not (Fig. 2.4C-2). The cell debris did not show immunoreactivity for p63, AR, or PCNA (Fig. 2.4A-C-2).

Type II showed the following characteristics: the regressed glands were lined by two epithelial layers that exhibited small cuboidal luminal cells (upper layer) and basal cells that were largely inflated and showed p63 immunoreactivity (lower layer) (Figs. 2.3E, F, and 2.4A-3), the glandular lumen was the most reduced of all the regressed glandular types and had cell debris in the acinus location (Figs. 2.3E, F, and 2.5A-2), and AR- and PCNA-positive reactions were recognized only in the basal cells (Fig. 2.4B-3, C-3).

Type III showed the following characteristics: the basal cells with p63 were flattened and slightly separated from each other by the insertion of luminal cells (Figs. 2.3H and 2.4A-4), the luminal cells that showed cuboidal or low columnar shape covered the basal cells (Figs. 2.3H and 2.4A-4), the size of the glandular lumen was the same as that of type I (Fig. 2.3C, G), most basal and luminal cells showed immunoreactivity for AR (Fig. 2.4B-4), and PCNA was expressed in many luminal and scattered basal cells (Fig. 2.4C-4).

In all regressed glandular types, the luminal cells of all types were PAS-positive in the apical areas of the cytoplasm (Fig. 2.5A), and all of the regressed prostate gland types revealed no AB-positive staining (Fig. 2.5B). The cell debris was PAS-positive and AB-negative (Figs. 2.5A, B-1, and B-2).

Table 2.1. shows the comparison between the developmental status of prostate glands and the presence of sperm in the epididymis in each season. The regressed prostate glands were observed in 40 raccoons (May, 5; June–August, spermatogenetic-declined season, 30; September, 3; October, 1;

November, 1). During the spermatogenetic-declined season, the presence of the regressed gland was approximately 73% (30/41), and 20 individuals showed no elongated spermatids or no sperm in the epididymis, accounting for approximately 49% of the total during these months (20/41). The rate of the regressed gland without completed spermatogenesis to all glands without completed spermatogenesis was approximately 79% (19/24). During February–April, no raccoons without completed spermatogenesis and with regressed prostate glands were observed.

Weight

The weight of the prostate glands varied with the season (Fig. 2.6). The developed prostate glands were found throughout the year, but the weight tended to be lighter in summer compared with other seasons, and the regressed prostate glands tended to be concentrated around summer and tended to be lighter in weight than the developed prostate glands in spring (Fig. 2.6).

Histological and immunohistochemical observation of glands during postnatal development

I divided the developmental stages of the prostate glands into three stages (immature, developing, and developed) in the postnatal development according to the degree of development in the prostate glands by 12 months old. The third developmental stage is histological structure in the mature state already described as developed prostate gland. Therefore, early two stages; immature and developing stages, were described here. Over 12 months of age, all prostate glands were decided to be mature stage, and either developed or regressed as previously described.

Immature stage of prostate glands:

The immature stage of prostate glands showed more clear distinction between tubular and alveolar parts of the gland and a larger proportion of interstitial tissue, than the mature prostate glands (Figs. 2.7A and 2.10A). In the immature stage, the epithelium of the prostate gland was lined by clear cuboidal basal cells and flattened to cuboidal luminal cells, and the lumens in the alveolar glands already formed in all samples examined (Fig. 2.7A-C). The luminal cells have PAS-positive granules in the cytoplasm at the immature stage, and the secretion was sometimes observed in the lumen (Fig. 2.8A). The immature stage was observed by 12 months old (Fig. 2.9), many individuals with the immature stage showed germ cells by spermatocytes (89%), and no completed spermatogenesis (sperm production) was detected in this stage (Table 2.2).

The developing stage of prostate glands:

The developing stage was characterized by a mixture of immature and developed area. Developed

glands which were consisted of mainly columnar luminal cells, was present at the proximal side (urethra side) of the prostate gland (Figs. 2.7F-J and 2.10B, C), and this area was symmetric (Fig. 2.10B, C). In the developing stages, the tubular glands developed from proximal to distal to become be lined by columnar luminal cells, and the development of marginal alveolar glands was later (Figs. 2.7F-J and 2.10B, C). At the transition between the immature and developing area, the luminal cells gradually changed from flat to columnar toward the distal part (Fig. 2.7F-H), and the basal cells also changed from dense to scattered with development of the glands (Fig. 2.7H, J). In the developed stage, the all glands were lined by columnar luminal cells with scattered basal cells (Figs. 2.7K-O and 2.10D). Granules in the cytoplasm of flattened luminal cells were dense, while granules in the cytoplasm of columnar luminal cells were dispersed (Figs. 2.2E and 2.8). The developing stage was observed between 5 months and 12 months old, when spermatogenesis in the testes was in progress or completed (Fig. 2.9, Table 2.2). This stage was not observed in raccoons whose spermatogenesis had not been initiated and in raccoons older than 12 months.

Collecting duct of the prostate gland

The collecting duct of the prostate glands opened into the prostatic urethra at the peripheral and caudal areas of the seminal colliculus. The epithelium of the collecting ducts changed from the transitional to pseudostratified epithelium with the transition from proximal to distal (Fig. 2.11A-D). The transitional epithelium of the collecting ducts near the urethra showed approximately four to five cell layers (Fig. 2.11A, B). In the distal part of the collecting ducts, on the other hand, the pseudostratified epithelium exhibited about two cell layers (Fig. 2.1C, D).

The epithelial cells, except for the cells in the most superficial layer, presented clear pale cytoplasm with oval-shaped or compressed nuclei (Fig. 2.11B). The superficial layer was composed of cuboidal cells, and its apical part was acidophilic (Fig. 2.11B). The lumen of the collecting ducts was often filled with secretion. In addition, the collecting duct contained intraepithelial cysts (Fig. 2.11B), and their epithelial cells were PAS- and AB-positive (arrows in Fig. 2.11E, F). However, the secretion within the cysts was AB-negative in many cases and occasionally positive (Fig. 2.11F), although the secretion always showed a PAS-positive response (Fig. 2.11E). Moreover, the superficial epithelial cells always showed PAS- and AB-positive responses (arrowheads in Fig. 2.11E, F). After digestion with diastase, PAS positivity did not disappear. These characteristics were common throughout all seasons and ages. The epithelial cells of the collecting duct showed immunoreactivity for p63 in the basal and the adjacent layers and AR in the basal layer (Fig. 2.11G, H). In the prostatic urethra, a superficial epithelial layer showed PAS-positive and AB-positive responses, and the distribution of p63 and AR was similar to that of the collecting duct (data not shown).

2.4 Discussion

Gross anatomy

All placental mammals have the prostate gland, which shows morphological variation among each species. The prostate glands of the raccoon consisted of the distinct body of the prostate and the disseminated part under the urethral muscle. The body of the prostate surrounded the prostatic urethra, similar to dogs (Berg, 1958) and ferrets (Bo et al., 2019), but the distribution pattern was different from cats, for which the gland does not surround the urethra at the ventral location (Aitken and Aughey, 1964).

Histology of the developed prostate glands

Histologically, the prostate glands of the raccoon appear as a homogeneous distribution like dogs (Leis-Filho, 2018). On the other hand, human prostate glands are divided into three zones depending on histological appearance and pathologic characteristics (McNeal, 1981). In the prostate glands of mice and gerbils, the prostate glands are divided into lobes, and the morphological difference in the glandular epithelium is seen between each lobe, and the glandular epithelial shape in the same lobe is different between the proximal and distal parts (Sugimura et al, 1986a; Rochel et al., 2007). The histological appearance of the prostate glands in the raccoons does not seem to form specific lobes, unlike those of humans, mice and gerbils.

The developed prostate glands of the adult raccoon were commonly lined by tall columnar cells, and these columnar cells were observed throughout all seasons. Therefore, this epithelial condition may be regarded as a common active feature of the glandular epithelium after reaching sexual maturity.

The secretion granules of the prostate gland in raccoons showed PAS-positive and AB-negative responses, meaning that the secretion of the prostate glands in raccoons was a serosity including neutral glycoprotein. These PAS-positive granules were not glycogen because the reaction remained after diastase digestion. These features of secretion were similar to dogs (Wrobel, 1972) and cats (Aitken and Aughey, 1964). While the prostatic glandular epithelium of rats (Tsukise and Yamada, 1981) and goats (Tsukise and Yamada, 1984) showed PAS- and AB-positive responses. Therefore, the property of secretion of the prostate gland appears to vary among species.

Histology of the regressed prostate glands

Raccoons with the regressed prostate gland were concentrated in the spermatogenetic-declined season (June–August). In this season, many raccoons (73%) had regressed glands, which showed decreases in the heights of the glandular epitheliums and relative cross-sections of the glands. Such a feature has been reported in some castrated animals and seasonal breeders in the non-breeding season. After castration, dogs (Huggins and Clark, 1940; Lai et al., 2008), rats (Huttunen et al., 1981), gerbils

(Góes et al., 2007; Oliveira et al., 2007) and ferrets (Bo et al., 2019) show the decreased height of luminal cells. In the non-breeding season, a decrease in the glandular epithelial height has been reported in donkeys (Abou-Elhamd et al., 2013), viscachas (Chaves et al., 2015), Tarabul's gerbils (Kheddache et al., 2017), and ground squirrels (Zhang et al., 2018).

In the raccoons, the epithelium of the developed prostate gland had some folds, but no folds were observed in the regressed prostate. The disappearance or decrease of folds has been reported in viscacha during the non-breeding season (Chaves et al., 2015) and in castrated dogs (O'shea, 1962). In the regressed prostate glands in raccoons, PAS-positive granules were densely observed in the supranuclear area of the luminal cells with various shapes, suggesting that the luminal cells also maintain the secretory function in the regressed prostate glands.

In general, the luminal cells highly depend on androgen and quickly respond to its absence. The plasma testosterone level of raccoons in Hokkaido is lower in the season when the spermatogenesis is markedly declined (Okuyama et al., 2012). In this study, the secretory granules are present in the luminal cells of regressed prostate glands also. In castrated dogs, however, the secretory granules are absent in the prostate luminal cells (Merk et al., 1980). These differences may be due to the situation of less or no testosterone. After castration, therefore, the treatment with testosterone causes the functional and morphological recovery of luminal cells in dogs (Zuckerman, 1936; Leav et al., 2001). Similarly, the morphological change of the luminal cells seen in this study might be due to the testosterone levels seasonally changed.

Progression and regeneration of the regressed prostate glands

In this study, three regressed glandular types were identified in the regressed prostate gland. I confirmed many cell debris of luminal cells without p63, the remaining tall luminal cells, and the transitional form of the basal cells in the type I unlike the type II. In type III, on the other hand, no cell debris, the large lumen same as the type I, and the cuboidal luminal cells with flat basal cells were confirmed. Therefore, I conclude that the transitional order of regressed prostate glands is type I, type II, and type III, and type III is the regeneration phase. Similar dynamics of the regression and regeneration in the prostate gland have not been reported in seasonal breeders, although the change of the glandular epithelial height during seasons has been demonstrated (Abou-Elhamd et al.,2013; Chaves et al., 2015; Kheddache et al., 2017; Zhang et al., 2018).

In this study on the raccoon prostates, the basal cells were enriched in the Type Ⅱ of the regressed glands. A similar basal cell-rich appearance was observed in castrated dogs with mild atrophy (Lai et al., 2008), castrated mice (Kurita et al, 2004; Wang et al., 2009) and castrated bats (Puga et al., 2016). Therefore, the survival of basal cells does not appear to be affected by low or no testosterone

concentration. This our finding of the basal cell-rich appearance during the seasonal change regression is the first reports.

The basal cell-rich condition in regressed prostates detected in the raccoons may result from both the atrophy caused by abrasion (decrease) of luminal cells and the increase of basal or basal stem cells. No immunoreactivity for p63 was detected in cell debris, indicating that basal cells do not show defluxion. Moreover, the cell proliferation activity of basal cells with p63 was detected in the regressed glands, especially in type II. It has been reported that the basal or basal stem cells with p63 can produce luminal cells without p63 (Wang et al., 2001; Kasper, 2008; Ousset et al., 2012; Toivanen and Shen, 2017), and this proliferation of basal cells is induced by the AR loss in stromal cells and subsequent exfoliation of luminal cells (Zhang et al., 2018; Zuckerman, 1936). In the prostate gland of type III (regeneration phase), moreover, the cell proliferative activity reappeared in luminal cells without p63 which could be due to both newly differentiated luminal cells from basal or basal stem cells (Toivanen and Shen, 2017; Xie et al., 2017) and survived luminal cells (Wang et al., 2009; Xie et al., 2017).

AR expression in the prostate gland

In the developed gland of the raccoon, AR expression was detected in the luminal and basal cells, and the luminal and basal cells with AR showed little proliferative activity. Therefore, androgens do not appear to be directly involved in the proliferation of both cell types. The AR of the luminal cell is necessary for the secretion of androgen-dependent proteins, such as PSA and prostatic acid phosphatase (PAP), and AR expression in the epithelial cells suppresses the epithelial proliferation (Donjacour and Cunha, 1993; Cunha et al., 2004; Wu et al., 2007; Niu et al., 2011; Xie et al., 2017). In the developed gland of the raccoon, AR of the luminal cell may mainly regulate the secretory functions of luminal cells.

On the other hand, in the regressed gland, the AR expression started to disappear from the luminal cells, and all AR disappeared completely as the regressed gland progressed. The functional luminal cells, which lost AR expression, fell off from the basement membrane in early regression. The disappearance of AR expression in the luminal cells signifies morphological changes and the loss of cell polarity (Wu et al., 2007; Xie et al., 2017). Moreover, in the prostate gland, the paracrine regulation by stromal cells to the epithelial cells has been reported, and it was demonstrated that AR expression is essential in the stromal cells, but not in luminal cells, for the survival of the luminal cells (Kurita et al., 2001; Neito et al., 2014). Therefore, in the raccoons, the stromal cells with AR may be unable to maintain the survival of the luminal cells in a paracrine manner when adequate androgen supply is lost. Moreover, previous reports indicate that AR expression in the epithelial cells suppresses the luminal cell proliferation (Wu et al., 2007; Niu et al., 2011; Xie et al., 2017), and the loss of luminal cells might induce the proliferation of basal or basal stem cells (Niu et al., 2011). These could explain the proliferation of the basal cell in

type Ⅱ following the loss of the luminal cell in type Ⅰ.

AR expression in luminal cells disappears once in type Ⅱ, and during the regeneration phase (type III), AR expression started to appear and develop in the luminal cells. In this study, on the other hand, basal cells continue to express AR through all phase. Xie et al. (2017) also demonstrated that AR expression of the basal cells is essential for the differentiation of basal cells to luminal cells. In the regeneration phase, therefore, it was likely to produce the new luminal cells with AR finally differentiated from daughter cells of basal or basal stem cells with AR.

The recovery of androgen levels restores the secretory functions of the luminal cells with AR expression and inhibit their proliferation again. The dynamics of prostate gland weight in raccoons during the year may be due to the disappearance and regeneration of luminal cells associated with the change of androgen levels. In the spermatogenetic-declined season of raccoons, the rate of the regressed prostate glands without spermatogenesis conditions showed a relatively high percentage (79%, 19/24). Thus, a decrease in androgen levels may simultaneously affect testicular spermatogenesis and glandular functions.

In the raccoons, the regression of the prostate glands symmetrically began from the craniodorsal and craniolateral regions. The regional heterogeneity of prostate glands in hormonal responses has been reported in other species such as Rodents (Sugimura et al., 1986a; 1986b; Góes et al., 2007), humans (McNeal, 1981) and dogs (Huggins and Clark, 1940). The raccoon prostate is also homogenous in appearance, but there is likely heterogeneity in hormonal responses. To clarify the origin of regional heterogeneity in the prostates of raccoons, we need to investigate prostatic local hormone levels such as androgen.

The prostate glands during postnatal development

The prostate glands are formed by canalization of solid prostatic buds arising from the urogenital sinus (Thomson, 2001; Marker et al., 2003). In rats and mice, the branching of the prostatic buds continues in postnatal and is completed by the end of puberty, and the prostatic buds begin to canalize in the neonatal period (Cunha et al., 2004). The canalization of the glands progresses distally from the urethral side, and the glandular epithelium differentiates into luminal and basal cells simultaneously with canalization (Marker et al., 2003; Cunha et al., 2004). In dogs, no lumens in the alveolar gland were seen at 0 weeks of age, and then lumens of the acini appeared at 8 weeks of age (Kawakami et al., 1991). The prostate glands of all raccoons examined in this study had lumens in the glands, and the youngest individual was 1 month old and had very small lumen. The study did not examine individuals younger than 1 month, so it is unclear exactly when the lumen is formed.

In humans, secretion from the prostate glands occurs during the fetal period, but in rats, on the

other hand, prostate secretion does not occur during the fetal period and dogs have no secretion of the prostate at birth (Picut et al., 2018). Androgen-dependent protein secretions such as PAP and PSA are secreted mainly after puberty, but in humans, first confirmed in the prostate glands when the prostate glands were canalized (Aumüller et al., 1983; Cunha et al., 2018). Secretion of PSA in the prostate gland appears at 12-20 days of age in rats and mice (Cunha et al., 2004). Androgen-dependent protein secretion is present at 4 months of age in dogs (Picut et al., 2018) Secretory granules of luminal cells were observed from an undeveloped stage in the raccoon prostate glands. I have not been able to pinpoint exactly when the prostate glands of the raccoon first begin to secrete, but it seems that secretion is already present in the immature state. In further study, the it is necessary to investigate the expression of PSA in raccoon prostate glands.

During puberty, epithelial proliferation in the rat prostate glands leads to the formation of epithelial infoldings, and the infoldings are stretched to extend the glands due to increased secretory activity (Vilamaior et al., 2006). In raccoons, the epithelial infoldings seen in rats were not observed. At the boundary between the undeveloped and developing parts of the raccoon prostate glands, the luminal cells developed stepwise from flat to columnar, and the basal cells changed from continuous to diffuse distribution as the epithelium became columnar. In developing stage, the developed area of the prostate glands was confined to the urethral side, suggesting that pubertal development occurs from the urethral side. This may be similar to the directionality of epithelial differentiation that accompanies canalization. In human, in early puberty, the prostate glands near the urethra are PAP-positive, while the peripheral prostate glands are PAP-negative (Aumüller et al., 1983). This report also supports a urethral-to-peripheral direction of the tubular development in the adolescent prostate glands. Although there is no description of the boundary between the developed and undeveloped regions, it has been reported that developed and undeveloped regions coexist in the canine prostate glands (Dorso et al., 2008). In this study on raccoon prostate glands, the feature of the boundary between developed and underdeveloped regions was revealed for the first time.

In raccoon prostate glands, the aspects of the postnatal development were similar to those of reorganization from the regressed prostate condition. The histology of luminal and basal cells of immature and developing stages in the postnatal development seem to correspond to that of regressed glandular types Ⅰ and types Ⅱ, respectively. It may be assumed that, therefore, the reorganization and postnatal development in prostate glands are carried out in the same mechanism.

The developmental state of the prostate was compared with the raccoon postnatal developmental stages determined in the Chapter 1. During infantile period by 5 months of age, raccoon prostates did not begin to develop, with one exception. A small number of prostate glands began to develop, and some completed development from 6 to 12 months of age. At 12 months of age, which is a subadult, more

than half of the prostate glands have begun to develop, and a few have completed development. Within the same age range of raccoons, there are individuals with different stages of prostate development, a characteristic similar to that of dogs (Dorso et al., 2008).

Collecting duct of the prostate gland

The epithelium of the collecting duct in the raccoons showed a secretory aspect in the most superficial layer (PAS- and AB-positive) and often had intraepithelial cysts filled with secretion PAS-positive and occasionally AB-positive). The superficial epithelial cells of the collecting ducts may secrete mucus including acidic glycoproteins that line the luminal surface. In the urinary transitional epithelium, it has been reported that the surface mucus secreted by surface epithelial cells (umbrella cells) may protect the epithelium from bacterial invasion or urinary toxic factors using the water trap effect by proteoglycans binding glycosaminoglycan (Parson, 2007). Surface mucus may have a similar protective effect in the prostate gland of raccoons. In this study on the raccoon prostate, the cysts were recognized within the epithelium of the collecting duct. There are no reports about intraepithelial cysts in the intact prostate collecting duct. In the raccoons, the secretion within the cysts was PAS-positive and mainly AB-negative, although the epithelial cells were PAS- and AB-positive. The epithelial cells of the cysts may produce surface mucus and leave secretion, mainly including neutral glycoprotein and occasionally including acidic glycoproteins. The appearance of the raccoon intraepithelial cysts were not incidental findings but one of the features of raccoon collecting ducts, as the cysts with specialized secretions are observed in most individuals.

In the raccoons, p63 expression was observed in basal layer cells of the prostatic collecting ducts and prostatic urethras. In observations of mouse urogenital epithelial development, p63 expression was detected in the urothelial and prostatic basal cells, but not in stromal cells and other epithelial cells. The urothelial and prostatic epithelium is differentiated from the epithelium of the urogenital sinus (Cunha et al., 2004). Therefore, the distribution of the basal or basal stem cells with p63 on each epithelial basal layer appears to be a common feature in the mammalian urothelial and prostatic epithelium to sustain the epithelium.

In our observation of the prostatic collecting duct and prostatic urethra, AR expression showed the same intraepithelial distribution as p63. It has been reported that strong AR immunoreactivity is detected in the basal cell layer of the human urethral epithelium and starts to disappear in the upper epithelial cells (Dietrich et al., 2004). It is thought that AR-positive cells are basal and basal stem cells. In the prostate glands, AR expression of the basal cells is involved in the differentiation of basal or basal stem cells to luminal cells (Xie et al., 2017). Therefore, in the epithelium of the prostatic collecting ducts and prostatic urethras of raccoons, AR expression in the ductal basal cells may be responsible for

differentiation into the upper layer epithelial cells like the acinar basal cells.

In conclusion, this study is the first report that clarified the seasonal dynamics of glandular structure, p63 and AR expression and proliferation in raccoon prostate glands, and reported that raccoon prostates exhibit seasonal variation of regression and regeneration. This seasonal variation may be reflected by the local growth factors in addition to seasonally fluctuating circular hormones, but further investigations are needed to understand the seasonal regulatory mechanism. In this study, moreover, the postnatal development in raccoon prostate glands was examined, and it was revealed that histological aspects in the postnatal development resemble to those of the reorganization in adult regressed prostate glands.

Table 2.1. The sperm existence and the prostate gland development during the year

Sperm existence / spermatogenic condition	January		February		March		April		May		June		July		August		September		October		Nobember		December	
	dev	reg	dev	reg	dev	reg	dev	reg	dev	reg	dev	reg	dev	reg	dev	reg	dev	reg	dev	reg	dev	reg	dev	reg
present/elongated	n	n	3	0	6	0	8	0	11	4	4	9	2	2	3	1	3	2	1	1	1	1	1	0
present/no elongated	n	n	0	0	0	0	0	0	1	0	0	0	1	0	0	0	0	0	0	0	0	0	0	0
no sperm/elongated	n	n	0	0	0	0	0	0	0	0	0	0	0	0	0	0	0	0	0	0	0	0	0	0
no sperm/no elongated	n	n	0	0	0	0	0	0	1	1	2	5	0	6	0	6	0	1	0	0	0	0	0	0

elongated, elongated spermatids were present.

no elongated, elongated spermatids were not present.

dev, developed prostate gland.

reg, regressed prosstate gland.

n, not corrected.

June-August was defined as spermatogenetic-declined season.

Table 2.2. Most advanced germ cells in each developmental stage of prostate glands in non adult raccoons

prosatate developmental stage during postnatal development	most advanced germ cell				
	gonocyte + spermatogonia	spermatocyte	round spermatid	elongated spermatid no sperm in epididymis	elongated spermatid sperm in epididymis
immature	34*(64**)	13(25)	3(6)	3(6)	0(0)
developing	1(6)	5(29)	4(24)	4(24)	3(18)
developed	0(0)	2(29)	0(0)	2(29)	3(43)

*, number; **, percentage (rounded to the first decimal place). Rounding errer is present in each stage.

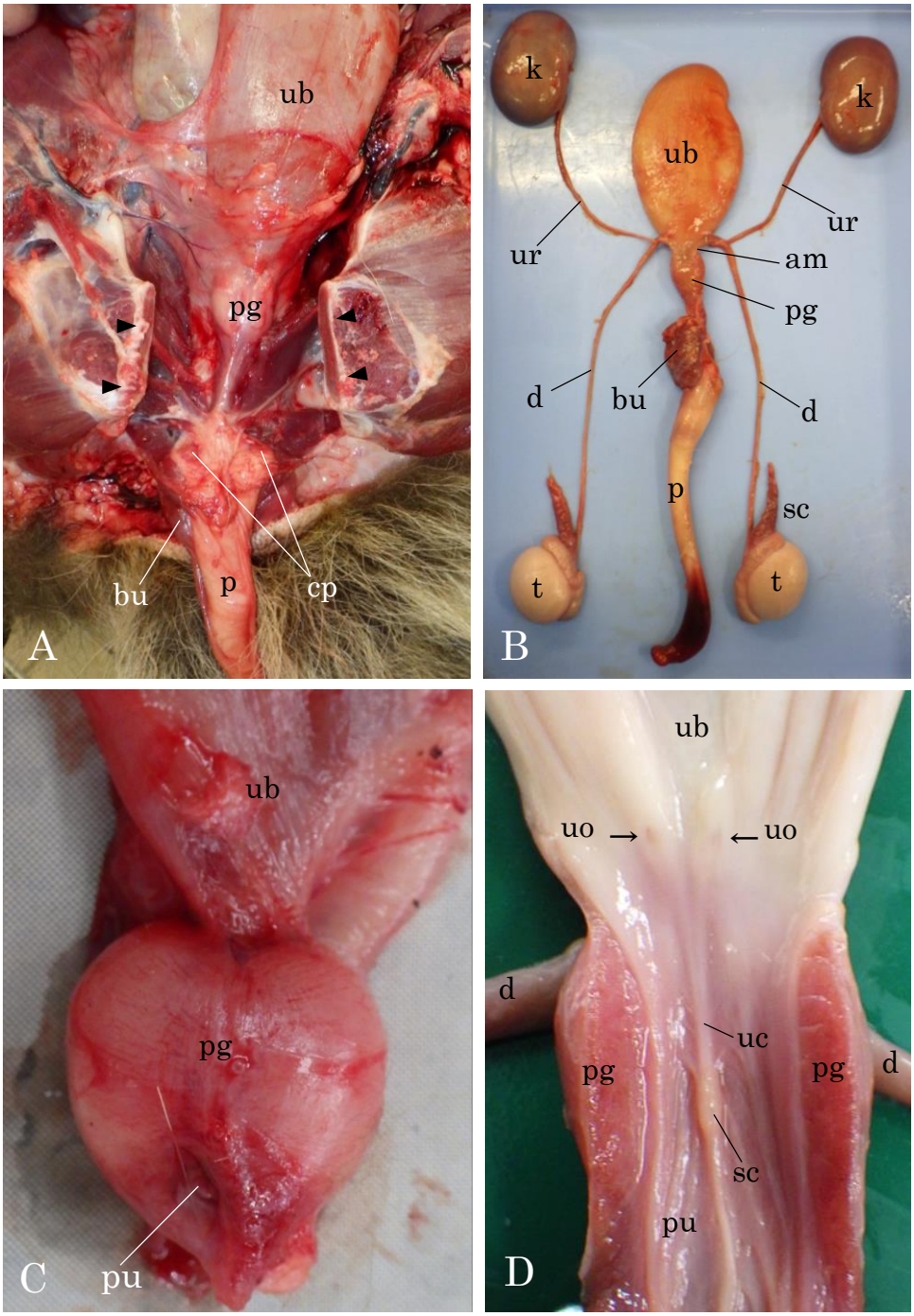

Fig. 2.1. Gross anatomy of the genital organs in male raccoons. (A) Ventral view of the prostate gland. Pelvic symphysis was cut open. The prostate gland was located caudal to the bladder. (B) Dorsal view of the removed male urogenital organs including the prostate gland. (C) Enlarged ventral view of the prostate gland. (D) Dorsal wall of the prostatic urethra. The ventral wall of the prostatic urethra was cut open. am, ampulla of the deferent duct; bu, bulbospongiosus muscle; cp, crura of the penis; d, deferent duct; k, kidney; p, penis; pg, prostate gland; pu, prostatic urethra; sc, spermatic cord; se, seminal colliculus; t, testis; ub, urinary bladder; uc, urethral crest; uo, ureteric orifice; ur, ureter.

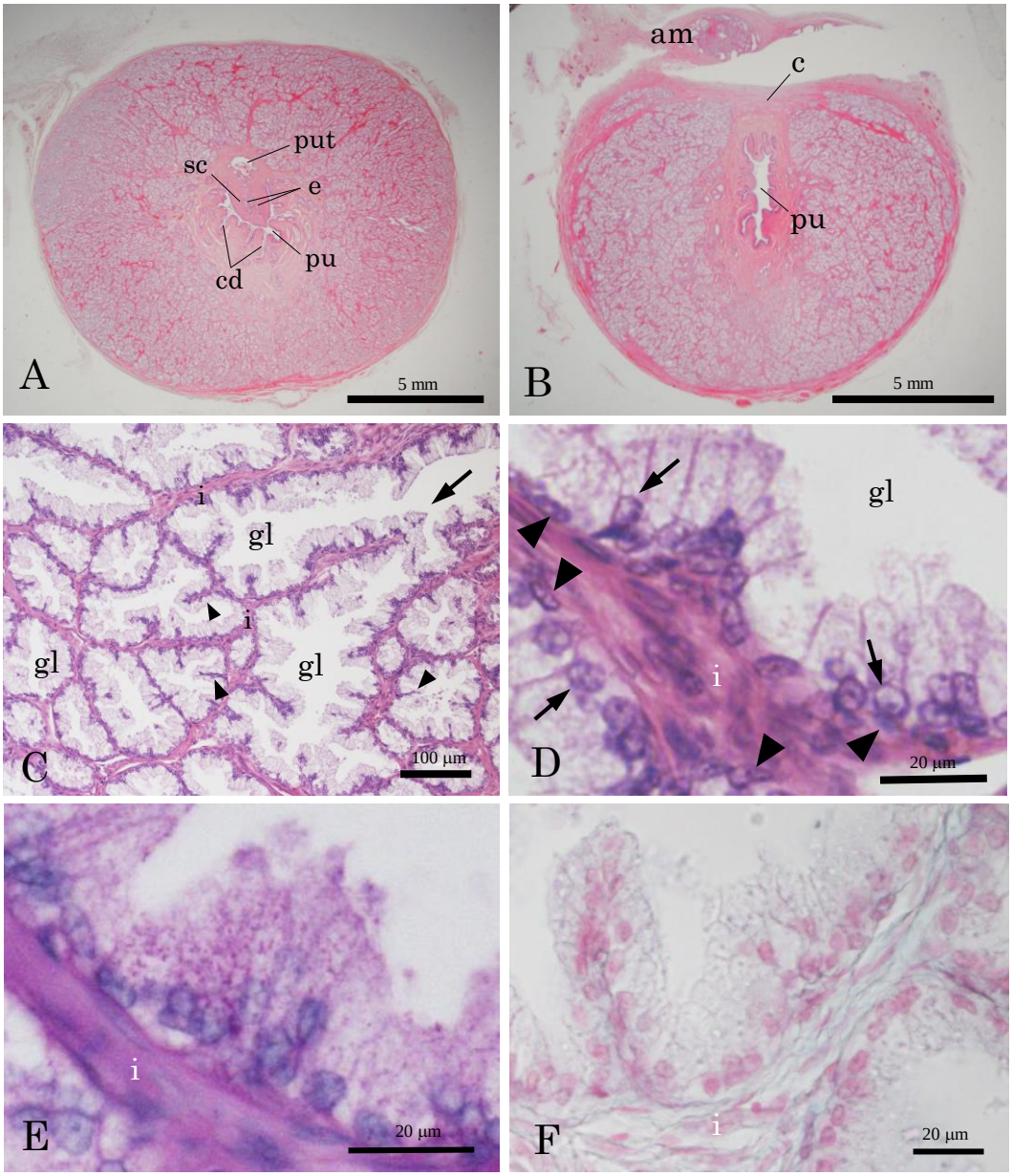

Fig. 2.2. Cross-sections of the developed prostate glands. (A) At approximately maximum diameter, the urethra was located in the central area and exhibited a U-shape due to the presence of the seminal colliculus. The prostate gland surrounded the urethra. (B) In the cranial part, the prostate gland was separated by the connective tissue in the dorsal part. (C) The prostate gland was a branched tubuloalveolar gland with folding (arrowheads), and its epithelium was pseudostratified. An arrow indicates the branch part. (D) Large magnification of glandular epithelium. Arrows indicate the luminal cells with a columnar shape, and the arrowheads indicate the basal cells with a flat shape. (E) The luminal cells had PAS-positive granules in the cytoplasm. (F) All glandular epithelial cells were AB-negative. am, ampulla of the deferent duct; c, connective tissue; cd, correcting duct; e, ejaculatory duct; gl, glandular lumen; i, interstitium; pu, prostatic urethra; put, prostatic utricle; se, seminal colliculus. A-D, HE staining; E, PAS staining; F, AB staining.

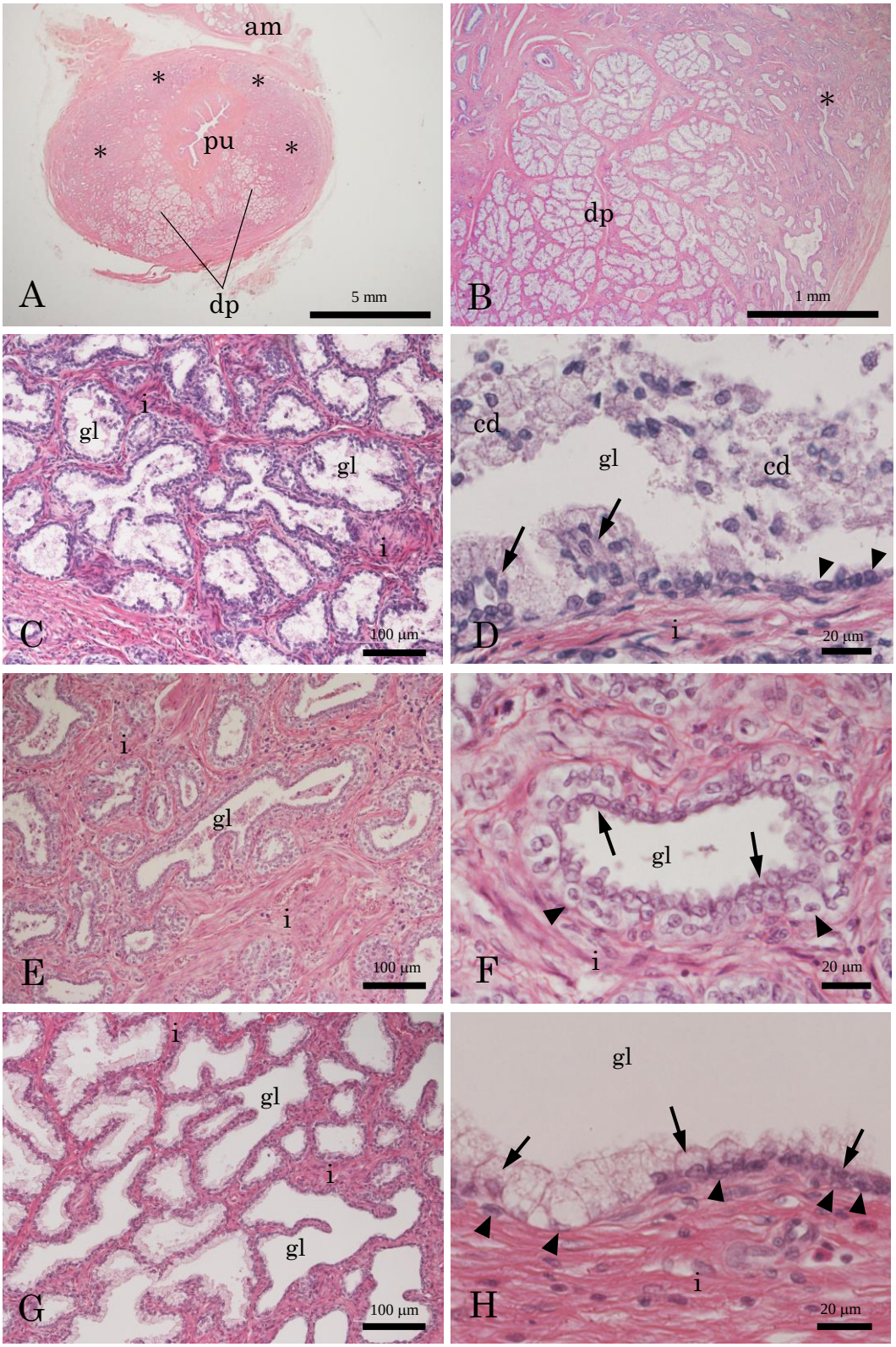
am
pu
dp
A
5 mm
dp
B
1 mm
gl
i
C
100 µm
cd
gl
D
20 µm
E
100 µm
F
20 µm
G
100 µm
H
20 µm

Fig. 2.3. Cross-section of the regressed prostate gland. (A) At the cranial part, some lobules were regressed (*) and other lobules (dp) appeared to be the same as developed prostate glands. The regressed glands tended to be observed on dorsal and lateral regions and seemed to be symmetrical. (B) Enlargement of the boundary between the developed (dp) and regressed glands (*). (C) The regressed glands (type I) are shown. Tall luminal cells fell out from the basement membrane to the lumen and the lumen of regressed glands filled with cell debris. (D) Large magnification of the regressed glands (type I). (E) The regressed glands (type II) are shown. The glands shrank to widen the area of the interstitium, and the epithelium did not have folding. (F) Large magnification of the regressed glands (type II). The epithelium was lined by two cell layers with cuboidal or flat luminal (upper layer, arrows) and basal (lower layer, arrowheads) cells. The basal cells largely expanded and showed an enlarged and pale cytoplasm and a round or oval nucleus. (G) The regressed glands (type III) are shown. Cuboidal and columnar liminal cells appeared. (H) Large magnification of the regressed glands (type III). Flattened basal cells were scattered in the glandular epithelium. arrows, luminal cells; arrowheads, basal cells; am, ampulla of the deferent duct; cd, cell debris; dp, developed glandular part; i, interstitium; gl, glandular lumen; pu, prostatic urethra. A-H, HE staining.

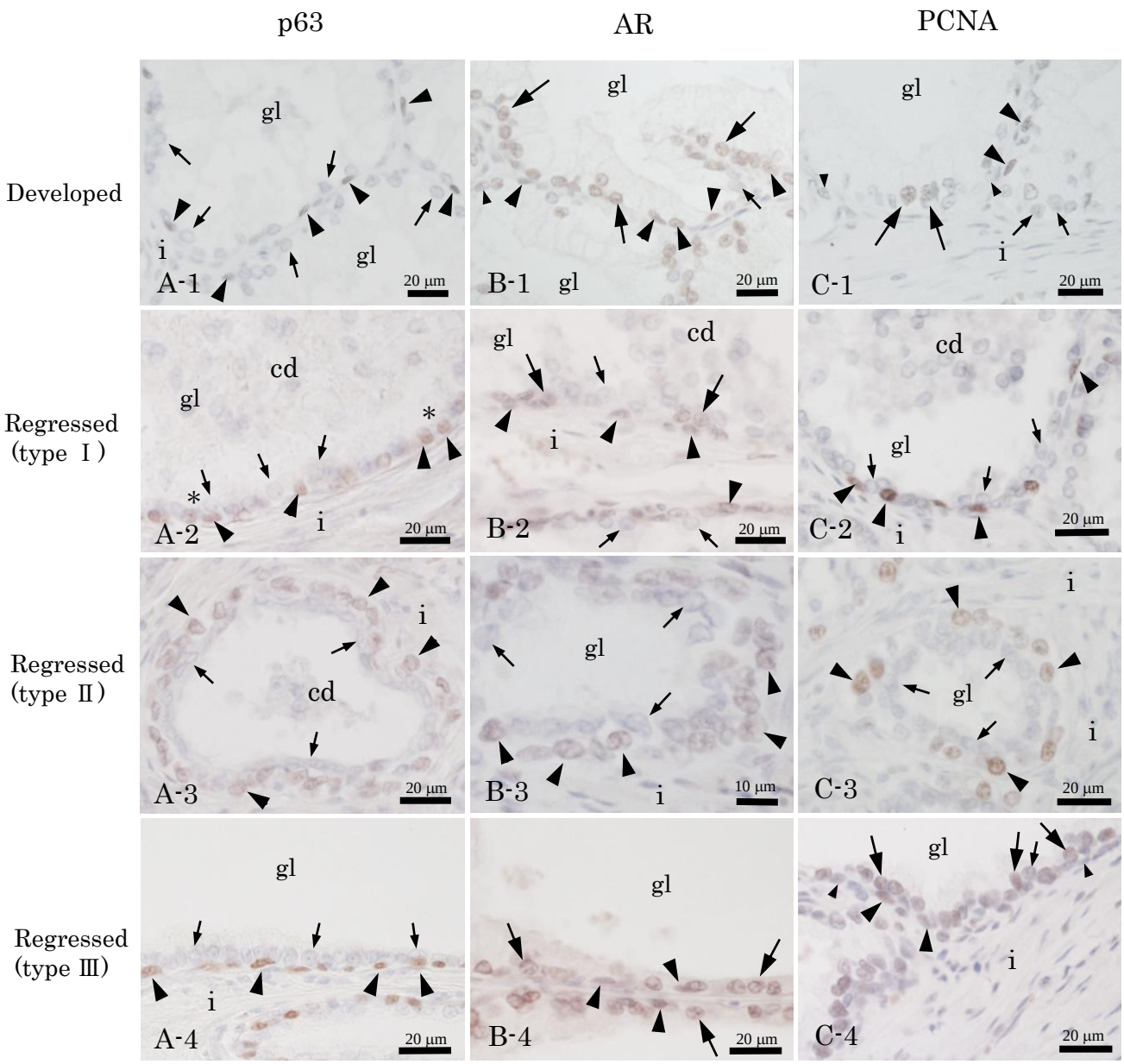

Fig. 2.4. Immunostaining of p63 (A), AR (B), and PCNA (C). 1, developed prostate gland; 2, regressed prostate gland (type I); 3, regressed prostate gland (type II); 4, regressed prostate gland (type III). In the developed gland, the basal cells with p63 are distributed scattered on the basal part (A-1). In type I of the regressed gland, basal cells showed fattened or cuboidal shape, and some cells lost the covering of luminal cells due to its defluxion (*), and basal cells got closer to each other as compared with the developed gland (A-2). In type II, largely expanded basal cells showed p63 immunoreactivity (A-3). In type III, basal cells exhibited a flattened shape and appeared closer to each (A-4). Concerning AR, the immunostaining of AR was shown in many luminal and basal cells in the developed gland (B-1). In type I of the regressed gland, AR-positive reactions were mainly detected in the basal cells, and some luminal cells had AR (B-2). While, in type II, luminal cells showed no AR immunoreactivity although most largely expanded basal cells had AR-positive reaction (B-3). In type III, most basal and luminal cells showed AR immunoreactivity (B-4). Concerning PCNA, very few PCNA reactive cells were shown in both basal and luminal cells (C-1). In type I of the regressed gland, PCNA immunoreactivity was detected in many basal cells, while not in the luminal cells (C-2). In type II also, PCNA immunoreactivity was detected only in the expanded basal cells (C-3). In type III, many luminal cells showed PCNA immunoreactivity (C-4). No cell debris showed immunoreactivity for p63, AR, and PCNA (A-C-2). large arrows, luminal cells with immunoreactivity; small arrows, luminal cells with no immunoreactivity; large arrowheads, basal cells with immunoreactivity; small arrowheads; basal cells with no immunoreactivity; cd, cell debris; i, interstitium; gl, glandular lumen.

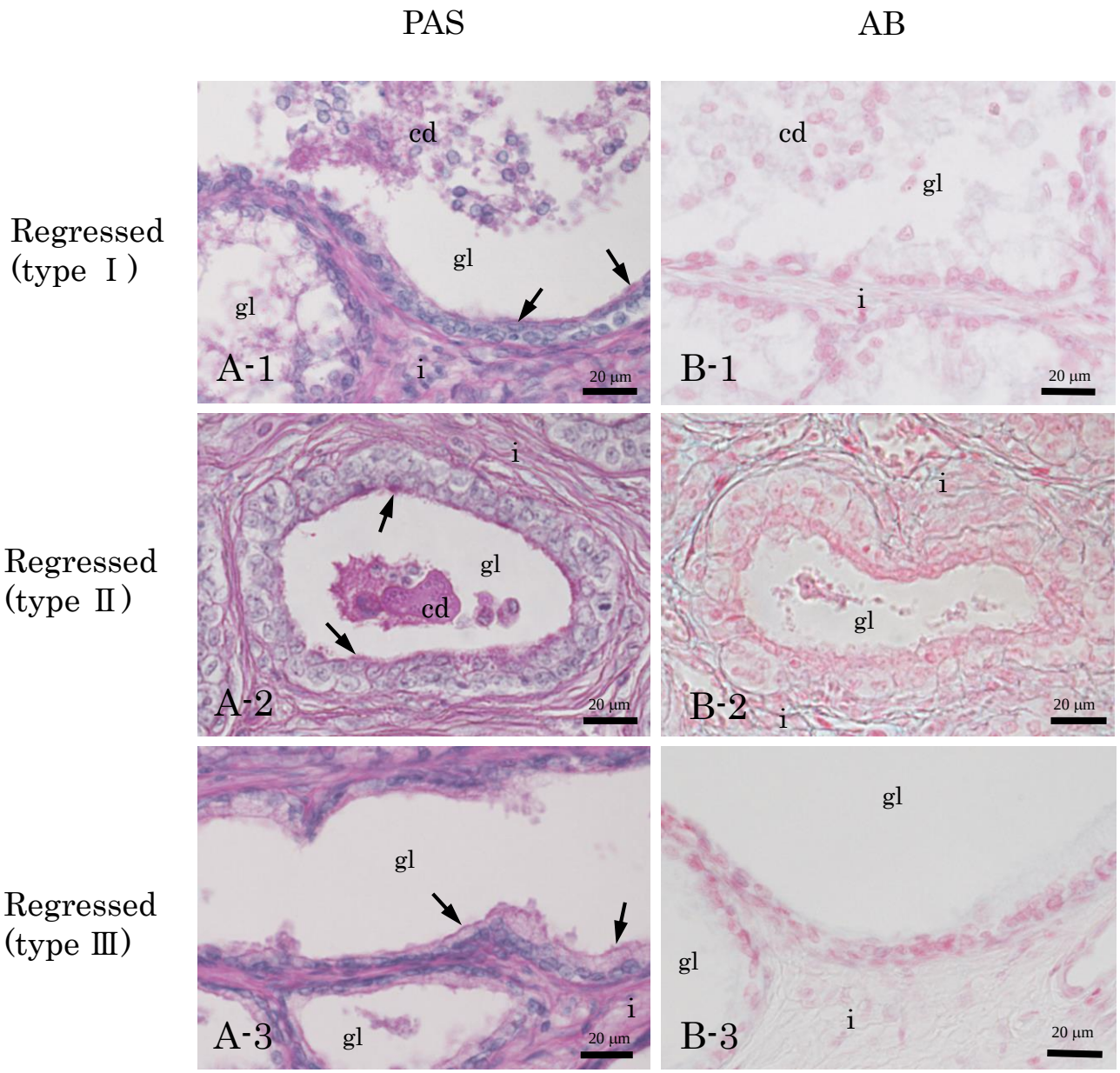

Fig. 2.5. PAS (A) and AB (B) staining of the regressed prostate gland. 1, regressed prostate gland (type I); 2, regressed prostate gland (type II); 3, regressed prostate gland (type III). In types I and II, PAS-positive cell debris was noticed in the lumen, and the luminal cells of all types were PAS-positive in the apical area of the cytoplasm. All types of the regressed prostate gland showed no AB-positive staining. arrows, PAS-positive luminal cells; am, ampulla of the deferent duct; cd, cell debris; dp, developed glandular part; i, interstitium; gl, glandular lumen; pu, prostatic urethra.

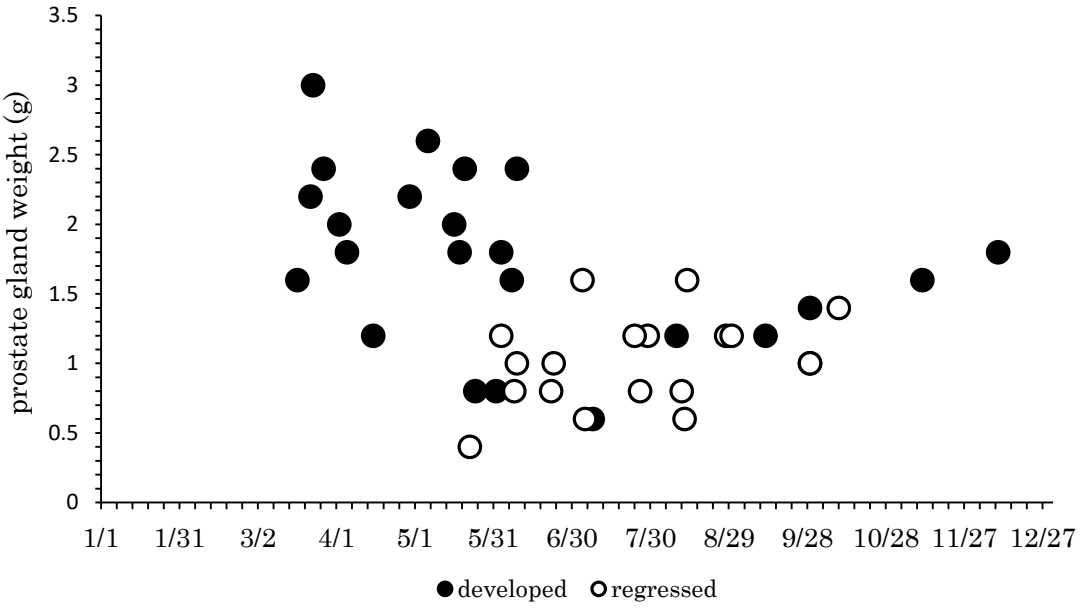

Fig. 2.6. Weight of prostate glands throughout the year (n=42). In summer, mainly the regressed prostate glands were observed, and this weight tended to be lighter. In spring, mainly the developed prostate glands were observed and the weight tended to be heavier.

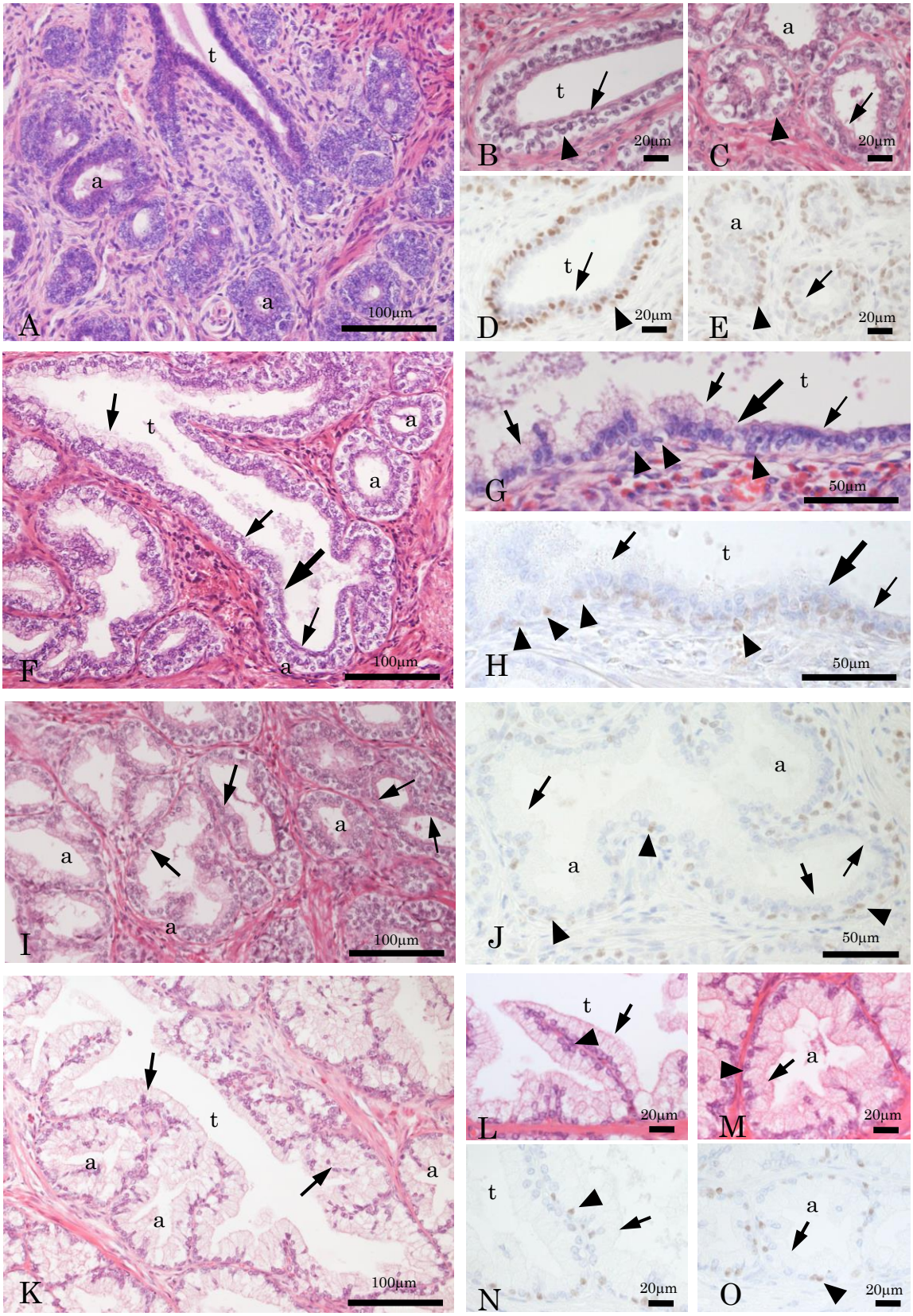
A
t
a
a
100μm
B
t
20μm
C
a
20μm
D
t
20μm
E
a
20μm
F
t
a
a
a
100μm
G
t
50μm
H
t
50μm
I
a
a
a
a
100μm
J
a
a
50μm
K
t
a
a
a
a
100μm
L
t
20μm
M
a
20μm
N
t
20μm
O
a
20μm

Fig. 2.7. Histological structure (HE staining) and p63 expression in each developmental stage. (A-E) Immature stage. (A) Histological image with tubular and alveolar gland parts, 8 months old. (B) Tubular gland part, 10 months old. (C) Alveolar gland part, 10 months old. (D) Tubular gland part, p63 immunostaining, 10 months old. (E) Alveolar gland part, p63 immunostaining, 10 months old. (F-J) Developing stage. (F) Histological image with tubular and alveolar gland parts in the proximal part of the tubular gland. 10 months old. (G) Tubular gland part, 12 months old. (H) Tubular gland part, 12 months old, p63 immunostaining. (I) Alveolar gland part, 6 months old. (J) Alveolar gland part, 6 months old, p63 immunostaining. (K-O) Developed stage. (K) Histological image with tubular and alveolar gland parts, adult. (L) Tubular gland part, adult. (M) Alveolar gland part, adult. (N) Tubular gland part, p63 immunostaining, adult. (O) Alveolar gland part, p63 immunostaining, adult. large arrow, border between columnar laminal cells and flattened or cuboidal laminal cells; middle arrows, columnar laminal cells; small arrows, flattened or cuboidal laminal cells; arrowheads, basal cells; a, alveolar gland; t, tubular gland.

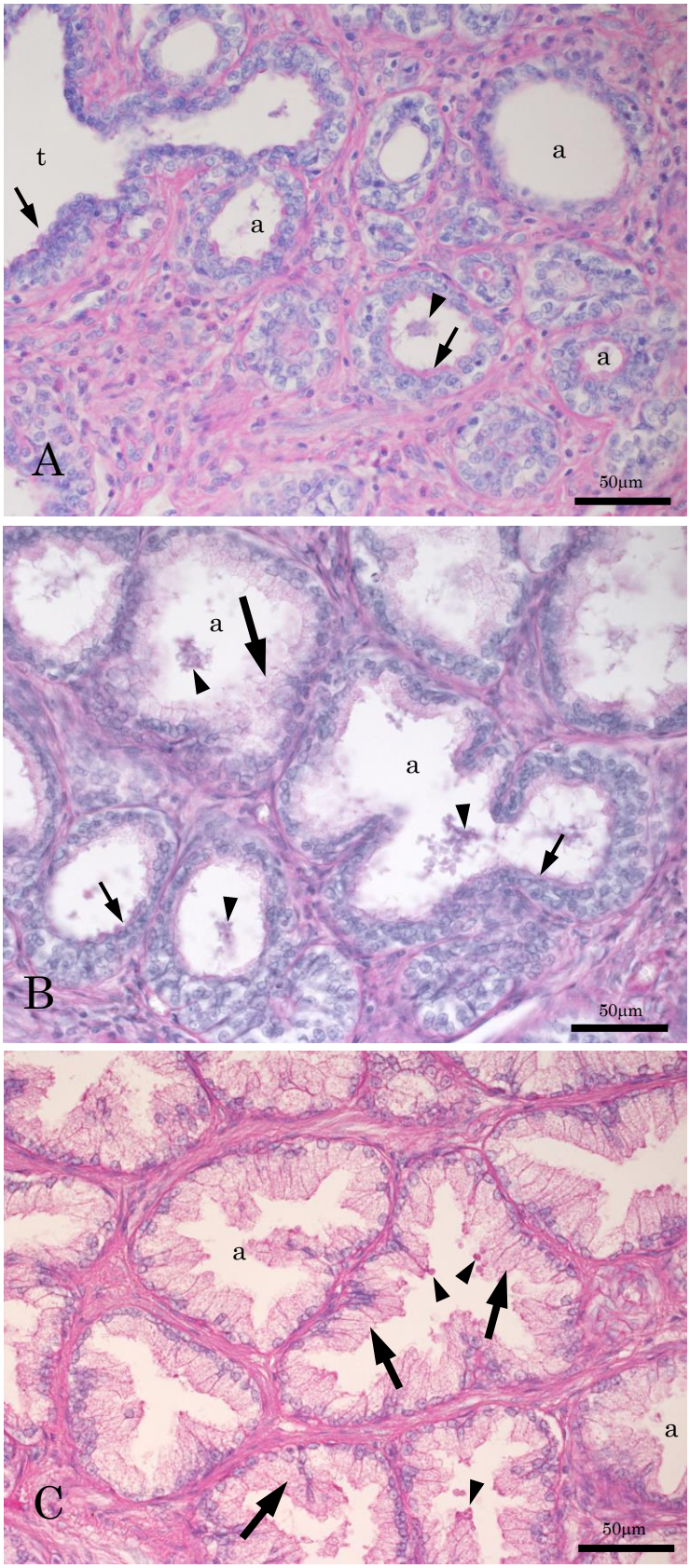

Fig. 2.8. PAS staining of each developmental stage of prostate glands. (A) Immature, 10 months old. (B) Developing, 8 months old. (C) Developed, adult. Large arrow, developed luminal cells with PAS-positive reactivity; small arrow, flatten or cuboidal luminal cells with PAS-positive reactivity; arrowhead, secretion; a, alveolar gland; t, tubular gland.

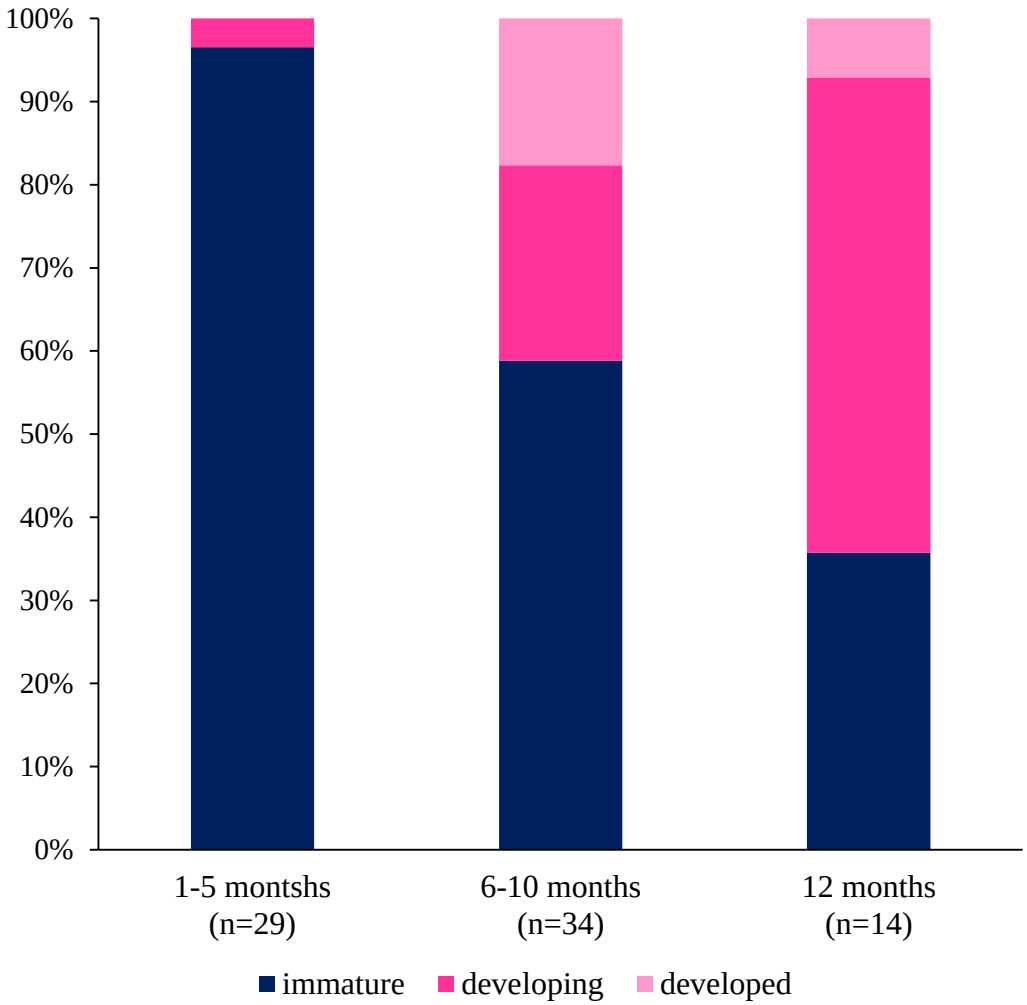

Fig. 2.9. Rate of each developmental stage of the prostate glands in three age groups of non-adult raccoons.

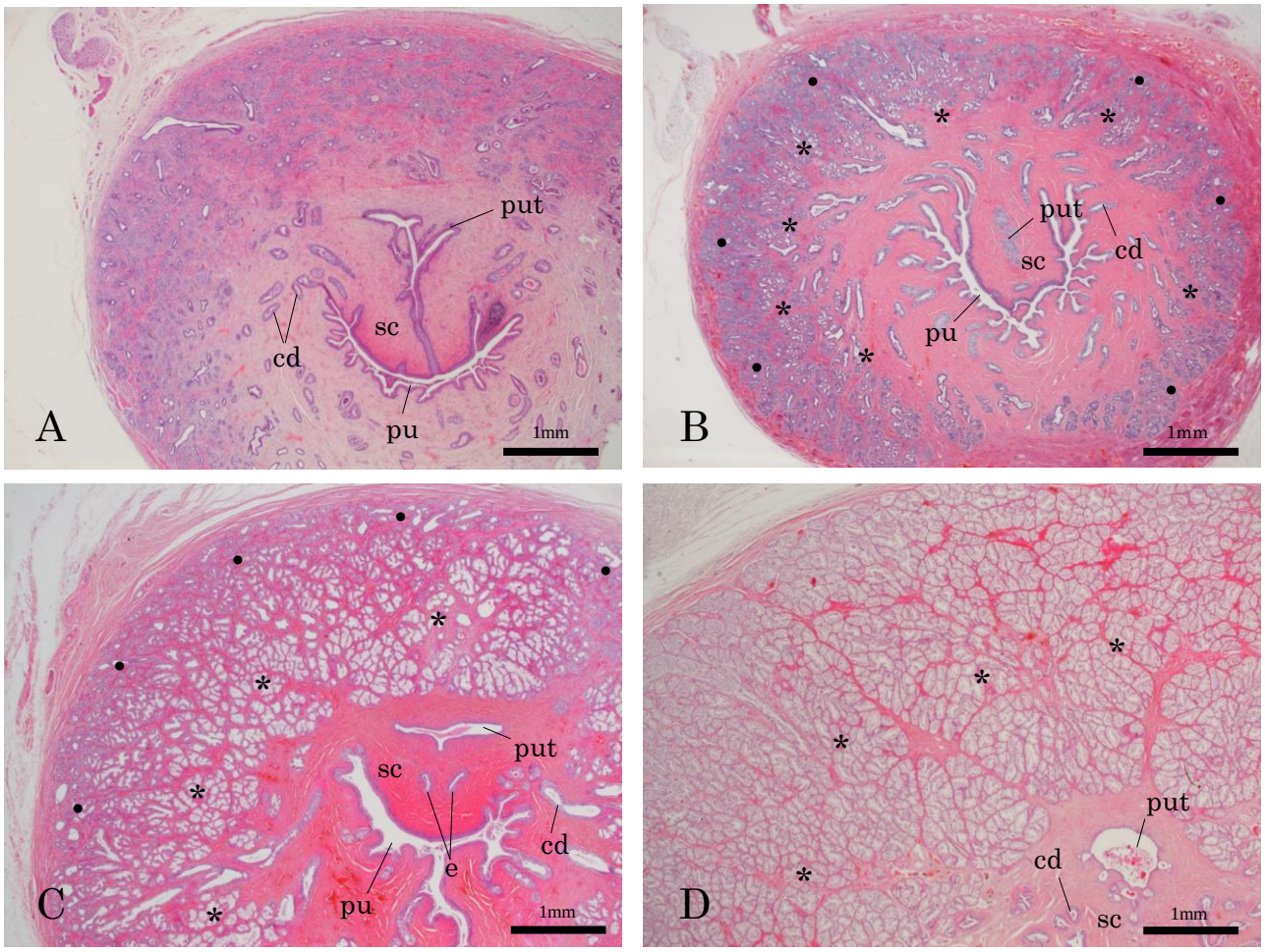

Fig. 2.10. Overall of the prostate glands in each developmental stage. (A) Immature, 8 months old. (B) Developing, 12 months old. (C) Developing, more developed than B, 10 months old. (D) Developed, adult. *, developed glandular part; ●, less developed glandular part; cd, correcting duct; e, ejaculatory duct; pu, prostatic urethra; put, prostatic utricle; se, seminal colliculus. HE staining.

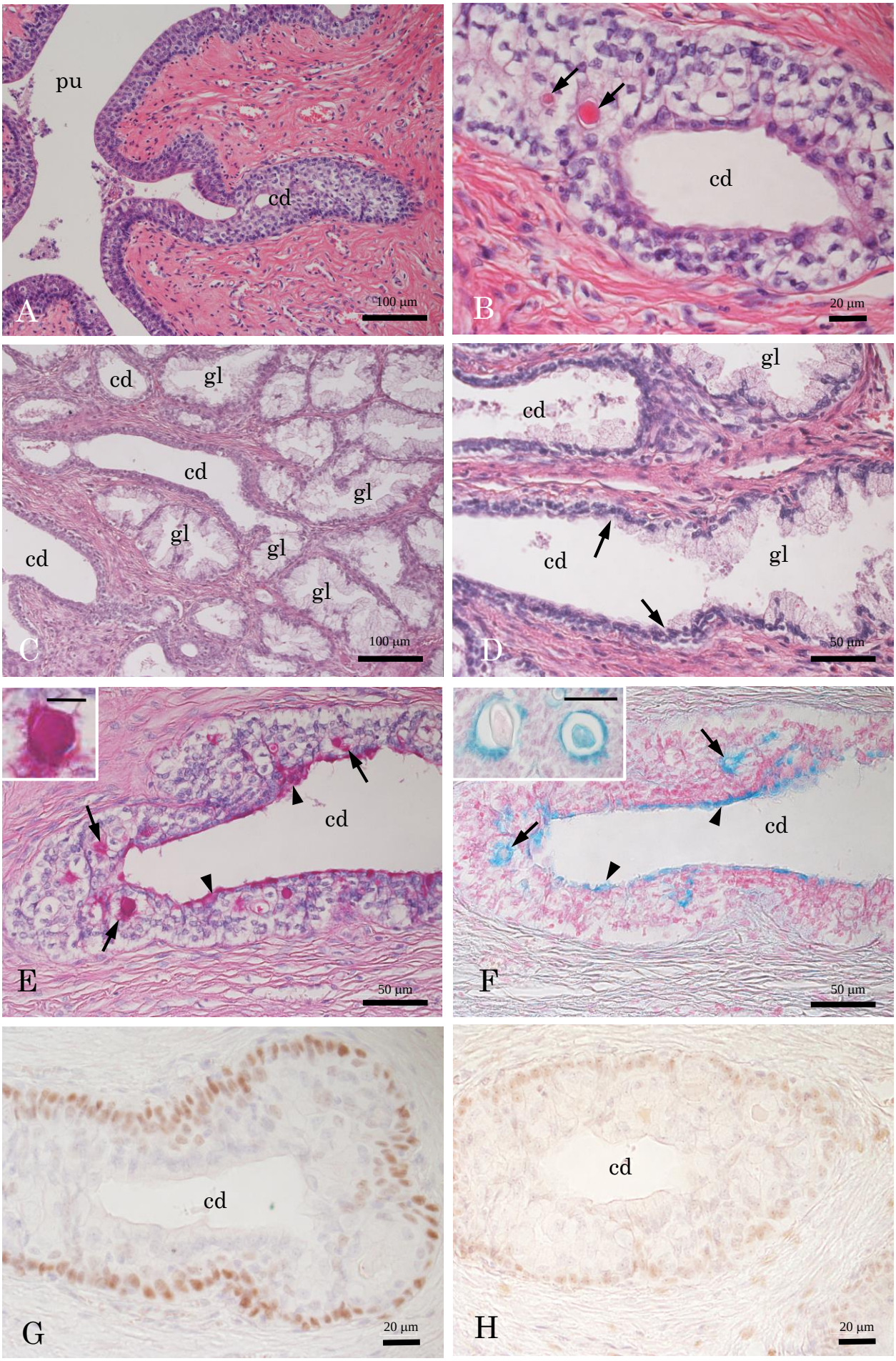
pu
cd
100 µm
A
cd
20 µm
B
cd
gl
cd
gl
gl
cd
gl
100 µm
C
gl
cd
cd
gl
50 µm
D
cd
50 µm
E
cd
50 µm
F
cd
20 µm
G
cd
20 µm
H

Fig. 2.11. The collecting duct of the prostate gland. (A) The collecting duct transferring to the prostatic urethra. The epithelial cells of the collecting duct were paler in color and swollen than those of the prostatic urethra. (B) The enlarged view of the collecting duct near the urethra. The most surficial cells were cuboidal in shape, and the cytoplasm was more acidophilic. The collecting duct had intraepithelial cysts with secretion (arrows). (C) The collecting ducts in the distal part. The number of epithelial cell layers decreased. (D) The enlarged view of the collecting ducts in the transitional part to the acinus (arrows). The epithelium of the collecting ducts showed almost two cell layers. (E) The intraepithelial cysts including secretion (arrows) and the superficial epithelial cells (arrowheads) of the collecting duct were PAS-positive. Insert shows enlargement of a cyst (bar =10 mm). (F) The superficial epithelial cells (arrowheads) and the epithelial cells which form the cysts (arrows) showed AB-positive. On the other hand, occasionally the secretion within the cysts was AB-positive although it was mainly AB-negative. An insert shows an enlargement of two cysts with different AB stainability in the secretion (bar = 50 mm). (G) The basal layer cells of the collecting duct showed p63 expression, but no p63 expression in the upper and middle part of the epithelial layer. (H) AR expression was also found mainly in the basal layer cells. cd, collecting duct; gl, glandular lumen; pu, prostatic urethra. A-D, HE staining; E, PAS staining; F, AB staining.

Chapter 3
Developmental Changes in the Prostatic Utricle of Raccoons

3.1 Introduction

The prostate gland often contains small sac-like structures called “prostatic utricle” within its tissue. The prostatic utricle is considered remnants of the female reproductive organs in males and has many other names that were once used, such as uterus masculinus, utriculus prostaticus, sinus prostate and sinus pocularis. Generally, the prostatic utricle is the blind-end structure found within the prostate gland located dorsal to the seminal colliculus, with an opening in the seminal colliculus. The prostate utricle has been reported in several animals (Zuckerman and Parkes, 1935; Sharma, 2010), including humans (Oh et al., 2009), but reports about it is not many. Among carnivores, the prostatic utricle has been reported to exist in dogs (Sharma, 2010) and minks (Basrur and Ramos, 1973), while in raccoons, there is no information about the prostatic utricle yet.

Formerly, the prostatic utricle with glandular structures was considered to correspond to the uterus, and the prostatic utricle lacking glandular structures was done to correspond to the vagina (Zuckerman and Parkes, 1935). In humans, glands were formed in the epithelium of the prostatic utricle during sexual maturation (Wernert et al., 1990), and it has been debated which it corresponds to the uterus or the vagina. Based on p63 expression, the human prostatic cavity is now thought to correspond to the vagina (Shapiro et al., 2004).

In this study, as a result of the investigation in Chapter 2, the prostatic utricle was found in the prostate gland of raccoons. In this Chapter, I examined the presence of the prostatic utricle in the prostate glands of raccoons at various developmental stages and the presence of gland structure in the epithelium of the prostatic utricle to characterize the prostatic utricle.

3.2 Materials and Methods

The prostate glands of 165 feral male raccoons were used in this study. Animals and sample preparations are described in the General Materials and Methods. Histological sections of the prostate gland were stained with HE, PAS, or AB. In addition, PAS staining was also performed after incubation with phosphate-buffered saline (PBS) containing 0.01% diastase for 50 min at 37°C. Moreover, the immunostaining for p63, PCNA was carried out. The prostate glands of under 6 months of age (n=29, infantile), between 6 and 12 months of age (n=48, juvenile) and over 12 months old (n=88, adult) were used for the observations of the prostatic utricle.

3.3 Results

The orifice of the prostatic utricle was located in the mid-line of the seminal colliculus, caudal to the ejaculatory duct (Fig. 3.1A). The prostatic utricle was located within the dorso-central connective tissue of the seminal colliculus (Figs. 3.1B and 3.2B-D) and was most commonly inverted flask-shaped that lodged within the prostate glands (Fig. 3.2C). In the length and shape of the prostatic utricle, there were large individual differences. The longest prostatic utricle was found within connective tissue between the ampulla of deferent ducts (Fig. 3.2A), and the shortest prostatic utricle was found only as a short and fine tubule structure at the orifice of the seminal colliculus (Fig. 3.2E). The prostatic utricles were blind and did not open to the body cavity (Fig. 3.3) and was not present in all raccoons (Fig. 3.2F). Table 3.1 shows the number of individuals with prostatic utricles in each developmental stage and in total number. There was little difference in the presence rate of prostatic utricles among developmental stages, and the rate to total number was 56%.

The prostatic utricle was frequently filled with secretions, and there were differences in the nature of the secretions (Fig. 3.4). In the infantile stage, secretion only with PAS- and AB- positive staining was observed (Fig. 3.4B1, C1). This secretion appeared to be secreted constantly regardless of developmental stages (Fig. 3.4B2, C2). Colloidal mass secretions began to appear from juvenile, were commonly observed in adults, and were positive for PAS but were negative for AB staining (Fig. 3.4B2, C2). These two types of secretions were present simultaneously in the prostatic utricle of the juvenile and adult stages (Fig. 3.4C2).

Occasionally, neutrophils, macrophages, cell debris and rarely eosinophils were observed in the prostatic utricle along with secretions (Fig. 3.5). when inflammatory cells were observed in the prostate utricle, infiltration of inflammatory cells into the prostatic utricle epithelium was observed (Fig. 3.5).

Mainly three characteristic structures were found in the epithelium of the prostatic utricle; sac-like glands, tubular glands and goblet cells. I described about the characteristics of three glands and infantile epithelium below. In the infantile stage, the prostatic utricle was stratified epithelium, and its luminal surface was positive for both PAS and AB (Fig. 3.6A). Formation of intraepithelial vacuoles was observed from the juvenile stage, and since the vacuoles contained secretions, they were regarded as intraepithelial glands called sac-like glands (Fig. 3.6B). The sac-like gland also contained PAS-positive and AB-negative colloidal mass secretions, and the area around the colloidal mass and the luminal surface of the vacuole showed AB positivity (Fig. 3.6B-2 and B-3). Multiple sac-like glands were scattered within the epithelium of the prostatic utricle, and the surface cells which composed the sac-like glands were thinly stretched (Fig. 3.6B). Tubular glands were absent during the infantile stage, but began to appear at the juvenile stage, and concomitant with sac-like glands in almost all cases in adult. Tubular glands extend basally and were composed of cells with pale cytoplasm (Fig. 3.6C-1). Like those of the sac-like glands, the tubular glands contained PAS-positive and AB-negative colloidal mass

secretions in the lumen, and the secretions surrounding the masses and luminal surfaces showed AB-positive (Fig. 3.6C-2 and C-3). Goblet cells were observed equally recognized at all developmental stages. All of observed goblet cells were located in the superficial layer of the epithelium, and were present singly or in clusters (Fig. 3.6D). Goblet cells and their secretions were positive for both PAS and AB (Fig. 3.6D-2 and D-3). Adults showed higher appearance rate in all gland types than the other developmental stages (Fig. 3.7).

In the prostatic utricle, the basal cells of the epithelium showed p63-positive (Fig. 3.8), Basal cells of the prostatic utricle epithelium in the infantile stage were positive for p63 (Fig. 3.8A), Both basal cells of the epithelium and the cells surrounding the sac-like glands showed p63-positive reaction (Fig. 3.8B). Moreover, tubular glands were formed by involving p63-positive cells (Fig. 3.9C).

PCNA-positive cells in the epithelium of the prostatic utricle were found in both the basal and superficial layers (Fig. 3.9A). In the sac-like and tubular glands, the cells on the luminal side were positive for PCNA (Fig. 3.9B).

3.4 Discussion

The prostatic utricle is a remnant of the female reproductive organs in males. During fetal life, Müllerian ducts are formed following Wolffian duct formation in both males and females (Kobayashi and Behringer, 2003). When the uterus and vagina are formed in females, a vaginal disc is formed at the junction of the Müllerian duct and the urogenital sinus, and then becomes a lumen to form the vagina (Cunha et al., 2017). In males also, after the Müllerian duct joined the urogenital sinus, the formed Müllerian ducts degenerate under the influence of anti-Müllerian hormone (AMH) (Kobayashi and Behringer, 2003). At the time of regression, the difference probably occurs in the structure of the prostatic utricle depending on the degree of regression. The prostatic utricle has been called by various terms, but there seem to be two main types among them. As the first type, the prostatic utricle is essentially a small sac-like structure that resides within the prostate gland, and this structure has been reported to exist in humans (McCarthy, 1927), primates (Zuckerman and Parkes, 1935), rabbits (Sharma, 2010), rats (Sharma, 2010), dogs (Sharma, 2010) and minks (Basrur and Ramos, 1973). In humans, it is now thought that a portion corresponding to the vagina remains in the prostate gland, and the name “male vagina” has been proposed (Puppo and Puppo, 2016). In this type, most of the uterus probably has regressed. As the second type, the term “uterus masculinus” also used in the past as another name for the prostatic utricle, has also been used in species that retain a uterine-like structure beyond the prostate glands, such as beavers (Conaway, 1958), European bisons (Swiezynski, 1968), donkeys (Shehata, 1978) and hoses (Shehata, 1978). These male animals have the bicornuate uterine-like structure at its upper end, and a recent study on bison prostate glands described the similar condition

which is known as the persistent Müllerian duct syndrome (PMDS) in humans. In this study, the second type was treated as PMDS and distinguish it from the term prostatic utricle.

Raccoons sometimes had prostatic utricles that extended beyond the prostate gland but were embedded within the connective tissue between the ejaculatory ducts and lacked a uterine-like structure. The raccoon prostatic utricle is located primarily within the prostate glands and was observed on the dorsal side of the seminal colliculus of the prostate. Therefore, the characteristics of the raccoon prostatic utricle seemed to be similar to those of the first type. There were large individual differences in the length and shape of the prostate utricles in raccoons, like in humans (McCarthy, 1927; Oh et al., 2009).

Furthermore, in this study, the appearance rate of prostate utricles in raccoons was 56% (93/165). In animals, percentage of presence was mentioned only in those considered to be PMDS; 75% (3/4) in horses, 100% (15/15) in donkeys (Sheata, 1978) and 83% in American beavers (Meier et al., 1998). Both PMDS and prostate utricles are treated as remnant structures, and the difference in the presence or absence and the shape probably reflects that the degree of degeneration varies from individual to individual. In the type of the prostate utricle, raccoons were classified into type 1 which was accompany by the large regression of the Müllerian duct although some individuals have a remnant structure with relatively long prostate utricles like PMDS. Therefore, lower presence rate of prostate utricles in raccoons than that in animals with type 2 may be due to a remarkable regression of the Müllerian duct. In raccoons, moreover, there was no large difference in the presence rate among each developmental stage, and thus there appears to be no regression or no emergence of the prostate utricles along with growth of postnatal development. Considering the fact that about half of the raccoons do not have prostate utricles, it is thought that the prostate utricles had no special functions.

The prostatic utricle opens into the seminal colliculus in all animals, but the positional relationship with the ejaculatory duct was different. In humans, the orifice of the prostatic utricle is located at approximately the same location as the ejaculatory duct on median line (Oh et al., 2009), and in dogs, the opening of the prostatic utricle is located slightly caudal to the opening of the ejaculatory duct (Sharma, 2010). In raccoons, the orifice was caudal to the opening of the ejaculatory duct, similar to that of dogs.

The epithelium of the prostatic utricle in raccoons showed multiple layers and was essentially p63-positive on the basal side. The human prostatic utricle becomes multi-layered during the fetal period (Shapiro et al., 2004), and the epithelium of the prostatic utricle in other animals has been reported to be pseudostratified (Zuckerman and Parkes, 1935) or stratified epithelium (Sharma, 2010). In humans, the p63-positive epithelium has suggested that the prostatic utricle originates from the urogenital sinus and primarily corresponds to the vagina (Shapiro et al., 2004). Thinking similarly, the prostatic utricle of raccoons was also equivalent to the vagina. In addition, as will be discussed in the Chapter 4, in

raccoons, the cervix is p63-positive stratified epithelium, so the prostatic utricle may correspond not only to the vagina but also to the cervix.

The epithelium of prostate utricles in the raccoon changed with sexual maturation. The epithelium of the prostatic utricles formed sac-like and tubular glands as it matured. In humans, the prostatic utricle also grows from fetal to adulthood, and in adult, the prostatic utricle shows similar morphology and similar immunoreactivity (PAP+, PSA+) to the prostate glands (Wernert et al., 1990). In raccoons, however, the morphology of the prostatic utricle does not resemble that of the prostate glands, and the appearance of the glands such as sac-like and tubular glands are clearly distinguishable from the prostate glands. The presence of p63-positive cells around the sac-like glands indicates that the sac-like gland is formed within the epithelium of the prostatic utricle. The tubular glands were continuous with the epithelium of the prostatic utricle and surrounded entirely by p63-positive cells, suggesting that the tubular glands of the prostatic utricle may derive from the sac-like glands.

In the raccoon prostatic utricle, the properties of secretions changed with epithelial changes (Fig. 3.10). In the infantile stage, both PAS and AB positive secretions were predominant, and PAS positive and AB negative secretions were rarely observed (Fig. 3.10A). The sac-like and tubular glands, which increase with maturity, secreted the secretions with PAS positive and AB negative (Fig. 3.10C). Stainability of this secretion resembled that of the intraepithelial gland of the raccoon prostatic duct. Prostatic utricle secretions of rats, rabbits, dogs and humans show PAS-positive and AB-negative similar to those of raccoons. In postpubertal humans, the prostatic utricles resemble the prostate glands in the point that each gland secrets both of PAP and PSA, known as prostatic secretions (Wernert et al., 1990). In the raccoon, it is interesting to examine the secretory compositions in the prostatic utricles and prostate glands.

In conclusion, the presence of the prostatic utricle was revealed in the prostate glands of the raccoon for the first time. The prostatic utricle of raccoons showed various shapes and the basal side of its epithelium expressed p63-positive, suggesting that it is homologous to the vagina and cervix. The prostatic utricle had sac-like and tubular glands, and goblet cells. The sac-like and tubular glands first appeared in juvenile stage and increased with the maturation. Moreover, lumen had secretions with PAS- and AB-positive in infantile stage, on the other hand, in adults, the secretions with different properties such as PAS- and AB-positive, and PAS-positive and AB-negative secretion were secreted into the lumen from the sac-like and tubular glands. It was revealed that the prostatic utricle showed morphological and functional changes along with maturation.

Table 3.1. Number and appearance rate of the prostatic utricle in each postnatal developmental stage

age	number	percentage
infantile (n=29)	19	66%
juvenile (n=48)	26	76%
adult (n=88)	48	75%
total (n=165)	93	56%

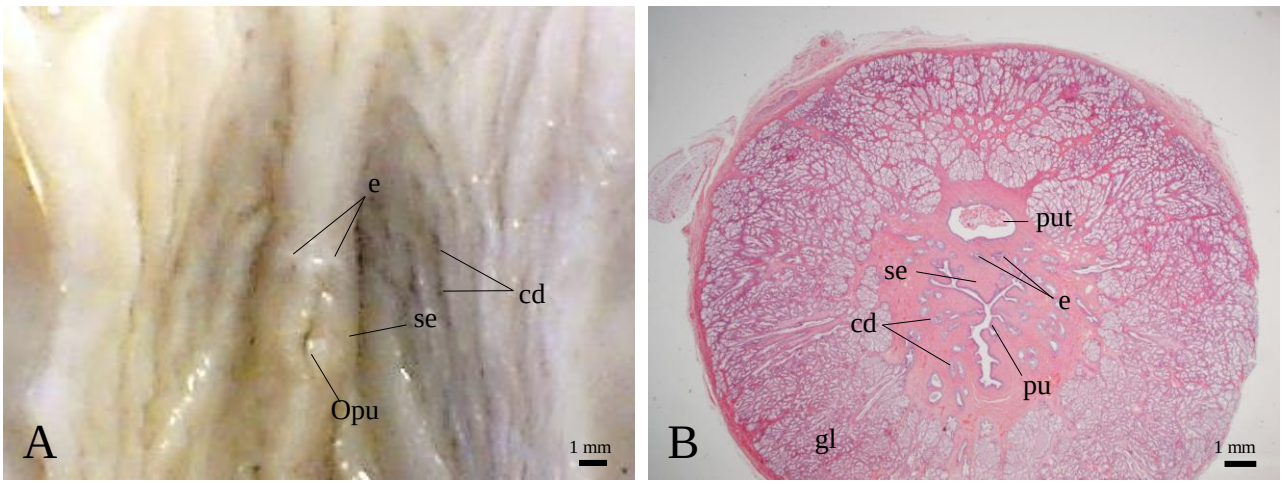

Fig. 3.1. Opening and location of the prostatic utricle. (A) Gross anatomy of the formalin fixed prostatic urethra. Ventral part of the prostatic urethra was cut open (ventral view). (B) Histological observation of the prostate gland cut at maximum diameter. cd, correcting duct; e, ejaculatory duct; gl, glandular lumen; Opu, orifice of prostatic utricle; pu, prostatic urethra; put, prostatic utricle; se, seminal colliculus.

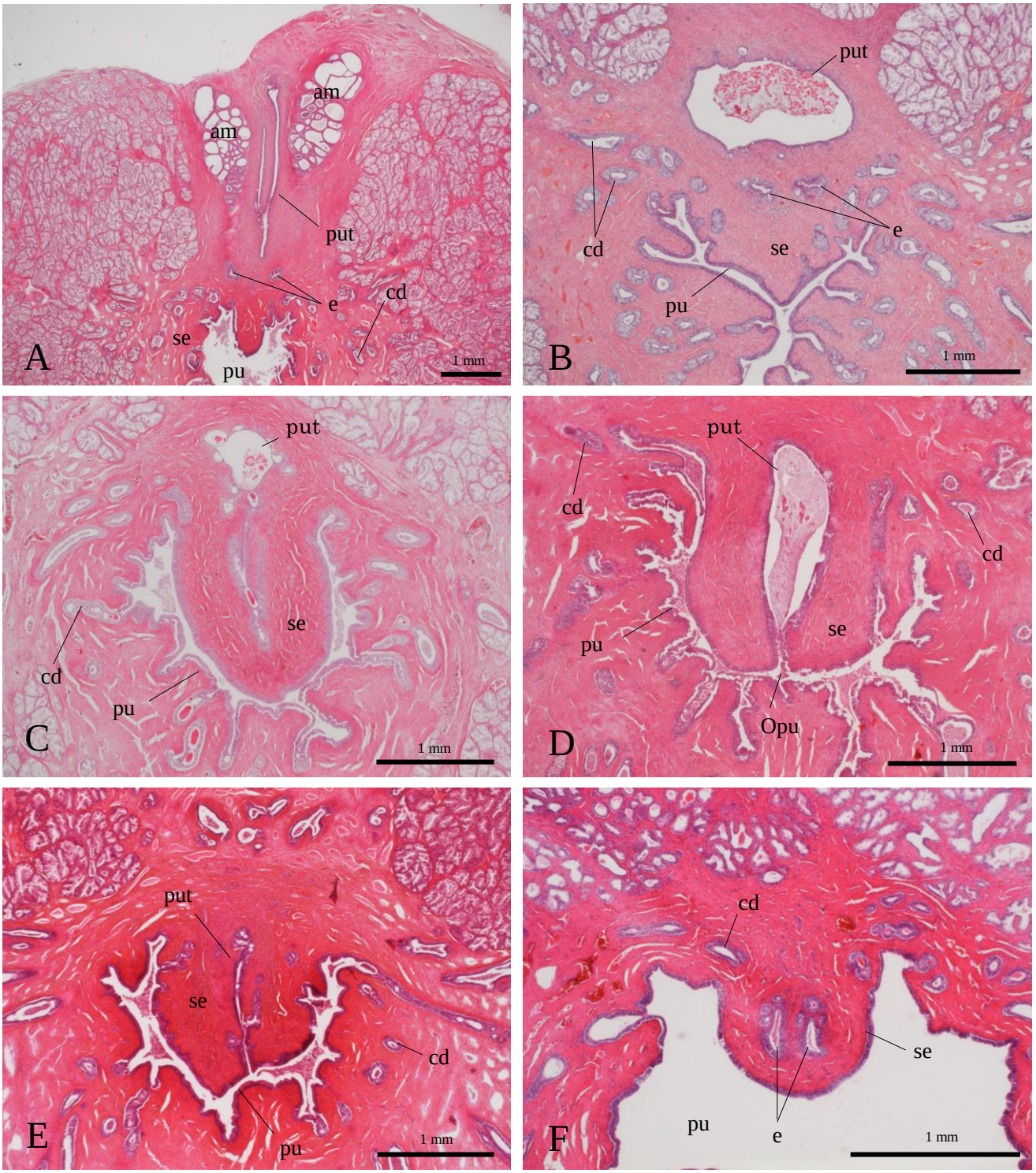

Fig. 3.2. Histological observation of the prostatic utricle. (A) Prostatic utricle between ampulla of the deferent ducts. (B) Prostatic utricle in the prostate gland cut at maximum diameter. (C) Prostatic utricle with inverted flask-shape. (D) Prostatic utricle continuing the orifice. (E) Prostatic utricle with short and fine tubule structure. (F) Prostate gland without the prostatic utricle. am, ampulla of the deferent duct; cd, correcting duct; e, ejaculatory duct; Opu, orifice of prostatic utricle; pu, prostatic urethra; put, prostatic utricle; se, seminal colliculus.

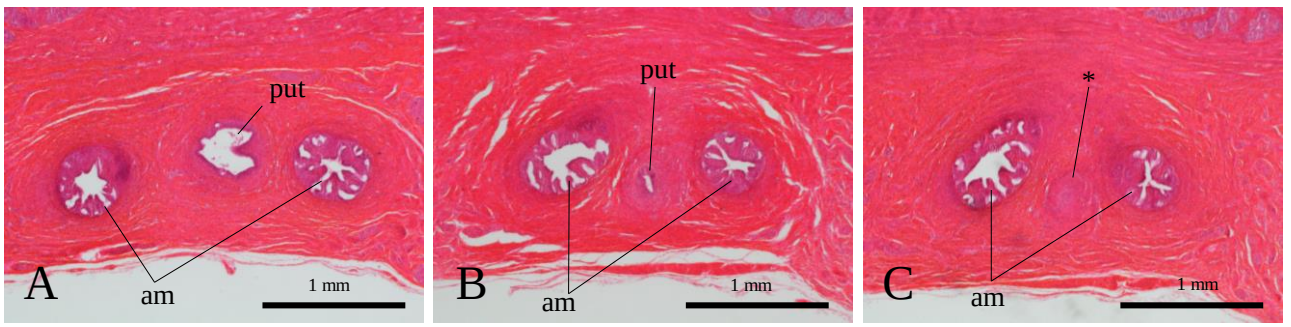

Fig. 3.3. Prostatic utricle with blind end in same infantile raccoon. (A) caudal part, (B) Prostatic utricle between A and C. (C) Cranial blind end part. *, blind end of prostatic utricle; am, ampulla of the deferent duct; e, ejaculatory duct; put, prostatic utricle.

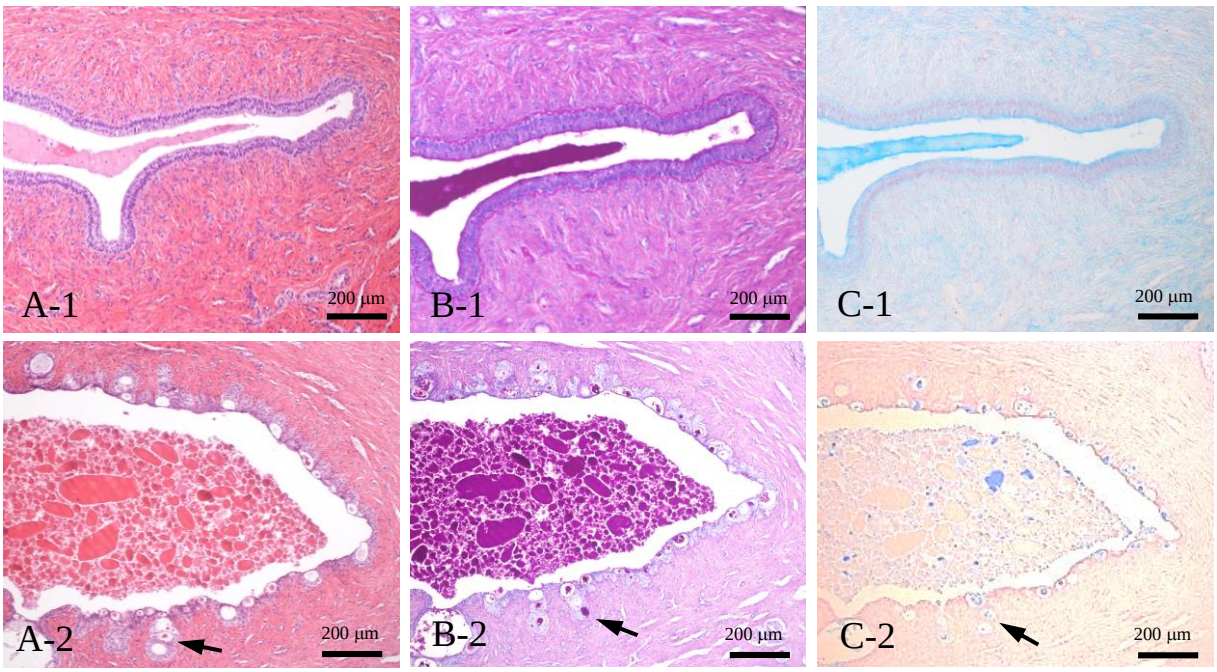

Fig. 3.4. PAS and AB staining of the prostatic utricle. (A) HE staining. (B) PAS staining. (C) AB staining. (1) Infantile. (2) Adult. Arrows indicate tubular gland.

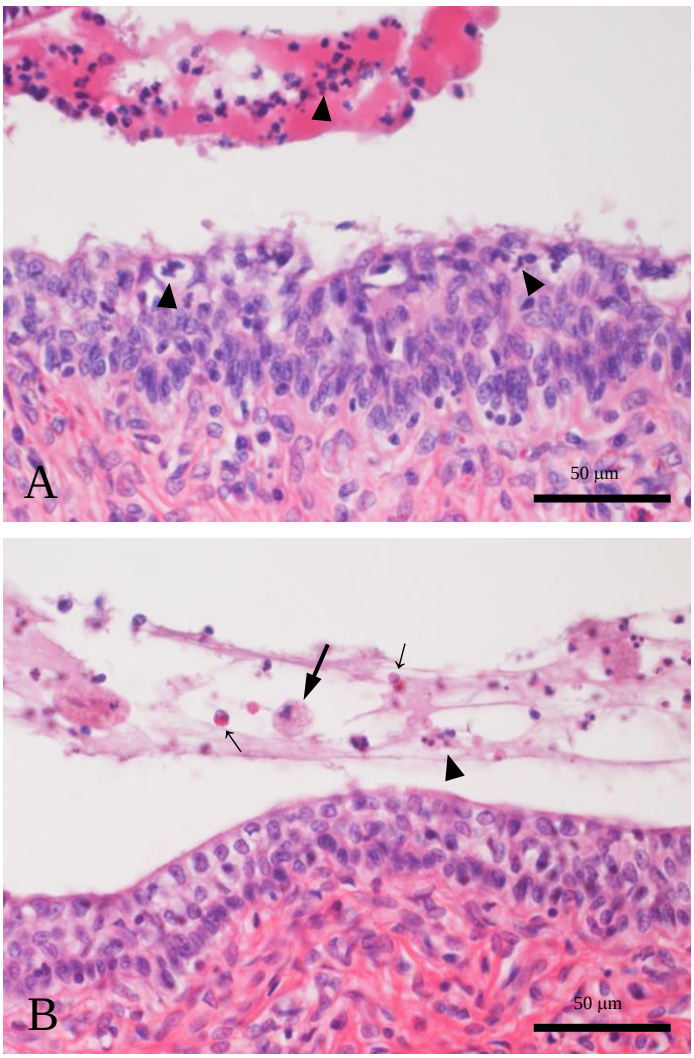

Fig. 3.5. Appearance of inflammatory cells in the prostatic utricle. (A) Infantile, the prostatic utricle with neutrophils (arrowheads). (B) Infantile, the prostatic utricle with neutrophils (arrowheads), eosinophils (small arrows) and macrophage (large arrow).

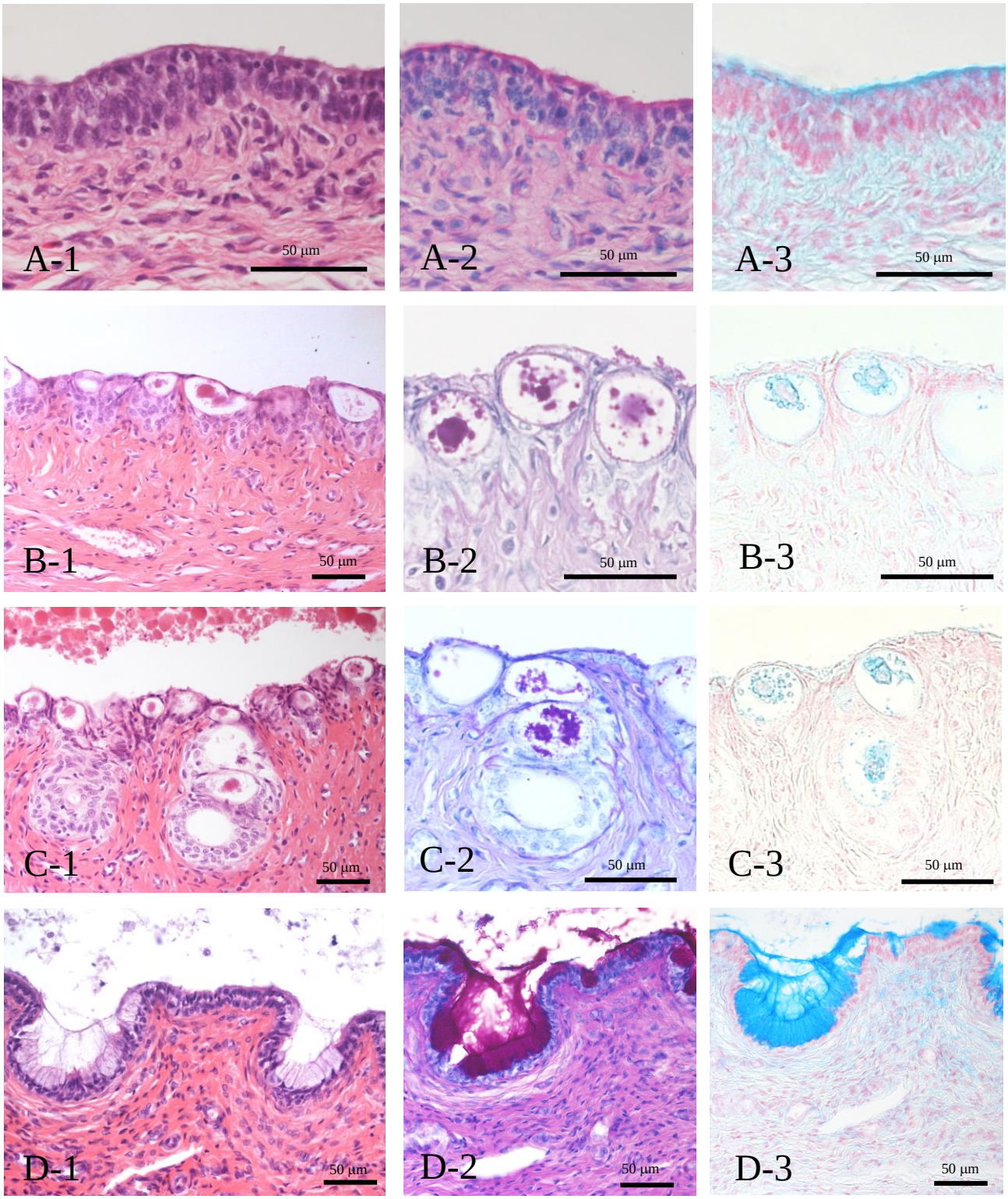

Fig. 3.6. Three epithelial gland structure in the prostatic utricle. (A) Epithelium of the prostatic utricle with a few gland structure, infantile. (B) Sac-like gland, adult. (C) Tubular gland, adult. (D) Goblet cells, adult. (1) HE staining. (2) PAS staining. (3) AB staining.

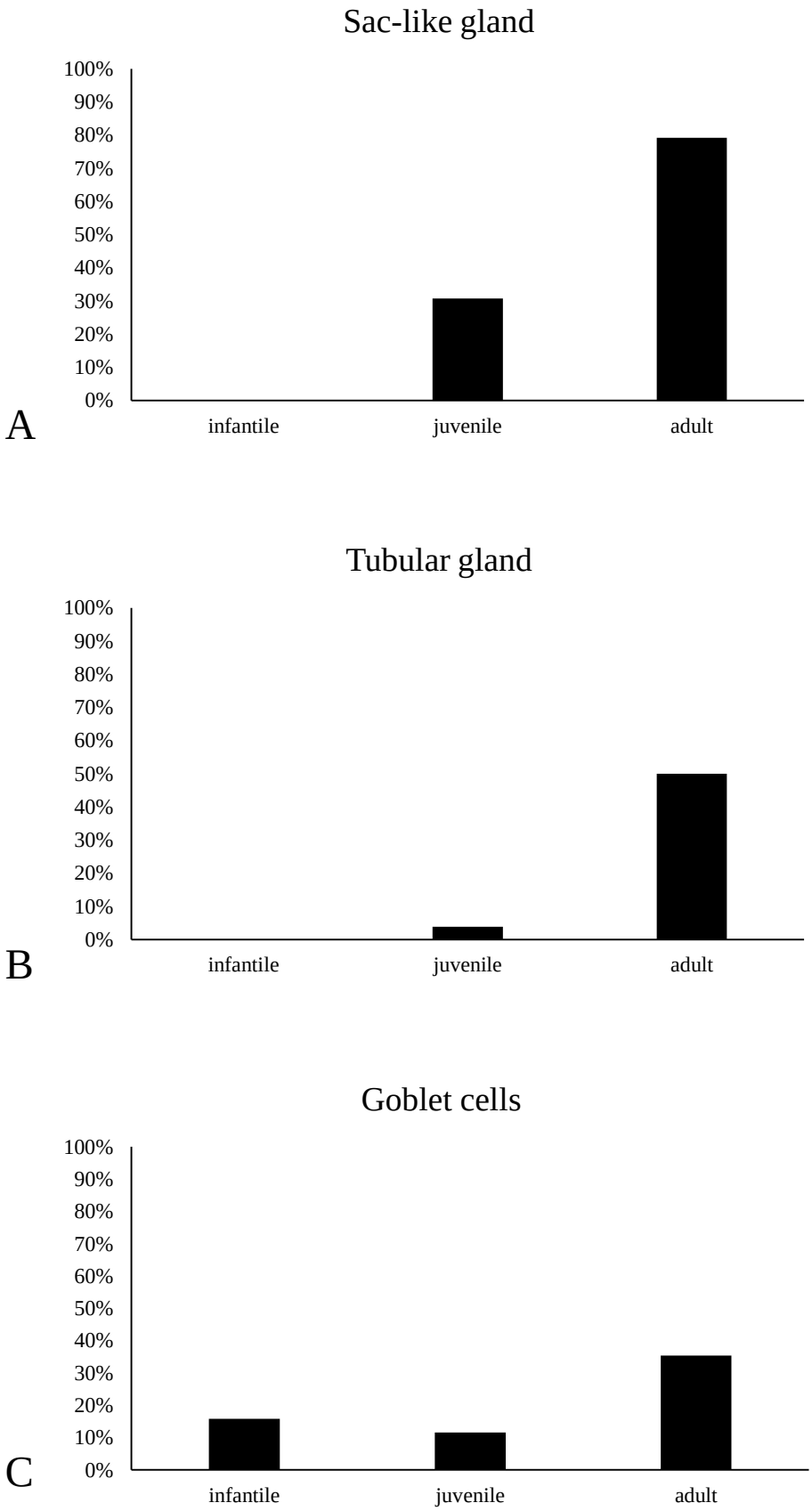

Fig. 3.7. Appearance rate of each gland type in the prostatic utricle at each developmental stage. (A) Sac-like gland. (B) Tubular gland. (C) Goblet cells.

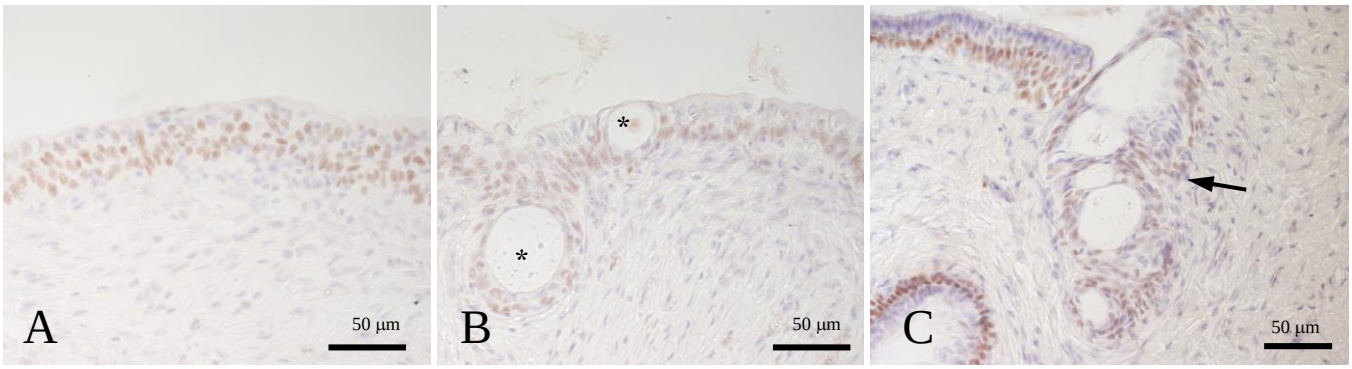

Fig. 3.8. Immunoreactivity for p63 in the epithelium of the prostatic utricle. (A) Infantile stage. (B) Sac-like gland. (C) Tubular gland. Arrow indicates tubular gland; *, sacklike gland.

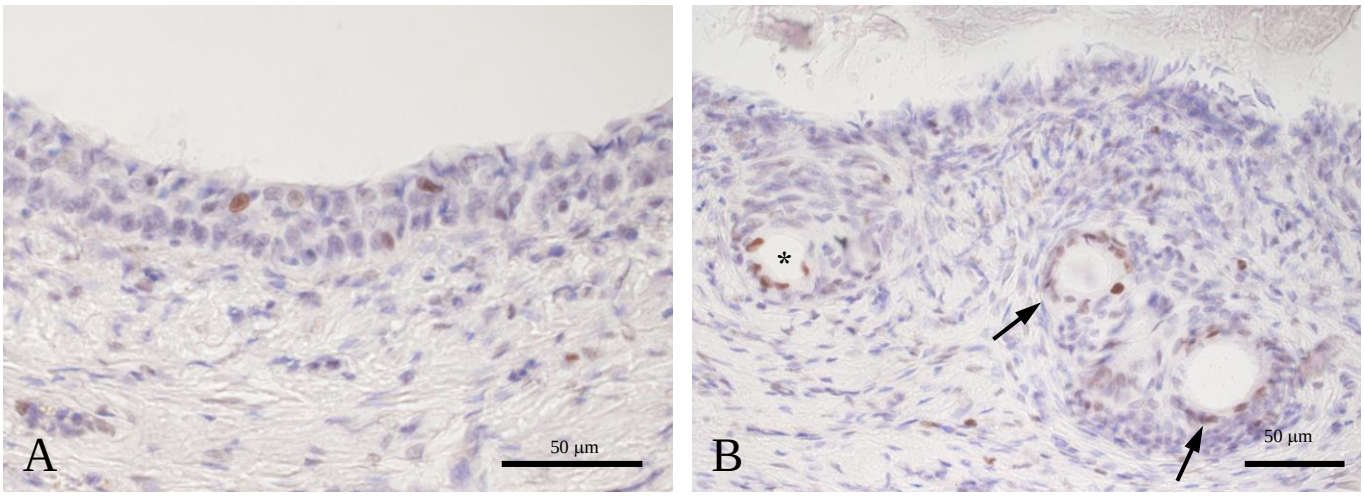

Fig. 3.9. Immunoreactivity for PCNA in the epithelium of the prostatic utricle. (A) Infantile stage. (B) Sac-like gland. Arrows indicate tubular gland; *, sac-like gland.

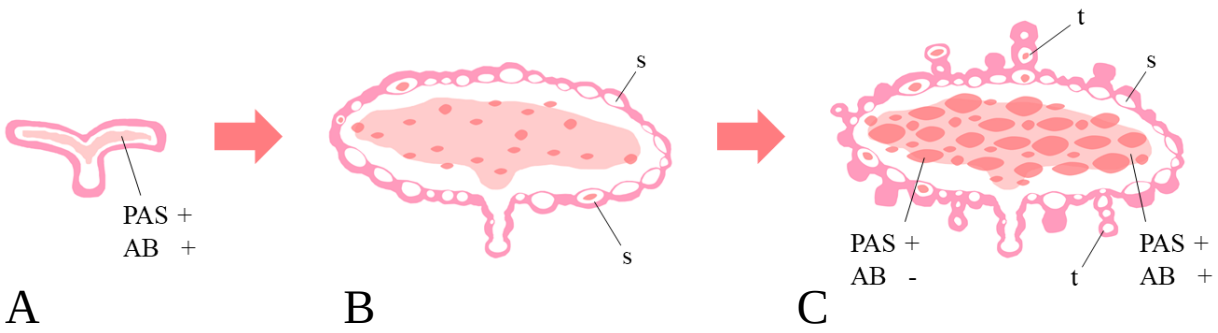

Fig. 3.10. Change in secretory component within the lumen of the prostatic utricle with postnatal development. (A) Infantile. (B) Juvenile. (C) Adult. s, sac-like gland; t, tubular gland.

Chapter 4
Morphological changes in the cervix of raccoons during pregnancy

4.1 Introduction

As a result of investigating the prostatic utricle of raccoons in Chapter 3, the prostatic utricle formed glands with sexual maturation. The formation of glands in the prostatic utricle suggested that the female genital organs retained in males have the capacity to form glands. However, in raccoons, because there are limited histological reports of female lower genital organs (reproductive tracts), it remained unclear whether the ability to form glands exists in the female genital organs. The female genital organs of raccoons have been reported in detail about ovary and uterus, and there are limited histological reports of the vagina and no histological reports of the cervix (Sanderson and Nalbandov, 1973).

Raccoons are pregnant for about 63 days (Sanderson and Nalbandov, 1973), and the corpus luteum is present throughout pregnancy (Sanderson and Nalbandov, 1973). Second estrus is known, in which estrus occurs again during pregnancy or when a child is lost soon after childbirth (Gehrt and Fritzell, 1996), and secondary estrus allows raccoons to reproduce reliably within the year. Characteristics that regain reproductive opportunities, such as secondary estrous, are known, but in raccoons, there is no information about regulatory mechanisms of female genital organs during pregnancy. Therefore, it was necessary to examine the role of cervix in pregnancy in raccoons.

An accumulation of mucus produced in the cervix is known as the cervical mucous plug (CMP) that protects the fetus during pregnancy (Becher et al., 2009; Timmons et al., 2010; Nott et al., 2016). The most important role of CMP is to prevent upward bacterial infection (Becher et al., 2009).

The epithelium of the cervix produces mucus. The cervix epithelium of the human is a simple columnar epithelium with folds (Nott et al., 2016), and the structures called cervical mucous glands in humans are actually folds of the epithelium (Nott et al., 2016). In humans, the stimulation by progesterone alters the properties of mucus, making it more viscous (Nott et al., 2016). On the other hand, the epithelium of the cervical canal was stratified epithelium in dogs (Goericke-Pesch et al., 2010). In the raccoon, however, the morphological structure and functions of the cervical epithelium are unknown. In this study, to clarify the characteristics of the cervix, I examined the raccoon cervical epithelium of non-pregnant and pregnant raccoons in detail.

4.2 Materials and Methods

The cervix of 46 (6 juveniles, 21 non-pregnant adults, and 19 pregnant adults) was examined in detail. The crown-rump length (CRL) of the fetus obtained from the pregnant individual was measured,

and the fetal age was estimated from CRL (Llewellyn, 1953), and classified into 6 age groups: 0-9 days, 10-19 days, 20-29 days, 30-39 days, 40-49 days, 50-63 days. Animals and sample preparation are described in the General Materials and Methods. Histological sections of the cervix were stained with HE, PAS, or AB (pH 2.5). The immunostaining for p63 and PCNA was carried out.

4.3 Results

Non-pregnant

In raccoons, the large vaginal fornix located dorsolateral to the vaginal part of cervix (Fig. 4.1B, C). The external uterine orifice was opened caudodorsally (Fig. 4.1A-C). The external uterine orifice was small and not opened in non-pregnant adult raccoons (Fig. 4.1A). Cervical and vaginal epithelia were continuous and had no clear boundary, and both epithelia showed p63 positive in basal side (Fig. 4.1D, E).

The cervix of raccoons was generally multilayered in 6 months old and adult (Fig. 4.2). Both non-adult and adult cervical epithelia had scattered goblet cells on the surface (Fig. 4.2F-H), and sometime had intraepithelial cyst (Fig. 4.2A, B, E). The cervix had 7-9 longitudinal folds (Fig. 4.2A, B).

Pregnant

At 27 days of gestation, the vaginal part of cervix was protruded more dorsally than non-pregnant raccoons, and its external uterine orifice was not opened (Fig. 4.3A). At 60 and 63 gestation days, viscous mucus was observed macroscopically to accumulate from the cervix to the vagina (Fig. 4.3B-D). This mucus was tightly packed in the cervical canal and vaginal fornix, blocking the canal (Fig.4.3B-E). At 63 days of gestation, the external uterine orifice was dilated, but was not opened to the outside world because it was densely packed with mucus (Fig. 4.3D).

In pregnant individuals, the surface layer of the cervical epithelium was replaced by goblet cells or columnar mucus cells (Fig. 4.4), and the epithelial replacement progressed with increasing of gestational days (Fig. 4.4). As epithelial replacement progressed, mucus secretion increased, and viscous mucus with AB and PAS-positive accumulated in the cervical cavity (Figs. 4.4 and 4.5; PAS staining, data not shown). In particular, raccoons with more than 30 days of gestation had so much cervical mucus that it blocked the lumen of the cervix (Fig. 4.5, Table 4.1). During progression of pregnancy, the cervical epithelium remained multilayered, and epithelial layers was present beneath the mucous cells (Fig. 4.4).

As the gestational day increases, the cervical lumen was dilated. In particular, the dilating was remarkable in raccoons whose estimated gestational days exceeded 57 days, and folds of the cervical epithelium were papillary as a result of dilation (Figs. 4.5A-4, 5 and Fig. 4.6). At this time, most of the cervical epithelium showed folding of epithelium without stroma was observed (Figs. 4.4A-4, 5 and Fig.

4.6E). Although most of the cervical epithelium was replaced by mucous cells at full-term gestation (63 days), p63-positive cells remained present on its basal side (Fig. 4.6).

In the internal uterine orifice, the cervical epithelium and endometrial epithelium were partially mixed in the cross section (Fig. 4.7). The endometrium is single-layered with uterine glands and showed p63 negativity, distinguishing it from the multilayered cervical epithelium with p63 (Fig. 4.7). At full-term gestation, the cervical epithelium of the internal cervical orifice was also papillary and replaced by mucous epithelium (Fig. 4.7B, C). Occasional cervical epithelium overlying the uterine gland was seen (Fig. 4.7B).

Differentiation into mucous cells was often seen in the basal to intermediate layers of the multilayered epithelium (Fig. 4.8), and differentiation into mucous cells was also observed in intraepithelial cysts (Figs. 4.8B and 4.9). Both intraepithelial cysts and mucous cells were present in the cervical epithelium at 6 months of age (Fig. 4.9A). Intraepithelial cysts were most common on day 27 of gestation (Fig. 4.9B). Intraepithelial cysts often contained cell debris, neutrophils and secretions (Fig. 4.9B-D), and similar objects were also present around folding of epithelium (arroehead in Fig. 4.9D).

Many cells in the cervix were not positive for PCNA in both juvenile and non-pregnant adult, and PCNA-positive cells were distributed in the epithelial surface layer (Fig. 4.10A). In particular, PCNA positive cells localized around invagination of the epithelium (Fig. 4.10A, D). At 27 days of gestation, mucus cells in the surface layer of the epithelium were PCNA-positive, and the cells in the luminal surface of the intraepithelial cysts were also PCNA-positive (Fig. 4.10C). PCNA positivity was also observed in the superficial mucous cells of the multilayered epithelium and around the intraepithelial cyst in the early pregnancy (Fig. 4.10C). At 51 days of gestation, PCNA-positive cells were found in both the basal and superficial layers of the epithelium, and mucous cells were also PCNA-positive. At full-term gestation (63 days), PCNA positivity was observed in sporadically in epithelial basal layer and mucous cells, and PCNA positive was observed in the lower layer of intraepithelial cysts (Fig. 4.10E, F).

4.4 Discussion

The deepest part of the vaginal fornix in raccoons was located dorsally. However, the vaginal fornix of cats is on the ventrolateral to the cervix (Zambelli and Cunto, 2005), the vaginal fornix of minks is deeper ventrally than dorsally (El-Banna and Hafez, 1972), and the vaginal fornix of dogs lies cranioventral to the cervix (Evans and Christensen, 1979). Different positions of the vaginal fornix relative to the cervix suggested different positions of the junction of the vagina and the cervix. Such positional differences of the cervix occurring within the order Carnivora may be due to differences in fetal development.

The cervical epithelium of non-pregnant adult raccoons was stratified epithelium similar to that of dogs (Goericke-Pesch et al., 2010). Near the internal uterine orifice of raccoons, at transition between stratified epithelium and simple columnar epithelium, uterine glands sometimes were beneath the stratified epithelium. In microminipigs, the cervical epithelium is simple columnar epithelium, and nodular area of stratified epithelium is seen below the columnar epithelium at the transition part near the external uterine orifice (de Rijk et al., 2014).

As pregnancy progressed, the stratified epithelium was replaced by mucous cells in raccoons. The mucus seen in late gestation of raccoons was abundant, filling the lumen of the cervix and pooled in the vaginal fornix. Referring to the definition of CMP in humans (Becher et al., 2009), the abundant mucous seen in the cervix of raccoons was CMP. Epithelial mucification of the vaginal epithelial associated with pregnancy is known in the mouse (Sugiyama et al., 2021), and mucification epithelium forms mucous plug (Lacroix et al., 2020). The mouse vagina normally is squamous epithelium, but as pregnancy progresses, the thick mucous cell layer was formed in the surface layer of the squamous epithelium (Sugiyama et al., 2021). In the experiment of progesterone administration, mucification of the vaginal epithelium in mice is reportedly due to progesterone stimulation (Gopinath, 2013). Progesterone stimulation switches the cervical mucus to a viscous character, resulting in CMP formation (Becher et al., 2009). Considering that raccoons have a corpus luteum throughout pregnancy (Sanderson and Nalbandov, 1973), in this study, mucification of the cervical epithelium and CMP formation were suggested to be induced by progesterone from corpus luteum during pregnancy.

Suprabasal mucus cells exist just above the basal layer and are thought to be the progenitor cells of mouse mucus cells (Sugiyama et al., 2021). In raccoons, differentiation of mucus cells occurs in the basal-to-intermediate layers in the cervical epithelium, and mucin cell progenitors of raccoons may be present above the basal layer as in mice. In non-pregnant mice, only the basal side of the vaginal epithelium became PCNA-positive (Sugiyama et al., 2021), whereas in non-pregnant raccoons, the superficial layer of the cervical epithelium was often PCNA-positive. In pregnant mice, mucous cells were not PCNA-positive (Sugiyama et al., 2021), but in pregnant raccoons, mucous cells were also PCNA-positive. In raccoons, differentiated mucous cells may be able to proliferate independently, and this feature distinguished them from mice.

In dogs, administration of progesterone resulted in the formation of numerous intraepithelial cysts in the cervical epithelium (Nelson and Kelly, 1976). A large number of intraepithelial cysts may be formed in raccoons as well due to the effects of progesterone during pregnancy. In raccoons, the intraepithelial cysts may spread from the inside because the lining cells of the intraepithelial cysts showed PCNA-positive. As mucous cells proliferate within the intraepithelial cysts and secrete mucus, the intraepithelial cysts expand from the inside, and the surface epithelium of the intraepithelial cysts

may become thin and stretched (Fig 4.11). Intraepithelial cysts that could no longer withstand expansion from the inside may rupture and may release their contents (Fig 4.11). It was suggested that the rupture of intraepithelial cysts form the epithelial folds by the ripped surface epithelium (Fig 4.11). In raccoons, intraepithelial cysts often contained neutrophils and were released into the CMP by cyst rupture. CMP not only provide mechanical barrier function, but also contain immunoglobulin and neutrophils (Becher et al., 2009). Neutrophils released from intraepithelial cysts were suggested to contribute to the barrier function of CMP.

Mucus cells formed during pregnancy slough off two days after delivery in mice (Sugiyama et al., 2021). In non-pregnant adult raccoons confirmed to have given birth in the past based on placental scars, there were little mucus cells remaining. This suggests that in raccoons, mucus cells which developed as pregnancy progressed shed after postpartum, although the exact timing was unknown. In raccoons, p63-positive cells were appeared under the mucous cells in the epithelium and shows PCNA positivity at full-term gestation. In humans, reserve cells (p63-positive) are present beneath the columnar epithelium in a specialized area (transformation zone) where are squamous metaplasia after birth (Witkiewicz et al., 2005). Similar to human reserve cells, raccoon p63-positive cells may proliferate basally and revert to normal cervical epithelium in non-pregnant adult.

Raccoon cervix was significantly dilated near the end of pregnancy (around 57 day of gestation). Hours before delivery in mice and days to weeks before delivery in humans, loss of cervical compliance occurs and the cervix dilates sufficiently to allow passage of the fetus (Timmons et al., 2010). Epithelial folds formed by rupture of intraepithelial cysts may help increase epithelial surface. Increased epithelial surface area may accommodate cervical dilation and may retain more mucous cells that produce CMP. CMP block the lumen of the dilated cervix and protect the fetus from ascending bacterial infection.

In conclusion, the cervical epithelium of raccoons showed stratified epithelium unlike humans, and had the ability to form glands during pregnancy. The epithelium in raccoons had goblet cells, columnar mucus cells and intraepithelial cysts. As pregnancy progressed, the cervical epithelium was replaced by goblet cells or columnar mucus cells, intraepithelial cysts with mucous were expanded and secretion increased to close the cervical orifice. It is suggested that the rupture of intraepithelial cysts may form the epithelial folds by the ripped surface epithelium. In this chapter, I clarified the characteristics of the cervix in non-pregnant raccoon and the gland and CMPs formation process during pregnancy.

Table 4.1. The fetal age and the presence of cervical mucus in pregnant raccoons

fetal age (days)	0-9	10-19	20-29	30-39	40-49	50-63
pregnant raccoon (number)	5	2	1	4	2	5
cervical mucous (number)	0	1	0	3	2	5

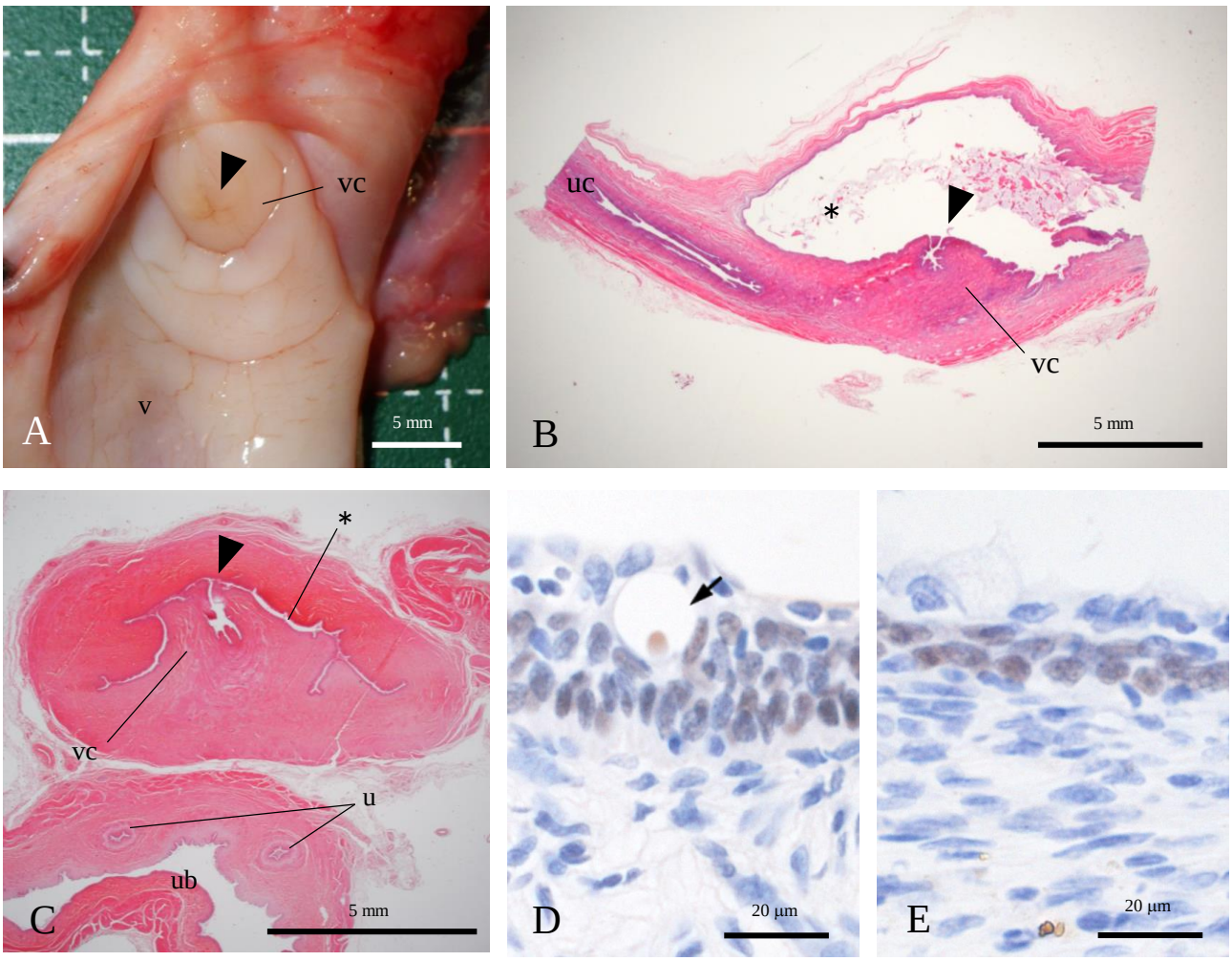

Fig. 4.1. Gross anatomy of the cervix (A), HE staining (B, C) and immunostaining for p63 (D, E) of non-pregnant raccoons. (A) Dorsal wall of the vagina was cut open. Dorsal view. (B) Longitudinal section of the transitional part between the vagina and the cervix. (C) Cross section at vaginal part of cervix. (D) p63 immunoreactivity of the epithelium of vagina in adult. (E) p63 immunoreactivity of the epithelial of cervix in adult. (A, B, D, E) Non-pregnant adult. (C) 6 months old. u, ureter; ub, urinary bladder; v, vagina; vc, vaginal part of cervix; arrowheads, external uterine orifice; arrow, intraepithelial cyst; *, vaginal fornix.

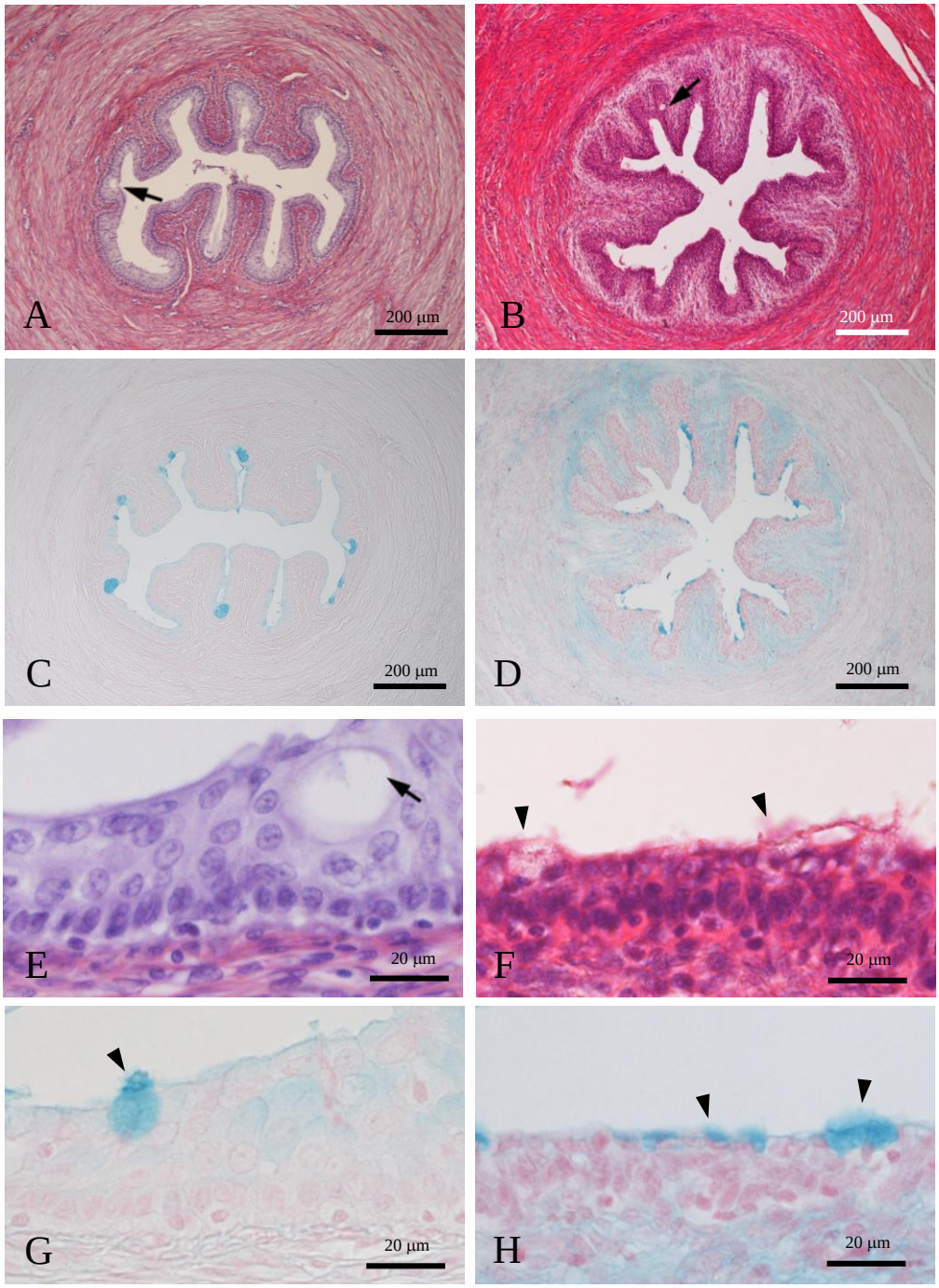

Fig. 4.2. Histological aspects of the cervix. (A, B, E, F) HE staining. (C, D, G, H) AB staining. (A, C, E, G) 6 months old, juvenile. (B, D, F, H) Non-pregnant adult. Arrow, intraepithelial cyst; arrowheads, mucous cell.

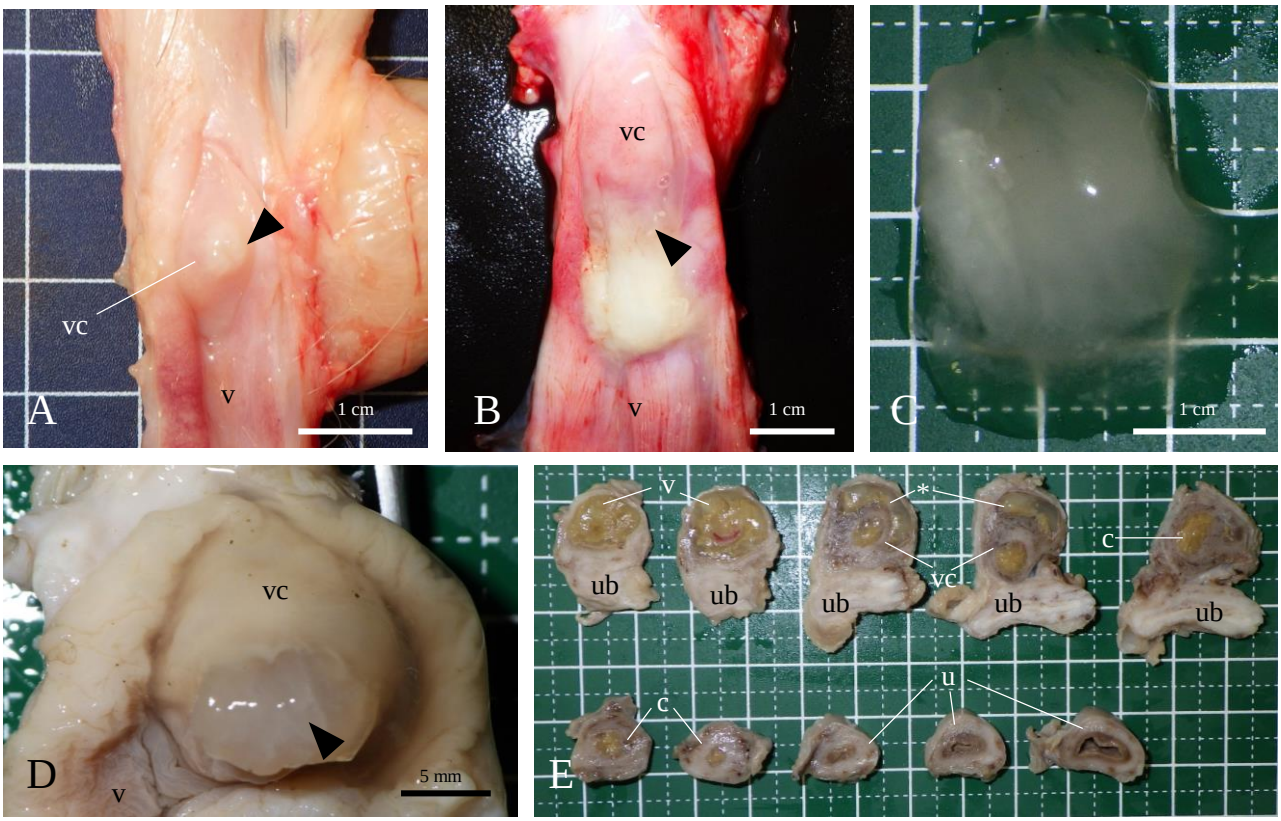

Fig. 4.3. Gross anatomy of the cervix in pregnant raccoons. B-D was the same specimen. (C-E) Formalin-fixed specimen. (A) Dorsal view. The dorsal wall of the vagina was cut open. 27 days of gestation. (B) Dorsal view. The dorsal wall of the vagina was cut open. 63 days of gestation. Mucous accumulation from the cervix to the vagina. (C) Mucous in the vagina at 63 days of gestation. (D) The cervical orifice is filled with mucus at 63 day of gestation. (E) Transverse slices from the vagina to the uterus. The upper left was the vagina, the right was the cranial side, and the lower right was the uterus. Mucous accumulation from the cervix to the vagina at 60 day of gestation. c, cervix; u, utricle; ub, urinary bladder; v, vagina; vc, vaginal part of cervix; arrowheads, external uterine orifice; *, vaginal fornix.

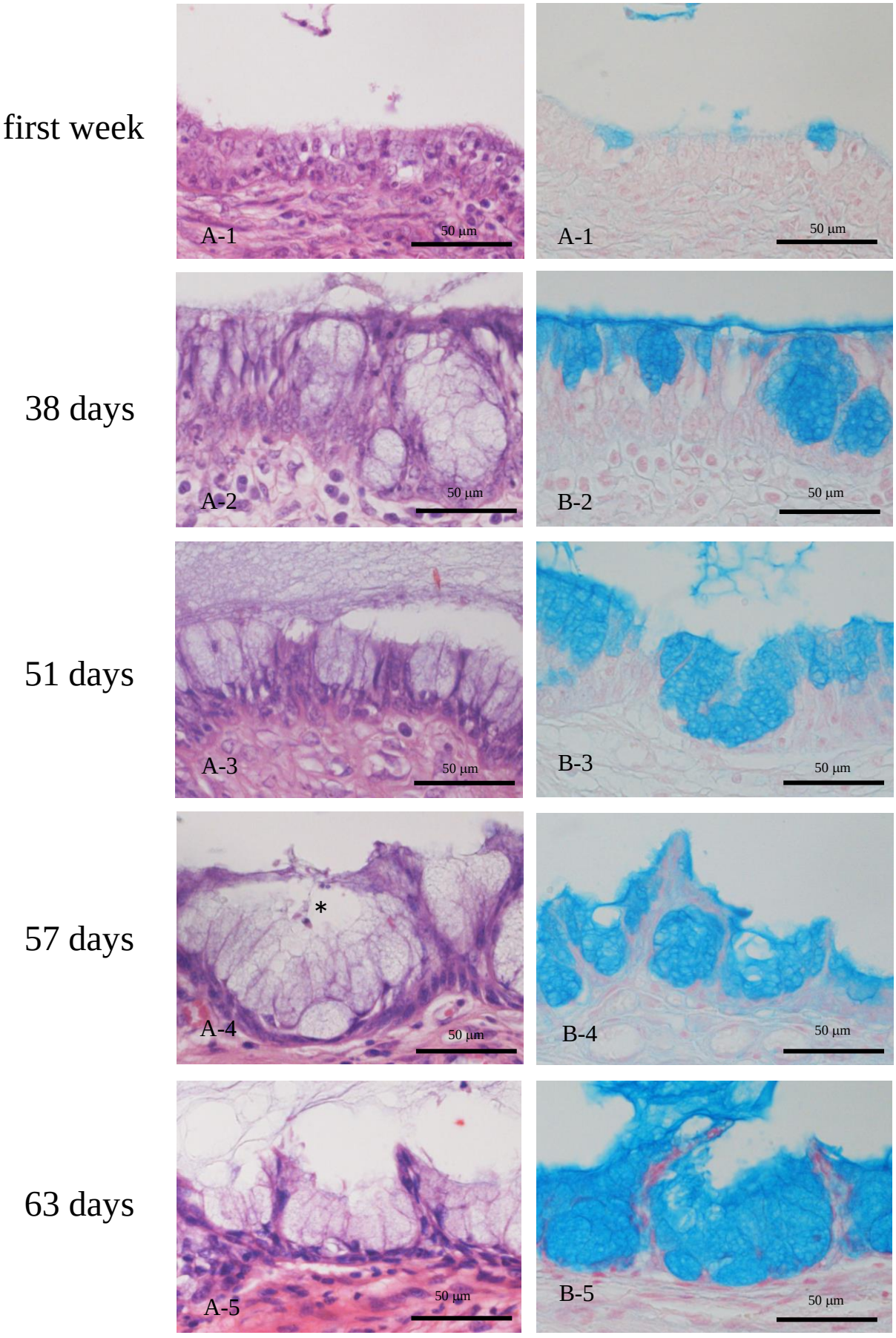
HE
AB pH2.5
first week
38 days
51 days
57 days
63 days
A-1
A-1
A-2
B-2
A-3
B-3
A-4
B-4
A-5
B-5
50 µm
*

Fig. 4.4. Pregnancy progression and differentiation of cervical epithelium into mucous cells. HE staining (A) and AB pH2.5 staining (B). Mucous cells differentiated within the epithelium. Cervical epithelium was replaced by mucous cells as pregnancy progressed. After 50 days of gestation, the epithelium was micropapillary with mucous cells. *, intraepithelial cyst.

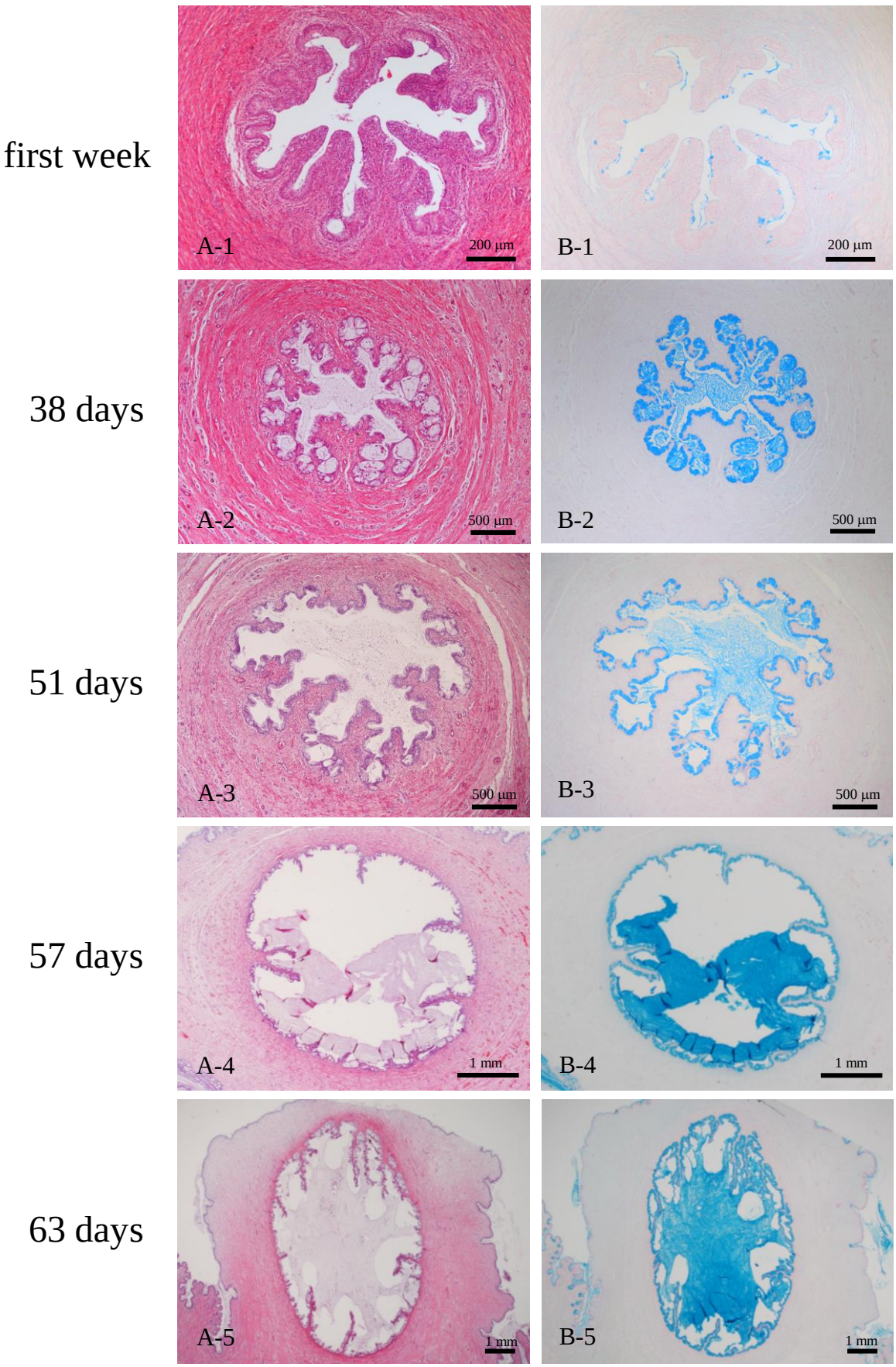
HE
AB pH2.5
first week
38 days
51 days
57 days
63 days
A-1
200 µm
B-1
200 µm
A-2
500 µm
B-2
500 µm
A-3
500 µm
B-3
500 µm
A-4
1 mm
B-4
1 mm
A-5
1 mm
B-5
1 mm

Fig. 4.5. Pregnancy progression and mucus retention in the cervix. (A) HE staining and (B) AB pH2.5 staining. (A) As the pregnancy progressed, the cervix dilated. Papillary folds were seen on the cervix after 57 days of gestation. (B) After 30 days of gestation, the cervix fills with mucus.

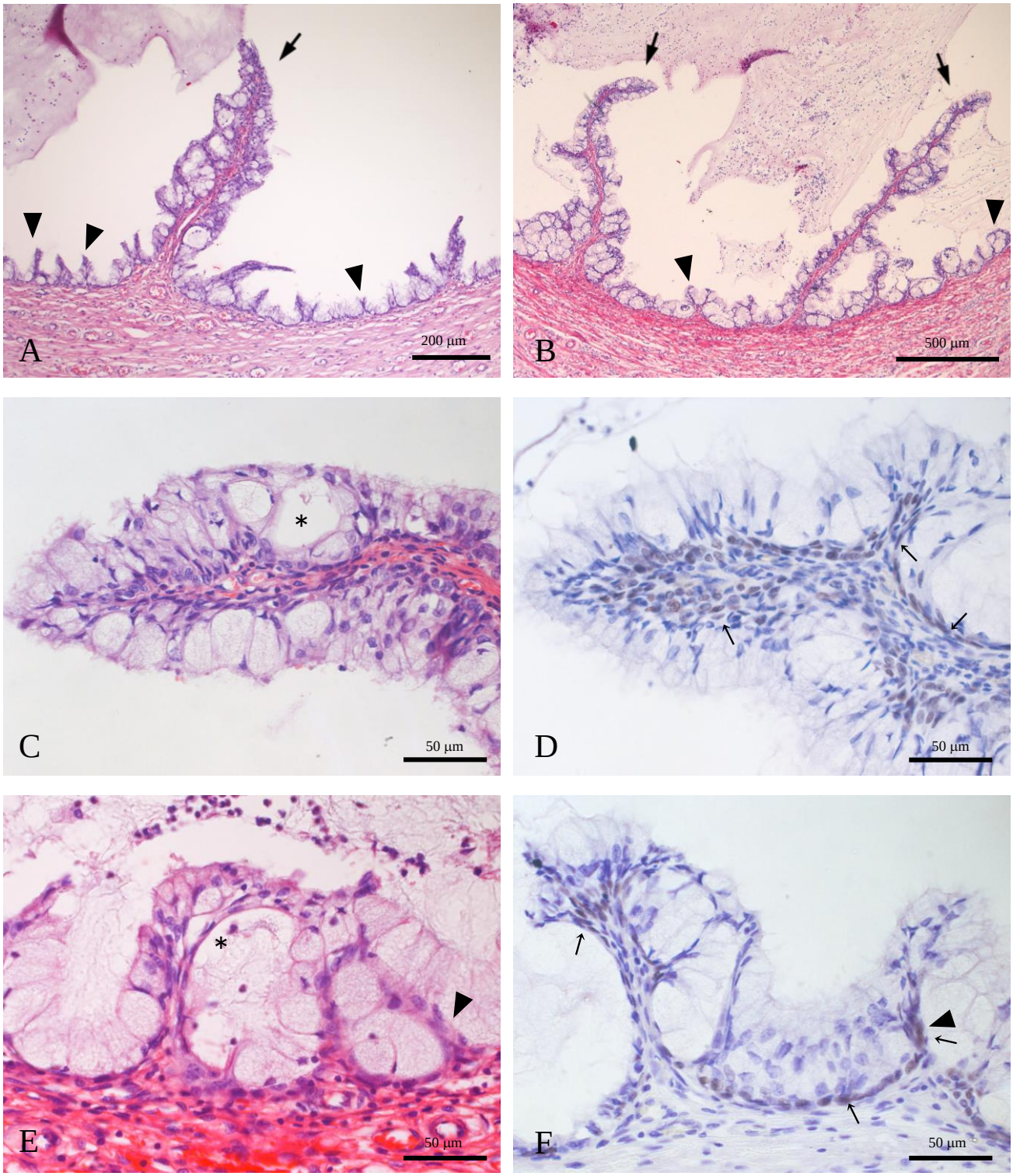

Fig. 4.6. The cervical epithelium over 57 days of gestation. HE staining (A, B, C, E) and immunostaining for p63 (D, E). (A) At 57 days of gestation. (B-F) At 63 days of gestation. (C, D) Tips of papillary folds. (E, F) Micropapillary with mucous cells of cervical epithelium. Large arrows, papillary fold; small arrows, p63 positive cell; arrowheads, folding of epithelium without stroma; asterisk, intraepithelial cyst.

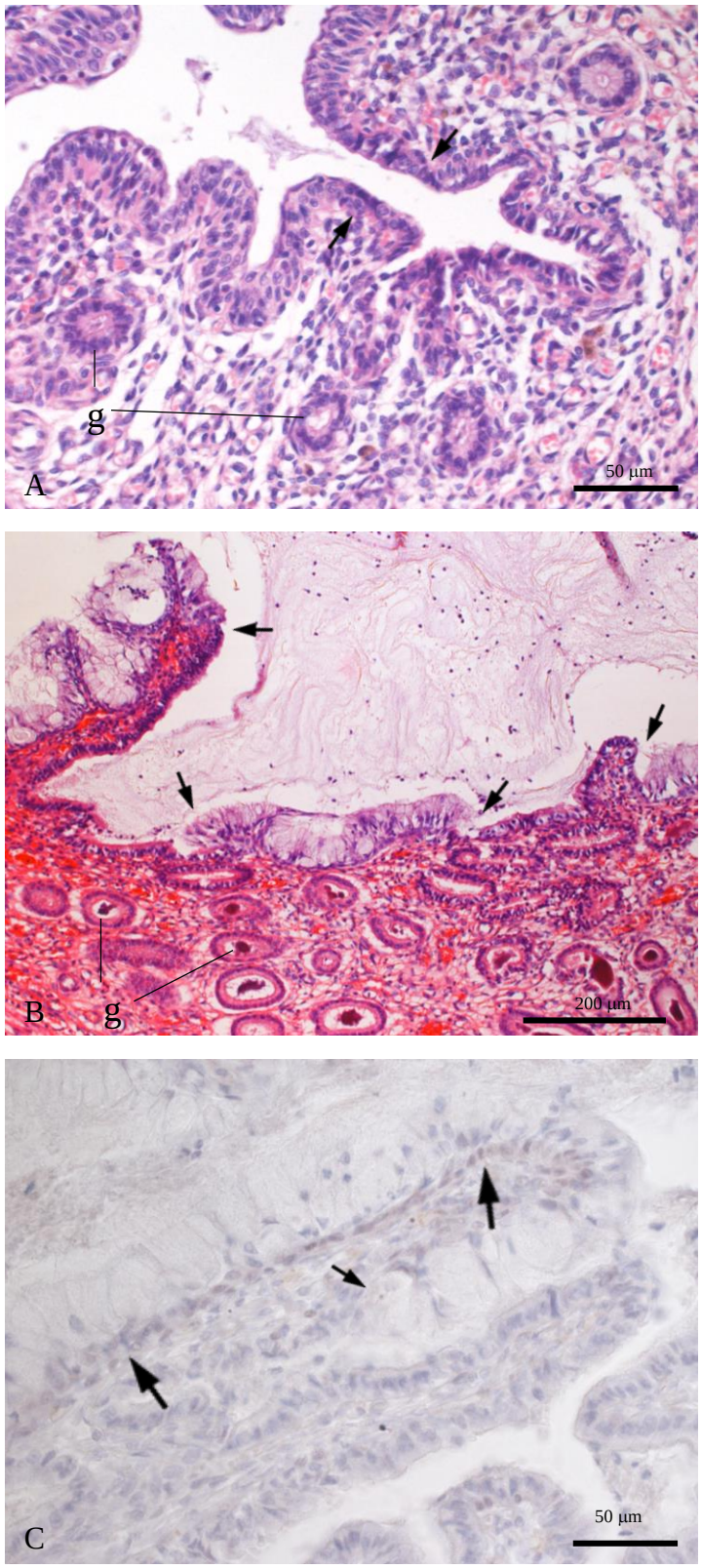

Fig. 4.7. Internal uterine orifice. HE staining (A, B) and immunostaining for p63 (C). (A) Internal uterine orifice of non-pregnant adult. (B) Internal uterine orifice at 63 days of gestation. (C) Internal uterine orifice at 63 days of gestation. Cervical epithelium with p63 positive (large arrows) on the left of border and uterine epithelium on the right of border. g, uterine gland; small arrows, epithelial border.

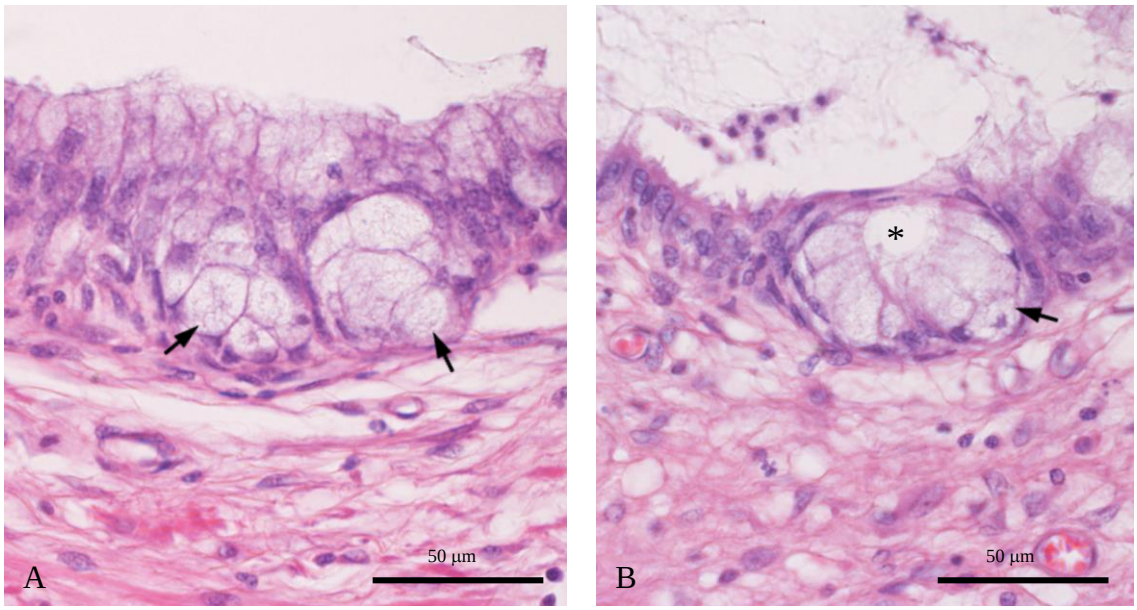

Fig. 4.8. Differentiation of goblet cells in the cervical epithelium. (A) Within the multilayered epithelium, goblet cells (arrows) differentiated from the basal side. (B) There was cyst (*) in the upper layer of the differentiated population of goblet cells (arrows), and the top layer of epithelium was stretched. HE staining.

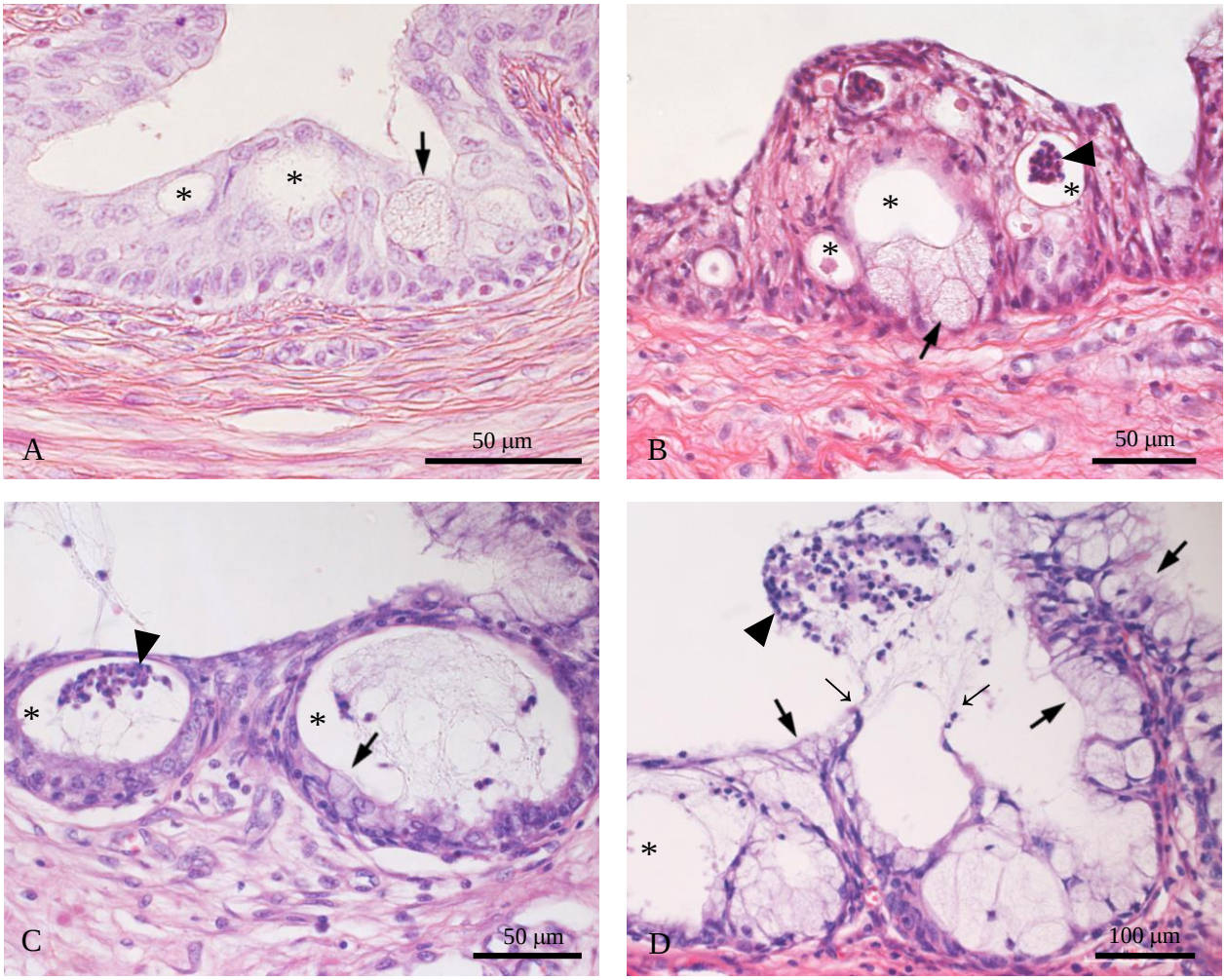

Fig. 4.9. Pregnancy progression and formation of intraepithelial cysts. (A) 6 months old (juvenile). (B) At 27 days of gestation. (C) At 57 days of gestation. (D) At 63 days of gestation. Large arrows, mucous cells; small arrows, folding of epithelium; *, intraepithelial cyst; arrowhead, contents of intraepithelial cyst (cell debris, neutrophils and secretions). HE staining.

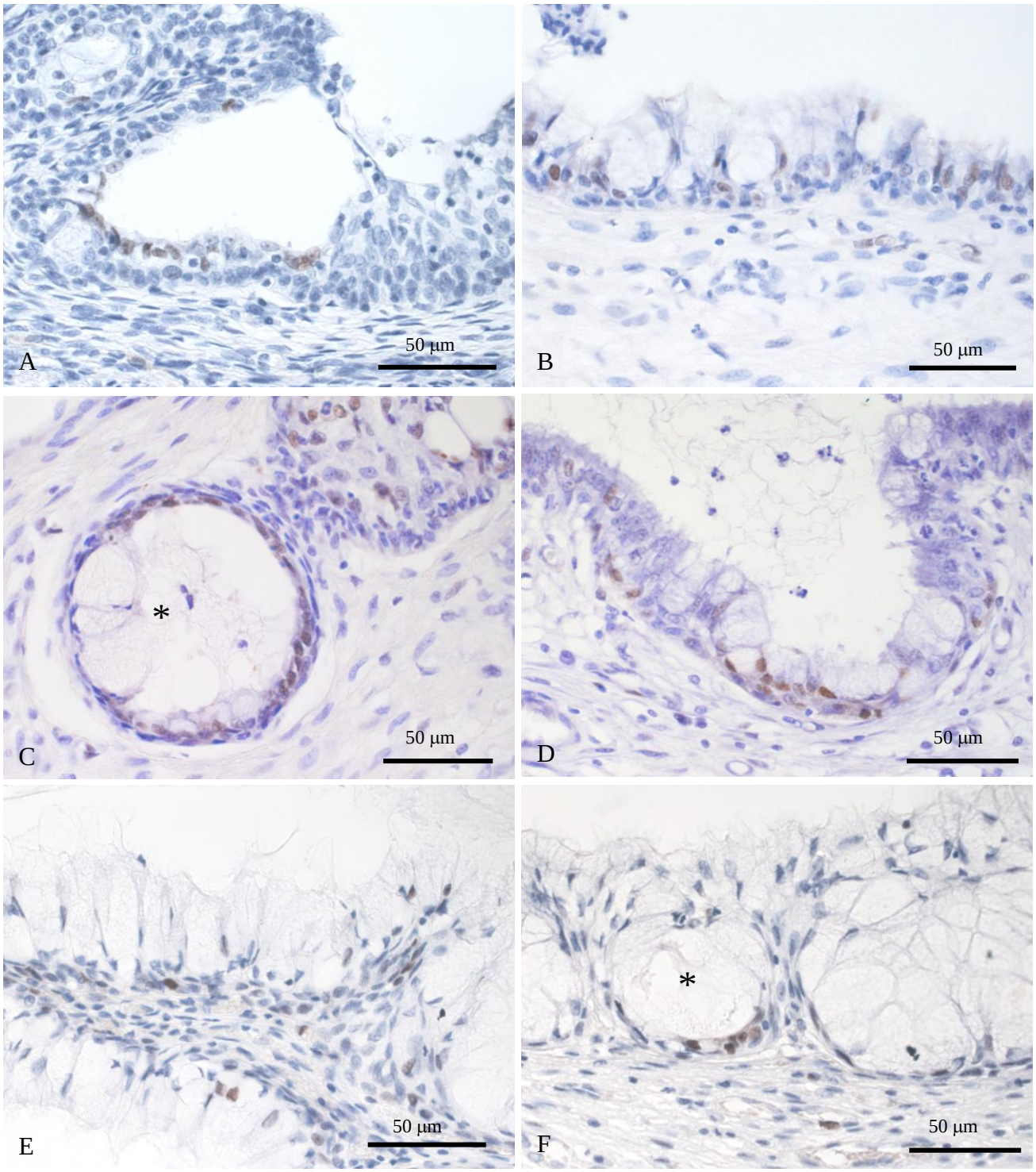

Fig. 4.10. Immunoreactivity for PCNA in the cervix of the pregnant raccoon. (A) Non-pregnant adult. (B) At 27 days of gestation. (C) At 27 days of gestation. (D) At 57 days of gestation. (E) At 63 days of gestation. (F) At 63 days of gestation. *, intraepithelial cyst.

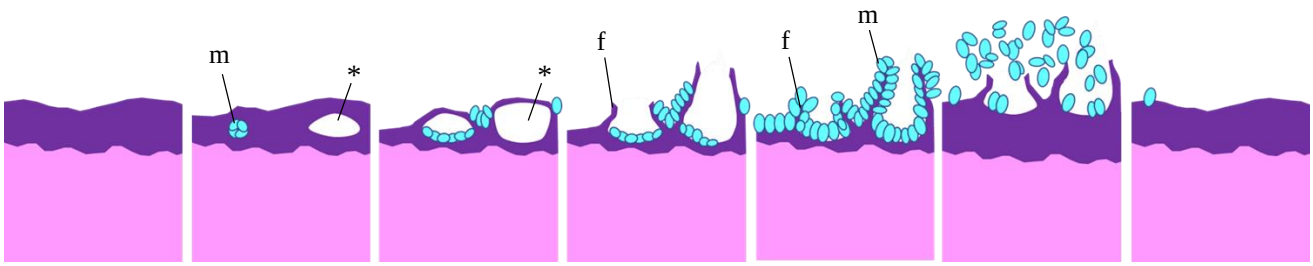

Fig. 4.11. A series of changes in the cervical epithelium throughout pregnancy. *, intraepithelial cyst; f, folding of epithelium without stroma; m, mucous cells.

General Conclusion

In the Chapter 1, developmental and seasonal changes in the testis of raccoons, the testes of raccoons were histologically, histochemically and immunohistochemically examined. The raccoon testes showed seasonal changes, and I identified the period of June to August as the spermatogenetic-declined season in the Tokachi region. In the regressed testes, the spermatids and spermatocytes were lost in spite of the maintenance of proliferation ability in germ cells, meaning that continuous germ cells shedding causes sperm depletion in the spermatogenetic-declined season. In addition, in the spermatogenetic-declined season, the loss of germ cells and decrease in the number and size of Leydig cells affected to the decrease in testicular weight. In this chapter, I also revealed the postnatal testicular development of the raccoon testis. The canalization of the testes began at 6 months of age and changed the distributional pattern of vimentin in the Sertoli cells, and this pattern was maintained in adult also despite developed and regressed conditions. Raccoons reach sexual maturity after 12 months of age. Based on these testicular characteristics, the developmental stages of raccoons were classified into infantile (under 6 months old), juvenile (6-12 months old), and adult (over 12 months old), and adults showed seasonal changes.

In the Chapter 2, developmental and seasonal changes in the prostate gland of raccoons, the prostate glands of raccoons were anatomically, histologically, histochemically and immunohistochemically examined, based on the developmental stages of the testis as defined in Chapter 1. This study is the first report that clarified the seasonal dynamics of glandular structure, p63 and AR expression and cell proliferation in raccoon prostate glands, and revealed that raccoon prostates exhibit seasonal variation of regression and regeneration. In this study, moreover, the postnatal development in raccoon prostate glands was examined, and it was revealed that the distribution of basal cells changed from dense to scattered at the boundary between the developed and undeveloped regions of the prostate gland. Comparing postnatal development with regeneration from seasonal regression, both showed transitional pattern of basal cells from dense to diffuse, and it was revealed that histological aspects in the postnatal development resemble those of the reorganization in adult regressed prostate glands.

In the Chapter 3, developmental changes in the prostatic utricle of raccoons, the prostatic utricles within the prostate glands of raccoons were anatomically, histologically, histochemically and immunohistochemically examined, based on the developmental stages of the testis as defined in Chapter 1. The presence of the prostatic utricle with various shapes was revealed in the prostate glands of the raccoon for the first time. the prostatic utricle of raccoons had sac-like and tubular glands, and goblet cells. The sac-like and tubular glands first appeared in juvenile stage and increased with the maturation. Moreover, lumen had secretions with PAS- and AB-positive in infantile stage, on the other hand, in

adults, the secretions with different properties such as PAS- and AB-positive, and PAS-positive and AB-negative secretion were secreted into the lumen from the sac-like and tubular glands. It was revealed that the prostatic utricle showed morphological and functional changes along with maturation. Moreover, p63 expression in the prostatic utricle indicated that the prostatic utricle of raccoons might correspond to the female vagina and cervix considering the result of Chapter 4.

In the Chapter 4, morphological changes in the cervix of raccoons during pregnancy, the cervices of the uterus were anatomically, histologically, histochemically and immunohistochemically examined. The cervical epithelium of raccoons showed stratified epithelium unlike humans. The epithelium in raccoons had goblet cells, columnar mucus cells and intraepithelial cysts. As pregnancy progressed, the cervical epithelium was replaced by goblet cells or columnar mucus cells, intraepithelial cysts with mucous were expanded, and secretion increased to close the cervical orifice. It is suggested that the rupture of intraepithelial cysts may form the epithelial folds by the ripped surface epithelium. This chapter clarified the process by which glands are formed in the stratified epithelium of the raccoon cervix. The formation of glands in the stratified epithelium was carried out by the extension of intraepithelial glands, which was similar to the epithelium of the prostatic utricle examined in Chapter 3. This confirms that the prostatic utricle is homologous to the cervix, and clarifies the formation process of glands in the stratified epithelium.

In these studies on the genital organs of raccoons, I revealed various characteristics of raccoon genital organs. In particular, I show for the first time that the prostate gland of raccoons exhibits seasonal regression during the spermatogenetic-declined season. During the spermatogenetic-declined season, many raccoons with regressed testes had regressed prostates, whereas there were also raccoons with both developed testes and prostate glands, and raccoons with developed testes and regressed prostate glands. The successful breeding in male raccoons may depend on not only testicular spermatogenic capacity but also prostatic function. To accurately understand the fertility of male raccoons during the spermatogenetic-declined season, future studies need to examine also function of the prostate gland in detail. In addition, male raccoons show individual differences in testicular and prostate development during the spermatogenetic-declined season, meaning that individual differences exist in the regulatory mechanism for reproduction of male raccoons. In this study, however, it is not known how those individual differences are regulated. In further study, I want to clear this reproductive phenomenon in raccoons.

The investigation of the seasonal changes and postnatal development in prostate glands of raccoons revealed the similar morphological and functional changes of the basal cells. It is important to deepen the understanding the property of basal cells as progenitor cells in prostate glands, and basal cells of the prostate gland may play a similar role during postnatal development and regeneration from regressed

condition. In the testes also, the common mechanisms may be used in both sexual maturity and regeneration from seasonal regression. Thus, regeneration from seasonal regression and maturation of male genital organs may be regulated by the same mechanism. In order to deepen our understanding of sexual maturation in seasonal breeding animals, it will be necessary to clarify the seasonality of adult animals at the same time.

In this study on the cervix of female raccoons, I was able to suggest the morphological and functional dynamics of the epithelial cells. It is thought that these results can explain clearly the mechanism of increased production of cervical mucus to protect fetus as pregnancy progress. In addition, the male prostatic utricle and the female cervix were suggested to be homologous, with glandular formation in stratified epithelium in both tissues. In both tissues, glands began as intraepithelial glands in stratified epithelium and formed by progression. This type of gland formation may be a common ability of female reproductive organs derived from the urogenital sinuses. These studies help elucidate the process of gland formation into the female reproductive organs.

These studies reveal the variable capacity of raccoon reproductive organs and contribute to the understanding of raccoon reproductive capacity. Furthermore, it will help us better understand the seasonal changes that occur in the reproductive organs of seasonally breeding animals.

Abstract

The raccoon (*Procyon loter*) is a member of Procyonidae belonging to Carnivora, which is a middle-sized mammal and skillfully use the forelimbs. The raccoon native to North America was introduced into Japan in 1970s and has been naturalized in almost every prefecture of Japan. In Hokkaido, Japan, their population has increased, and many problems are induced by them.

Raccoons are considered seasonal breeders, and in Hokkaido, the mating season peaks in February. Mated female raccoons stays pregnant for about 63 days and give birth to an average of 3-4 cubs。 However, information on morphological changes in the raccoon genital organs with postnatal development, with seasonal change and during pregnancy is limited. In this study, therefore, morphological and functional changes were examined in the testes and prostate glands of male raccoons, during developmental and seasonal changes, and in female, morphological and functional dynamics of the uterus, especially cervix during pregnancy were investigated.

In the examination of the raccoon testes, the regression of spermatogenesis was detected from June to August, although not all individuals. Moreover, the decline in the functions of Leydig cells was suggested. In the regression of spermatogenesis, there were no changes in the proliferative activity of the germ cells. Therefore, the regression was thought to be caused by shedding of germ cells. In the postnatal testicular development, testes began to the canalize at 6 months of age, and all individuals reached sexal maturation over 12 months old.

In the studies on the prostate glands, the seasonal dynamics of glandular structure, p63 and AR expression and proliferation in raccoon prostate glands were examined. Raccoon prostates exhibit seasonal variation of regression and regeneration. Moreover, in the postnatal development, it was revealed that histological aspects in the postnatal development resemble those of the reorganization in adult regressed prostate glands.

In the examination of the prostatic utricle, in the prostate glands of the raccoont, the prostatic utricle with various shapes was recognized. The prostatic utricle of raccoons had saclike and tubular glands and goblet cells. The saclike and tubular glands first appeared in juvenile stage, but not infantile. The lumen had secretions with PAS- and AB-positive in infantile stage, on the other hand, in adults, the secretions with PAS- and AB-positive, and PAS-positive and AB-negative secretion were secreted. Therefore, the prostatic utricle showed morphological and functional changes along with maturation.

In the studies on the cervix, histological changes was revealed during pregnancy. As pregnancy progressed, the intraepithelial cysts with mucous were expanded, and secretion increased to close the cervical orifice. It is suggested that the rupture of intraepithelial cysts may form the epithelial folds by the ripped surface epithelium.

要旨

アライグマ（*Procyon loter*）は，食肉目アライグマ科に属する中型の哺乳類で，水辺を好み器用に前肢を使用することが知られている。アライグマは，1970 年代に北アメリカから移入され，現在野生化して日本全国にその分布を広めている。北海道においても，アライグマはその分布を広めており，様々な問題を引き起こしている。

アライグマは季節繁殖動物と考えられており，北海道では交尾期のピークが 2 月にあると報告されている。アライグマの妊娠期間は 63 日で，3 から 4 頭の子を出産する。しかし，生後発達，季節変化，そして妊娠といった期間におけるアライグマの生殖器の形態学的な変化の情報はほとんどない。本研究では，雄のアライグマにおいて，生後発達および季節変化における精巣や前立腺の形態学的および機能学的変化を調べ，さらに雌では，妊娠にともなう子宮頸の形態学的および機能学的動態を検索した。

アライグマの精巣の検索では，全ての個体ではないが 6 月から 8 月の間に精子形成の退行が認められ，さらにライディッヒ細胞の機能の低下を示唆することができた。精子形成の退行において，生殖細胞の増殖能には変化がなかったことから，生殖細胞の脱落が精子形成の退行を引き起こしていると考えられた。また，生後発達においてアライグマの精巣では，生後 6 か月で精細管の管腔形成が生じ，また 12 か月以上で全ての個体が性成熟に達することが明らかになった。

前立腺では，管腔構造，p 63 や AR の発現，そして細胞増殖能の季節動態が調べられ，アライグマは，前立腺の退縮と再発達にともなうこれらの変化を示すことを明らかになった。さらに，前立腺の生後発達の解析では，生後発達の組織学的様相が，成体の退縮した前立腺が再発達する際の特徴と類似することを明らかにした。

前立腺小室の検索では，アライグマの前立腺に様々な形の前立腺小室が認められた。アライグマの前立腺小室には，管状腺，嚢状腺そして杯細胞といった腺構造が認められ，管状腺と嚢状腺は幼若個体には認められず，若年個体になって初めて出現する。幼若個体では，前立腺小室の管腔内に PAS と AB に陽性を示す分泌物が認められ，成体では PAS 陽性と AB 陰性の分泌物がさらに分泌されるようになる。このように，前立腺小室は成長にともなって形態学的，機能学的な変化を示した。

雌の生殖器である子宮頸の組織学的検索では，妊娠期に組織学的変化が認められた。妊娠の進行にともなって，粘液を保有した上皮内嚢胞は拡張し，子宮頸の分泌は増加して子宮口は塞がれた。また，上皮内嚢胞の破裂が上皮ヒダの形成に関与している可能性が示唆された。

Acknowledgements

I would like to express my sincere gratitude to my supervisor Prof. Motoki Sasaki, Laboratory of Anatomy, Obihiro University of Agriculture and Veterinary Medicine for his support to the completion of my dissertation. I would like to express my deepest gratitude to Emer. Prof. Nobuo Kitamura, Obihiro University of Agriculture and Veterinary Medicine and Dr. Emi Yamaguchi, National Agriculture and Food Research Organization, Dr. Anni Nurliani, Lambung Mangkurat University, for their valuable suggestions. I am grateful to the members of the supervising mumbers, Prof. Tatsuo Oshida, Prof. Yoshiyasu Kobayashi, Prof. Motozumi Matsui, Obihiro University of Agriculture and Veterinary Medicine, for the constructive advice. I would like to express my special gratitude to Emer. Prof. Kunitoshi Imai, Prof. Hidefumi Furuoka, Assoc. Prof. Shinya Fukumoto, Assoc. Prof. Kotaro Matsumoto, Obihiro University of Agriculture and Veterinary Medicine, for his support for sampling. I also extend my gratitude to all members of the Laboratory of Anatomy, Obihiro University of Agriculture and Veterinary Medicine for their support may studies.

References

1. Abou-Elhamd AS, Salem AO, Selim AA. 2013. Histomorphological studies on the prostate gland of Donkey Equus Asinus during different seasons. *J Histol Article* ID 643287: 19.
2. Aitken RNC, Aughey E. 1964. A histochemical study of the accessory genital glands of the male cat. *Res Vet Sci* **5**: 268–276.
3. Asano M, Matoba Y, Ikeda T, Suzuki M, Asakawa M, Ohtaishi, N. 2003. Reproductive characteristics of the feral raccoon (*Procyon lotor*) in Hokkaido, Japan. *J Vet Med Sci* **65**: 369–373.
4. Aumüller G, Seitz J, Bischof W. 1983. Immunohistochemical study on the initiation of acid phosphatase secretion in the human prostate cytochemistry and biochemistry of acid phosphatases IV. *J Androl* **4**: 183−191.
5. Barsanti JA, Finco DR. 1986. Canine prostatic diseases. *Vet Clin North Am Small Anim Pract* **16**: 587–99.
6. Basrur PK, Ramos AS. 1973. Seasonal changes in the accessory sex glands and gonaducts of male mink. *Can J Zool* **51**: 1125−1132.
7. Becher N, Waldorf KA., Hein M, Uldbjerg N. 2009. The cervical mucus plug: structured review of the literature. *Acta Obstet Gynecol Scand* **88**: 502−513.
8. Beguelini MR, Goes RM, Rahal P, Morielle–Versute E, Taboga SR. 2015. Impact of the processes of testicular regression and recrudescence in the prostatic complex of the bat *Myotis nigricans* (Chiroptera: Vespertilionidae). *J Morphol* **276**: 721–732.
9. Berg OA. 1958. The normal prostate gland of the dog. *Eur J Endocrinol* **27**: 129–139.
10. Bergmann M, Dierichs R. 1983. Postnatal formation of the blood-testis barrier in the rat with special reference to the initiation of meiosis. *Anat Embryol* **168**: 269−275.
11. Blottner S, Hingst O, Meyer HHD. 1996. Seasonal spermatogenesis and testosterone production in roe deer (*Capreolus capreolus*). *Reproduction* **108**: 299−305.
12. Bo P, Tagliavia C, Canova M, De Silva M, Bombardi C, Grandis A. 2019. Comparative characterization of the prostate gland in intact, and surgically and chemically neutered ferrets. *J Exot Pet Med* **31**: 68–74.
13. Bonkhoff H, Remberger K. 1996. Differentiation pathways and histogenetic aspects of normal and abnormal prostatic growth: A stem cell model. *Prostate* **28**: 98–106.
14. Bronson FH. 2009. Climate change and seasonal reproduction in mammals. *Phil Trans R Soc B* **364**: 3331–3340.

15. Chatani H, Kandori H. 2017. Male Reproductive Organs. pp347−378 In: Toxicologic histopathology. (Japanese Society of Toxicologic Pathology ed.) Nishimuasyoten, Tokyo.
16. Chaves M, Aguilera-Merlo C, Cruceño A, Fogal T, Mohamed F. 2015. Morphological study of the prostate gland in viscacha (*Lagostomus maximus maximus*) during periods of maximal and minimal reproductive activity. *Anat Rec* **298**: 1919–1931.
17. Conaway, C. H. 1958. The uterus masculinus of *Castor canadensis*. *J Mammal* **39**: 97−108.
18. Costa GMJ, Avelar GF, Guimarães DA, França LR. 2019. Postnatal testis development in the collared peccary (*Tayassu tajacu*), with emphasis on spermatogonial stem cells markers and niche. *Gen Comp Endocrinol* **273**: 98−107.
19. Cunha GR, Kurita T, Cao M, Shen J, Robboy, S, Baskin L. 2017. Molecular mechanisms of development of the human fetal female reproductive tract. *Differentiation* **97**: 54−72.
20. Cunha GR, Ricke W, Thomson A, Marker PC, Risbridger G, Hayward SW, Wang YZ, Donjacour AA, Kurita T. 2004. Hormonal, cellular, and molecular regulation of normal and neoplastic prostatic development. *J Steroid Biochem Mol Biol* **92**: 221–236.
21. Cunha GR, Vezina CM, Isaacson D, Ricke WA, Timms BG, Cao M, Franco O, Baskin LS. 2018. Development of the human prostate. *Differentiation* **103**: 24−45.
22. Dadhich RK, Barrionuevo FJ, Real FM, Lupiañez DG, Ortega E, Burgos M, Jiménez R. 2013. Identification of live germ-cell desquamation as a major mechanism of seasonal testis regression in mammals: a study in the Iberian mole (*Talpa occidentalis*). *Biol Reprod* **88**: 101−1.
23. de Rijk E, van den Brink H, Lensen J, Lambregts A, Lorentsen H, Peter B. 2014. Estrous cycle-dependent morphology in the reproductive organs of the female Göttingen minipig. *Toxicol Pathol* **42**: 1197−1211.
24. Devkota B, Sasaki M, Takahashi KI, Matsuzaki S, Matsui M, Haneda S, Takahashi M, Osawa T, Miyake YI. 2006. Postnatal developmental changes in immunohistochemical localization of α-smooth muscle actin (SMA) and vimentin in bovine testes. *J Reprod Dev* **52**: 43−49.
25. Dietrich W, Haitel A, Huber JC, Reiter W. 2004. Expression of estrogen receptors in human corpus cavernosum and male urethra. *J Histochem Cytochem* **52**: 355–360.
26. Di Sant'Agnese PA, 1992. Neuroendocrine differentiation in carcinoma of the prostate.

diagnostic, prognostic, and therapeutic implications. *Cancer* **70**: 254–268.

27. Donjacour AA, Cunha GR. 1993. Assessment of prostatic protein secretion in tissue recombinants made of urogenital sinus mesenchyme and urothelium from normal or androgen-insensitive mice. *Endocrinology* **131**: 2342–2350.
28. Dorso L, Chanut F, Howroyd P, Burnett R. 2008. Variability in weight and histological appearance of the prostate of beagle dogs used in toxicology studies. *Toxicol Pathol* **36**: 917–925.
29. Dutourné B. Saboureau M. 1983. An endocrine and histophysiological study of the testicular annual cycle in the hedgehog (*Erinaceus europaeus* L.). *Gen Com Endocrinol* **50**: 324–332.
30. El-Banna AA, Hafez ESE. 1972. The uterine cervix in mammals. *Am J Obstet Gynecol* **112**: 145–164.
31. Evans H, Christensen GC. 1993. The Urogenital Apparatus. pp554–601. In: Miller's Anatomy of the Dog. 2nd ed. W. B. Saunders Company, New York.
32. Farias TDO, Figueiredo AFA, Wnuk NT, Ferraz FS, Talamoni SA, Costa GMJ. 2020. Male reproductive morphofunctional evaluation of a Neotropical sperm-storing vespertilionid bat (*Myotis levis*) in an environmental context. *Cell Tissue Res* **382**: 639–656.
33. Gehrt SD. 2003. Raccoons. pp. 611–634. In: Wild Mammals of North America: Biology, Management, and Conservation. 2nd ed. (Feldhamer GA, Thompson BC, Chapman JA eds.), Johns Hopkins University Press, Baltimore, Maryland.
34. Gehrt, SD., Fritzell, EK. 1996. Second estrus and late litters in raccoons. *J Mammal* **77**: 388–393.
35. Gobello C, Castex G, Corrada Y. 2002. Serum and seminal markers in the diagnosis of disorders of the genital tract of the dog: A mini-review. *Theriogenology* **57**: 1285–1291.
36. Goedken MJ, Kerlin RL, Morton D. 2008. Spontaneous and age-related testicular findings in beagle dogs. *Toxicol Pathol* **36**: 465–471.
37. Goericke-Pesch S, Schmidt B, Failing K, Wehrend A. 2010. Changes in the histomorphology of the canine cervix through the oestrous cycle. *Theriogenology* **74**: 1075–1081.
38. Goeritz F, Quest M, Wagener A, Fassbender M, Broich A, Hildebrandt TB, Hofmann RR, Blottner, S. 2003. Seasonal timing of sperm production in roe deer:

interrelationship among changes in ejaculate parameters, morphology and function of testis and accessory glands. *Anat Histol Embryol* **59**: 1487–1502.

39. Góes RM, Zanetoni C, Tomiosso TC, Ribeiro DL, Taboga SR. 2007. Surgical and chemical castration induce differential histological response in prostate lobes of Mongolian gerbil. *Micron* **38**: 231–236.
40. Gopinath C. 2013. Toxicology and pathology of female reproductive tract. *Cell Biol Toxicol* **29**: 131−141.
41. Grau GA, Sanderson GC, Rogers JP. 1970. Age determination of raccoons. *J Wildl Manage* **34**: 364–372.
42. Haruyama E, Suda M, Ayukawa Y, Kamura K, Mizutamari M, Ooshima Y, Tanimoto A. 2012. Testicular development in cynomolgus monkeys. *Toxicol Pathol* **40**: 935−942.
43. Hayakawa D, Sasaki M, Suzuki M, Tsubota T, Igota H, Kaji K, Kitamura N. 2010. Immunohistochemical localization of steroidogenic enzymes in the testis of the sika deer (*Cervus nippon*) during developmental and seasonal changes. *J Reprod Dev* **56**: 117−123.
44. Hochereau-de Reviers MT, Perreau C, Lincoln GA. 1985. Photoperiodic variations of somatic and germ cell populations in the Soay ram testis. *Reproduction* **74**: 329−334.
45. Hoffmann K. 1978. Effects of short photoperiods on puberty, growth and moult in the Djungarian hamster *(Phodopus sungorus*). *Reproduction* **54**: 29−35.
46. Huggins C. 1945. The physiology of the prostate gland. *Physiol Rev* **25**: 281–295.
47. Huggins C, Clark PJ. 1940. Quantitative studies of prostatic secretion II. The effect of castration and of estrogen injection on the normal and on the hyperplastic prostate glands of dogs. *J Exp Med* **72**: 747–762.
48. Huttunen E, Romppanen T, Helminen HJ. 1981. A histoquantitative study on the effects of castration on the rat ventral prostate lobe. *J Anat* **132**: 357–370.
49. Ikeda T, Asano M, Matoba Y, Abe G. 2004. Present status of invasive alien raccoon and its impact in Japan. *Glob Environ Res* **8**: 125–131.
50. Ismail AHR, Landry F, Aprikian AG, Chevalier S. 2002. Androgen ablation promotes neuroendocrine cell differentiation in dog and human prostate. *Prostate* **51**: 117–125.
51. James RW, Heywood R. 1979. Age-related variations in the testes and prostate of beagle dogs. *Toxicology* **12**: 273−279.

52. Johnson L, Tatum ME. 1989. Temporal appearance of seasonal changes in numbers of Sertoli cells, Leydig cells, and germ cells in stallions. *Biol Reprod* **40**: 994–999.
53. Junge R, Hoffmeister DF. 1979. Age determination in raccoons from cranial suture obliteration. *J Wildl Manage* **44**: 725–729.
54. Kamioka M, Sasaki M, Yamada K, Endo H, Oishi M, Yuhara K, Tomikawa S, Sugimoto M, Oshida T, Kitamura N. 2017. Mobility of the forearm in the raccoon (*Procyon lotor*), raccoon dog (*Nyctereutes procyonoides*) and red panda (*Ailurus fulgens*). *J Vet Med Sci* **79**: 224–229.
55. Kaneko K, Akiya Y, Sato H, Tanaka A, Aoki H, Miyoshi M, Abukawa T, Mochizuki M, Kawakami S. 2005. Seasonal influence on testicular function of male raccoons, *Procyon lotor*. *J Reprod Dev* **51**: 477−482.
56. Kangawa A, Otake M, Enya S, Yoshida T, Shibata M. 2016. Histological development of male reproductive organs in microminipigs. *Toxicol Pathol* **44**: 1105−1122.
57. Kangawa A, Otake M, Enya S, Yoshida T, Shibata M. 2019. Histological changes of the testicular interstitium during postnatal development in microminipigs. *Toxicol Pathol* **47**: 469−482.
58. Kasper S. 2008. Exploring the origins of the normal prostate and prostate cancer stem cell. *Ste. Cell Rev* **4**: 193–201.
59. Kato T, Ichida Y, Tei K, Asano M, Hayama SI. 2009. Reproductive characteristics of feral raccoons (*Procyon lotor*) captured by the pest control in Kamakura, Japan. *J Vet Med Sci* **71**: 1473−1478.
60. Kaur G, Thompson LA, Dufour JM. 2014. Sertoli cells–immunological sentinels of spermatogenesis. *Semin Cell Dev Biol* **30**: 36−44.
61. Kawakami E, Tsutsui T, Ogasa A. 1991. Histological observations of the reproductive organs of the male dog from birth to sexual maturity. *J Vet Med Sci* **53**: 241−248.
62. Kheddache A, Moudilou ENT, Zatra Y, Aknoun-Sail N, Amirat Z, Exbrayat JM, Khammar F. 2017. Seasonal morphophysiological variations in the prostatic complex of the Tarabul's gerbil (*Gerbillus tarabuli*). *Tissue Cell* **49**: 345–357.
63. Kliesch S, Schweifer B, Niklowitz P, Nieschlag E, Bergmann M. 1991. The influence of LH and/or FSH on Leydig and Sertoli cell morphology after testicular involution in the Djungarian hamster, *Phodopus sungorus*, induced by hypophysectomy or short photoperiods. *Andrologia* **23**: 99−107.
64. Klonisch T, Schön J, Hombach-Klonisch S, Blottner S. 2006. The roe deer as a model for studying seasonal regulation of testis function. *Int J Androl* **29**: 122−128.

65. Kobayashi A, Behringer RR. 2003. Developmental genetics of the female reproductive tract in mammals. *Nat Rev Genet* **4**: 969–980.
66. Koizumi N, Uchida M, Makino T, Taguri T, Kuroki T, Muto, M, Kato Y, Watanabe H. 2009. Isolation and characterization of *Leptospira* spp. from raccoons in Japan. *J Vet Med Sci* **71**: 425–429.
67. Komatsu T, Yamamoto Y, Atoji Y, Tsubota T, Suzuki Y. 1997. Seasonal changes in subcellular structures of Leydig and Sertoli cells in the Japanese black bear, *Ursus thibetanus japonicus*. *Arch Histol Cytol* **60**: 225–234.
68. Komatsu T, Yamamoto Y, Atoji Y, Tsubota T, Suzuki Y. 1998. Immunohistochemical demonstration of cytoskeletal proteins in the testis of the Japanese black bear, *Ursus thibetanus japonicus*. *Anat Histol Embryol* **27**: 209–213.
69. Kopecky M, Semecky V, Nachtigal P. 2005. Vimentin expression during altered spermatogenesis in rats. *Acta histochem* **107**: 279–289.
70. Kormano M, Hovatta O. 1972. Contractility and histochemistry of the myoid cell layer of the rat seminiferous tubules during postnatal development. *Z Anat Entwickl* **137**: 239-248.
71. Kurita T, Medina RT, Mills AA, Cunha, GR. 2004. Role of p63 and basal cells in the prostate. *Development* **131**: 4955–4964.
72. Kurita T, Wang YZ, Donjacour AA, Zhao C, Lydon JP, O'Malley BW, Isaacs JT, Dahiya R, Cunha GR. 2001. Paracrine regulation of apoptosis by steroid hormones in the male and female reproductive system. *Cell Death Diff* **8**: 192–200.
73. Lacroix G, Gouyer V, Gottrand F, Desseyn JL. 2020. The cervicovaginal mucus barrier. *Int J Mol Sci* **21**: 8266.
74. Lai CL, van den Ham R, van Leenders G, van der Lugt J, Teske E. 2008. Comparative characterization of the canine normal prostate in intact and castrated animals. *Prostate* **68**: 498–507.
75. Leav I, Schelling KH, Adams JY. Merk FB, Alroy J. 2001. Role of canine basal cells in postnatal prostatic development, induction of hyperplasia, and sex hormone-stimulated growth; and the ductal origin of carcinoma. *Prostate* **48**: 210–224.
76. Leis-Filho AF, Fonseca-Alves CE. 2018. Anatomy, histology, and physiology of the canine prostate gland. *Vet Anat Physiol* ID: 233394869.
77. Li Q, Zhang F, Zhang S, Sheng X, Han Y, Yuan Z, Weng Q. 2015. Seasonal expression of androgen receptor, aromatase, and estrogen receptor alpha and beta in the testis of the wild ground squirrel (*Citellus dauricus* Brandt). *Eur J Histochem* **59**: 9–16.

78. Llewellyn LM. 1953. Growth rate of the raccoon fetus. *J Wildl Manage* **17**: 320–321.
79. Marker PC, Donjacour AA, Dahiya R, Cunha GR. 2003. Hormonal, cellular, and molecular control of prostatic development. *Dev Biol* **253**: 165−174.
80. Massoud D, Lao-Perez M, Hurtado A, Abdo W, Palomino-Morales R, Carmona FD, Burgos M, Jiménez R, Barrionuevo FJ. 2018. Germ cell desquamation-based testis regression in a seasonal breeder, the Egyptian long-eared hedgehog, *Hemiechinus auritus*. *PLoS One* **13**: e0204851.
81. McCarthy JF, Bitter JS, Klemperer P. 1927. Anatomical and histological study of the verumontanum with especial reference to the ejaculatory ducts. *J Urol* **17**: 1−16.
82. McNeal JE. 1981. The zonal anatomy of the prostate. *Prostate* **2**: 35–49.
83. McNeal JE. 1988. Normal histology of the prostate. *Am J Surg Pathol* **12**: 619–633.
84. Meier C, Partlow GD, Fisher KR, Rennie B. 1998. Persistent paramesonephric ducts (masculine uterus) in the male North American beaver (*Castor canadensis*). *Can J Zool* **76**: 1188−1193.
85. Merk FB, Leav I, Kwan PW, Ofner P. 1980. Effects of estrogen and androgen on the ultrastructure of secretory granules and intercellular junctions in regressed canine prostate. *Anat Rec* **197**: 111–132.
86. Montgomery GC. 1964. Tooth eruption in preweaned raccoons. *J. Wildl. Manage.* **28**: 582–584.
87. Morales A, Mohamed F, Cavicchia JC. 2007. Apoptosis and blood–testis barrier during the first spermatogenic wave in the pubertal rat. *Anat Rec* **290**: 206−214.
88. Morton D, Weisbrode SE, Wyder WE, Maurer JK, Capen CC. 1986. Spermatid giant cells, tubular hypospermatogenesis, spermatogonial swelling, cytoplasmic vacuoles, and tubular dilatation in the testes of normal rabbits. *Vet pathol* **23**: 176−183.
89. Neito CM, Rider LC, Cramer SD. 2014. Influence of stromal–epithelial interactions on androgen action. *Endocr Relat Cancer* **21**: 147–160.
90. Nelson LW, Kelly WA. 1976. Progestogen-related gross and microscopic changes in female Beagles. *Vet Pathol* **13**: 143−156.
91. Nikitin AY, Matoso A, Roy-Burman P. 2007. Prostate stem cells and cancer. *Histol Histopath* **22**: 1043–1049.
92. Nistal M, Codesal J, Paniagua R. 1986. Multinucleate spermatids in aging human testes. *Arch Androl* **16**: 125−129.
93. Niu Y, Wang J, Shang Z, Huang S-P, Shyr C-R, Yeh S, Chang C. 2011. Increased CK5/CK8-positive intermediate cells with stromal smooth muscle cell atrophy in the

mice lacking prostate epithelial androgen receptor. *PLoS ONE* **6**: e20202.

94. Nott JP, Bonney EA, Pickering JD, Simpson NA. 2016. The structure and function of the cervix during pregnancy. *Transl Res Anat* **2**: 1−7.
95. Oe S, Sashika M, Fujimoto A, Shimozuru M, Tsubota T. 2020. Predation impacts of invasive raccoons on rare native species. *Sci Rep* **10**: 1–12.
96. Oh CS, Chung IH, Won HS, Kim JH, Nam KI. 2009. Morphologic variations of the prostatic utricle. *Clin Anat* **22**: 358−364.
97. Okuyama MW, Shimozuru M, Abe G, Nakai M, Sashika M, Shimada K, Takahashi N, Fukui D, Nakamura R, Tsubota T. 2013. Timing of puberty and its relationship with body growth and season in male raccoons (*Procyon lotor*) in Hokkaido. *J Reprod Dev* **59**: 361–367.
98. Okuyama MW, Shimozuru M, Takahashi N, Fukui D, Nakamura R, Tsubota T. 2012. Seasonal changes in spermatogenesis and peripheral testosterone concentration in raccoons (*Procyon lotor*) in Hokkaido. *J Vet Med Sci* **74**: 727–732.
99. Okuyama MW, Shimozuru M, Yanagawa Y, Tsubota T. 2014. Changes in the immunolocalization of steroidogenic enzymes and the androgen receptor in raccoon (*Procyon lotor*) testes in association with the seasons and spermatogenesis. *J Reprod Dev* **60**: 155−161.
100. Oliveira SM, Vilamaior PSL, Corradi LS, Góes RM, Taboga SR. 2007. Cellular and extracellular behavior in the gerbil (*Meriones unguiculatus*) ventral prostate following different types of castration and the consequences of testosterone replacement. *Cell Biol Int* **31**: 235–245.
101. O'shea JD. 1962. Studies on the canine prostate gland: I. Factors influencing its size and weight. *J Comp Pathol Ther* **72**: 321–331.
102. Ousset M, Van Keymeulen A, Bouvencourt G, Sharma N, Achouri Y, Simons BD, Blanpain C. 2012. Multipotent and unipotent progenitors contribute to prostate postnatal development. *Nat Cell Biol* **14**: 1131–1138.
103. Parson CL. 2007. The Role of the urinary epithelium in the pathogenesis of interstitial cystitis/prostatitis/urethritis. *Urology* **69**: 9–16.
104. Pelletier RM. 1986. Cyclic formation and decay of the blood-testis barrier in the mink (*Mustela vison*), a seasonal breeder. *Am J Anat* **175**: 91−117.
105. Picut CA, Remick AK, de Rijk EP, Simons ML, Stump DG, Parker GA. 2015. Postnatal development of the testis in the rat: morphologic study and correlation of morphology to neuroendocrine parameters. *Toxicol Pathol* **43**: 326−342.

106.Picut CA, Ziejewski MK, Stanislaus D. 2018. Comparative aspects of pre-and postnatal development of the male reproductive system. *Birth Defects Res* **110**: 190–227.

107.Poglayen-Neuwall I, Shively JN. 1991. Testicular cycles of the ringtail, *Bassariscus astutus* (Carnivora: Procyonidae). *Zeitschrift für Säugetierkunde* **56**: 72−80.

108.Puga CC, Beguelini MR, Martins FF, Falleiros Jr LR, Morielle-Versute E, Vilamaior PS, Taboga SR. 2014. Seasonal changes in the prostatic complex of *Artibeus planirostris* (Chiroptera: Phyllostomidae). *Gen Comp Endocrinol* **197**: 33–42.

109.Puga CC, Beguelini MR, Morielle-Versute E, Vilamaior PS, Taboga SR. 2016. The effects of castration followed testosterone supplementation in prostatic complex of *Artibeus planirostris* (Chiroptera: Phyllostomidae). *Tissue Cell* **48**: 252–264.

110.Puppo V, Puppo G. 2016. Male vagina is a more accurate term than prostatic utricle. *Int J Urol* **23**: 108.

111.Qiang W, Murase T, Tsubota T. 2003. Seasonal changes in spermatogenesis and testicular steroidogenesis in wild male raccoon dogs (*Nyctereutes procynoides*). *J Vet Med Sci* **65**: 1087−1092.

112.Rehm S. 2000. Spontaneous testicular lesions in purpose-bred beagle dogs. *Toxicol Pathol* **28**: 782−787.

113.Robboy SJ, Hill EC, Sandberg EC, Czernobilsky B. 1986. Vaginal adenosis in women born prior to the diethylstilbestrol era. *Human Pathol* **17**: 488−492.

114.Rochel SS, Bruni–Cardoso A, Taboga SR, Vilamaior PSL, Góes RM. 2007. Lobe identity in the Mongolian gerbil prostatic complex: a new rodent model for prostate study. *Anat Rec* **38**: 231–236.

115.Ryman-Tubb T, Lothion-Roy JH, Metzler VM, Harris AE, Robinson BD, Rizvanov AA, Jeyapalan JN, James VH, England G, Rutland CS, Persson JL, Kenner L, Rubin MA, Mongan NP, de Brot S. 2022. Comparative pathology of dog and human prostate cancer. *Vet Med Sci* **8**: 110–120.

116.Sanderson GC, Nalbandov AV. 1973. The reproductive cycle of the raccoon in Illinois. *Illinois Nat Hist Surv Bull* **31**: 25–85.

117.Sasaki M, Endo H, Kimura J, Rerkamnuaychoke W, Hayakawa D, Bhuminand D, Kitamura N, Fukuta K. 2010. Immunohistochemical localization of the cytoskeletal proteins in the testes of the lesser mouse deer (*Tragulus javanicus*). *Mamm Study* **35**: 57−64.

118.Seco-Rovira V, Beltrán-Frutos E, Ferrer C, Saez FJ, Madrid JF, Canteras M, Pastor L

M. 2015. Testicular histomorphometry and the proliferative and apoptotic activities of the seminiferous epithelium in Syrian hamster (*Mesocricetus auratus*) during regression owing to short photoperiod. *Andrology* **3**: 598−610.

119. Sharma DK. 2010. Comparative study of prostatic utricle in rat, rabbit, dog and man. *J. Anat. Soc. India* **59**: 12−18.

120. Shapiro E, Huang H, McFadden DE, Masch RJ, Ng E, Lepor H, Wu XR. 2004. The prostatic utricle is not a müllerian duct remnant: immunohistochemical evidence for a distinct urogenital sinus origin. *J Urol* **172**: 1753−1756.

121. Shehata R. 1978. Male uterus in the donkey and horse. *Cells Tissues Organs* **101**: 245−248.

122. Štrbenc M, Fazarinc G, Bavdek SV, Pogačnik A. 2003. Apoptosis and proliferation during seasonal testis regression in the brown hare (*Lepus europaeus* L.). *Anat Histol Embryol* **32**: 48−53.

123. Sugimura Y, Cunha GR, Donjacour AA. 1986a. Morphogenesis of ductal networks in the mouse prostate. *Biol Reprod* **34**: 961–971.

124. Sugimura Y, Cunha GR, Donjacour AA. 1986b. Morphological and histological study of castration-induced degeneration and androgen-induced regeneration in the mouse prostate. *Biol Reprod* **34**: 973–983.

125. Sugiyama M, Machida N, Yasunaga A, Terai N, Fukasawa H, Ono HK, Kobayashi R, Nishiyama K, Hashimoto O, Kurusu S, Yoshioka K. 2021. Vaginal mucus in mice: developmental and gene expression features of epithelial mucous cells during pregnancy. *Biol Reprod* **105**: 1272−1282.

126. Swiezynski, K. 1968. The male reproductive organs of the European bison. *Acta Theriol* **13**: 29−34.

127. Thomson AA. 2001. Role of androgens and fibroblast growth factors in prostatic development. *Reproduction* **121**: 187−195.

128. Thuilliez C, Tortereau A, Perron-Lepage MF, Howroyd P, Gauthier B. 2014. Spontaneous testicular tubular hypoplasia/atrophy in the Göttingen minipig: a retrospective study. *Toxicol Pathol* **42**: 1024−1031.

129. Timmons B, Akins M, Mahendroo M. 2010. Cervical remodeling during pregnancy and parturition. *Trends Endocrinol Metab* **21**: 353−361.

130. Todhunter R, Gemmell RT. 1987. Seasonal changes in the reproductive tract of the male marsupial bandicoot, *Isoodon macrourus*. *J Anat* **154**: 173–186.

131. Toivanen R, Shen MM. 2017. Prostate organogenesis tissue induction, hormonal

regulation and cell type specification. *Development* **144**: 1382–1398.

132. Tsubota T, Nagashima T, Kohyama K, Maejima K, Murase T, Kita I. 2001. Seasonal changes in testicular steroidogenesis and spermatogenesis in a northern fur seal, *Callorhinus ursinus*. *J Reprod Dev* **47**: 415−420.

133. Tsukise A, Yamada K. 1981. The histochemistry of complex carbohydrates in the epithelium lining the ventral prostate of the rat. *Histochem* **72**: 215–227.

134. Tsukise A, Yamada K. 1984. Complex carbohydrates in the secretory epithelium of the goat prostate. *Histochem J* **16**: 311–319.

135. Uno T. 2015. Studies on Male Reproductive Characteristics of Feral Raccoons (*Procyon lotor*) in Kanagawa Prefecture, Japan. In: Doctoral Thesis, Nippon Veterinary and Life Science Univ.

136. Vanderstichel R, Forzan MJ, Perez GE, Serpell JA, Garde E. 2015. Changes in blood testosterone concentrations after surgical and chemical sterilization of male free roaming dogs in southern Chile. *Theriogenology* **83**: 1021–1027.

137. Vilamaior PS, Taboga SR, Carvalho HF. 2006. Postnatal growth of the ventral prostate in Wistar rats: a stereological and morphometrical study. *Anat Rec* **288**: 885−892.

138. Wang X, Hayward SW, Kristina MC, Thayer A, Cunha GR. 2001. Cell differentiation lineage in the prostate. *Differentiation* **68**: 270–279.

139. Wang X, Kruithof-de Julio M., Economides KD, Walker D, Yu H, Halili MV, Hu Y, Price SM, Abate-Shen C, Shen MM. 2009. A luminal epithelial stem cell that is a cell of origin for prostate cancer. *Nature* **461**: 495–500.

140. Weider K, Bergmann M, Giese S, Guillou F, Failing K, Brehm R. 2011. Altered differentiation and clustering of Sertoli cells in transgenic mice showing a Sertoli cell specific knockout of the connexin 43 gene. *Differentiation* **82**: 38−49.

141. Wernert N, Kern L, Heitz PH, Bonkhoff H, Goebbels R, Seitz G, Inniger R, Remberger, K, Dhom G. 1990. Morphological and immunohistochemical investigations of the utriculus prostaticus from the fetal period up to adulthood. *The Prostate* **17**: 19−30.

142. Witkiewicz AK, Hecht JL, Cviko A, McKeon FD, Ince TA, Crum CP. 2005. Microglandular hyperplasia: a model for the de novo emergence and evolution of endocervical reserve cells. *Hum Pathol* **36**: 154−161.

143. Wrobel M. 1972. Histochemische und elektronenmikroskopische untersuchungen an der prostata von Hund und Katze. *Zbl Vet Med* **C1**: 93–116.

144. Wu CT, Altuwaijri S, Ricke WA, Huang SP, Yeh S, Zhang C, Niu Y, Tsai MY, Chang C. 2007. Increased prostate cell proliferation and loss of cell differentiation in mice

lacking prostate epithelial androgen receptor. *Proc Natl Acad Sci USA* **104**: 12679–12684.

145. Xie Q, Liu Y, Cai T, Horton C, Stefanson J, Wang ZA. 2017. Dissecting cell-type-specific roles of androgen receptor in prostate homeostasis and regeneration through lineage tracing. *Nat Commun* **8**: 1–14.

146. Zambelli D, Cunto M. 2005. Vaginal and cervical modifications during the estrus cycle in the domestic cat. *Theriogenology* **64**: 679–684.

147. Zhang Y, Wang Y, Huang C, Wang Y, Qi H, Han Y, Yuan Z, Weng Q, Zhang H. 2018. Seasonal expression of 5α-reductases and androgen receptor in the prostate gland of the wild ground squirrel (*Spermophilus dauricus*). *Comp Biochem Physiol A Mol Integr Physiol* **226**: 11–16.

148. Zhu LJ, Zong SD, Phillips DM, Moo-Young AJ, Bardin CW. 1997. Changes in the distribution of intermediate filaments in rat Sertoli cells during the seminiferous epithelium cycle and postnatal development. *Anat Rec* **248**: 391–405.

149. Zuckerman S. 1936. The endocrine control of the prostate. *Proc Roy Soc Med* **29**: 1557–1568.

150. Zuckerman S, Parkes AS. 1935. Observations on the structure of the uterus masculinus in various primates. *J Anat* **69**: 484–496.9.